A FRAP Assay to determine the influence of Crumbs in membrane protein dynamics

Dissertation

zur Erlangung des akademischen Grades

Doctor of Philosophy

(Ph. D.)

vorgelegt
der Fakultät Mathematik und Naturwissenschaften
der Technischen Universität Dresden
von

João Pedro Bronze Firmino

geboren am 20. Dezember in Oeiras, Portugal

Gutachter:

Professor Dr. Elisabeth Knust	Max Planck Institute for Molecular Cell Biology and Genetics, Dresden
Professor Dr. Michael Brand	Technischen Universität Dresden, Dresden

Eingereicht am: 24th June 2011

To my mother and grandmother,

Declaration

I herewith declare that I have produced this paper without the prohibited assistance of third parties and without making use of aids other than those specified; notions taken over directly or indirectly from other sources have been identified as such. This paper has not previously been presented in identical or similar form to any other German or foreign examination board.

This thesis work was conducted from 1st March 2007 to 1st March 2011 under the supervision of Prof.Dr. Elisabeth Knust at the Max Planck Institute for Molecular Cell Biology and Genetics, Dresden.

I declare that I have not undertaken any previous unsuccessful doctorate proceedings.

I declare that I recognize the doctorate regulations of the Fakultät für Mathematik und Naturwissenschaften of the Technische Universität Dresden.

Dresden, June 24th, 2011

João Firmino

Table of Contents

Table of Figures

A. Introduction

D. Results

E. Discussion

F. Materials and Methods

DVD contents

Drosophila Embryogenesis

Example FRAP Movies (use FIJI for visualisation)

CasperSASVenus

Anterior

CasperSASVenus_anterior_withalignstacks.tif
CasperSASVenus_anterior_withoutalignstacks.tif

Posterior

CasperSASVenus_posterior_withalignstacks.tif
CasperSASVenus_posterior_withoutalignstacks.tif

*D*ECadGFP

Anterior

*D*ECadGFP_anterior_postbleach_fast.tif
*D*ECadGFP_anterior_postbleach_medium.tif
*D*ECadGFP_anterior_postbleach_slow.tif
*D*ECadGFP_anterior_prebleach.tif
*D*ECadGFP_anterior_withalignstacks.tif
*D*ECadGFP_anterior_withoutalignstacks.tif

Posterior

*D*ECadGFP_posterior_postbleach_fast.tif
*D*ECadGFP_posterior_postbleach_medium.tif
*D*ECadGFP_posterior_postbleach_slow.tif
*D*ECadGFP_posterior_prebleach.tif
*D*ECadGFP_posterior_withalignstacks.tif
*D*ECadGFP_posterior_withoutalignstacks.tif

LacGFP

Anterior

LacGFP_anterior_postbleach_fast.tif
LacGFP_anterior_postbleach_medium.tif
LacGFP_anterior_postbleach_slow.tif
LacGFP_anterior_prebleach.tif
LacGFP_anterior_withalignstacks.tif
LacGFP_anterior_withoutalignstacks.tif

Posterior

LacGFP_posterior_postbleach_fast.tif
LacGFP_posterior_postbleach_medium.tif
LacGFP_posterior_postbleach_slow.tif
LacGFP_posterior_prebleach.tif
LacGFP_posterior_withalignstacks.tif
LacGFP_posterior_withoutalignstacks.tif

SpiderGFP

Anterior

SpiderGFP_anterior_withalignstacks.tif
SpiderGFP_anterior_withoutalignstacks.tif

Posterior

SpiderGFP_posterior_withalignstacks.tif
SpiderGFP_posterior_withoutalignstacks.tif

Excel spreadsheet template

FIJI software for movie visualization (Windows and MacOSX installer)

GBE movies

GBE_stage8

GBE_stage9

MATLAB script

A. Introduction

1. Epithelial Cell Polarity

Cell polarity is an intrinsic and necessary property of every organism. It is involved in several processes such as epithelial morphogenesis, asymmetric cell division and cell migration and is characterised by differences in protein and lipid distribution, morphology and cell function (Knust and Bossinger, 2002).

Epithelial cell polarisation is a crucial event in development, since epithelia act as diffusion barriers thus allowing the specific transport of substances through the cell. Ultrastructurally, epithelia are characterised by the presence of cell-cell junctions that subdivide the cell membrane in morphologically and biochemically distinct compartments (Davies and Garrod, 1997).

1.1 Junctional complexes in *Drosophila*

There are two main adhesive cell-cell junction types in *Drosophila* epithelia – the Zonula Adherens (ZA) and Septate Junctions (SJ). The ZA is involved in cell-cell adhesion with its main protein components being *D*E-Cadherin, Armadillo (β-catenin) and α-catenin. Septate Junctions, on the other hand, have a barrier function and are characterised by electron dense septae between the lateral membranes.

The ZA assumes a very important role in apicobasal polarity since it marks the border between the apical and basal membrane compartments. This polarity is classically defined by three distinct protein complexes, two of which localise mostly in the subapical region (Bazooka/PAR3-*D*aPKC-*D*Par6 complex and the Crumbs-Stardust-*D*Patj complex) and the other in the basolateral membrane (Scribble-Dlg-Lgl complex) side of the Zonula Adherens (Johnson and Wodarz, 2003); (Laprise and Tepass, 2011); (Figure A1).

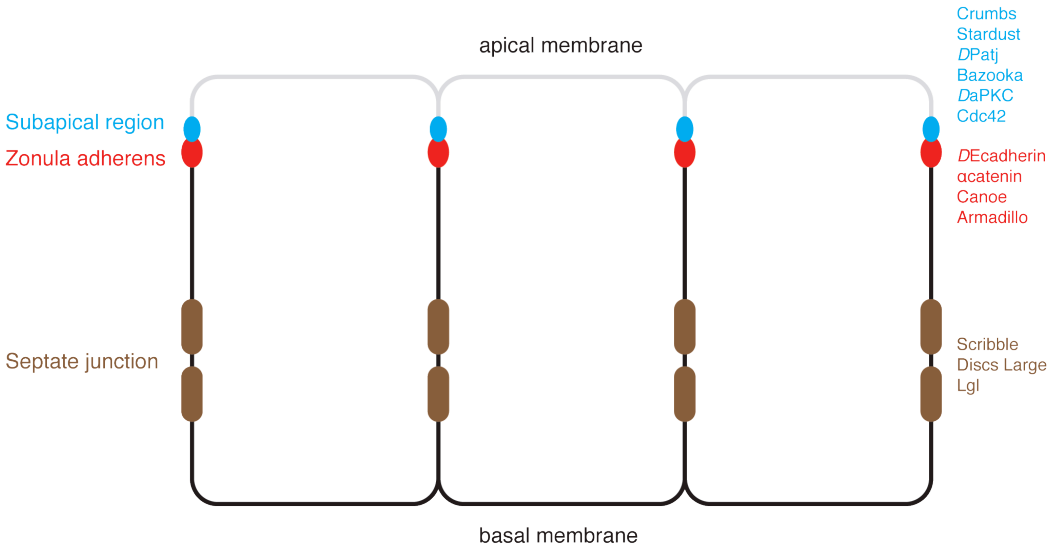

Figure A1 - Schematic representation of epithelial cell-cell junctions in *Drosophila melanogaster*. The type of junction is indicated on the left and the proteins localised in that subdomain are indicated on the right [adapted from (Knust and Bossinger, 2002)].

The blastoderm is the first epithelium formed in the *Drosophila* embryo and is the result of the process of cellularisation. It is characterised by the segregation of the 5000 nuclei present in the syncytium via growth and invaginations of the plasma membrane - cleavage furrows (Lecuit, 2004). Establishment of apicobasal polarity occurs as the plasma membrane is growing. As it grows, it is possible to observe the formation of transient basal adherens junctions (BAJ) composed by many of the future zonula adherens (ZA) proteins – *D*E-Cadherin, catenins – and the subapical region (SAR) component – *D*Patj. As cellularisation proceeds, Armadillo (ß-catenin) accumulates in spot junctions along the lateral membrane, which later coalesce apically to form a belt around the cell - the zonula adherens. Once the process is complete, distinct domains in the plasma membrane can be identified by the presence of specific proteins (Harris and Peifer, 2005).

1.1.1. Bazooka Complex

Bazooka acts upstream of zonula adherens formation in the primary epithelia of *Drosophila*, since embryos lacking Bazooka (Baz) or *D*aPKC fail to establish junctions altogether (Muller and Wieschaus, 1996). Although Bazooka/PAR3, *D*Par-6 and *D*aPKC are often assumed to function as a complex in epithelial cells, there is increasing evidence that Bazooka/PAR3 acts independently from *D*Par-6 and *D*aPKC in this cell type. Both *D*Par-6 and *D*aPKC interact with the Crumbs complex and both Stardust (Sdt) and Crumbs (Crb) can bind directly to the PDZ domain of *D*Par6, coprecipitating with *D*Par6 and *D*aPKC in mammals and *Drosophila* (Hurd et al., 2003); (Lemmers et al., 2004); (Wang et al., 2004); (Kempkens et al., 2006); (Nam and Choi, 2006). Furthermore, two conserved threonines in the cytoplasmic tail of Crb are *in vitro* phosphorylated by *D*aPKC and this is required for Crumbs activity (Sotillos et al., 2004).
Bazooka/PAR3, on the other hand, interacts with Armadillo (Arm), which binds directly to *D*E-Cadherin, as well as the Nectin-like protein, Echinoid, both of which are components of the adherens junction (Wei et al., 2005). Bazooka does play a key role in positioning the AJs in the primary epithelium of *Drosophila*, since it localises to the apical/lateral border before *DE*-Cadherin and Armadillo and is required for the coalescence of spot adherens junctions into the zonula adherens (Harris and Peifer, 2005); (McGill et al., 2009).
Baz fails to associate with *D*aPKC and *D*Par6 in epithelial cells because it is excluded from the complex by the combined action of the Crumbs complex and of its phosphorylation on serine 980 by *D*aPKC. This phosphorylation is not sufficient to prevent its association with *D*Par6/aPKC complex, since Baz can bind directly to the PDZ domain of *D*Par6. However, both Crb and Sdt bind to the same domain of *D*Par6, thus outcompeting Baz for binding (Morais-de-Sa et al., 2010). Another model was also proposed by (Krahn et al., 2010) in which the PDZ domain of Sdt binds to the region surrounding S980 of Baz - the phosphorylation target of *D*aPKC. As long as S980 is not phosphorylated by *D*aPKC, this complex is stable, and the PDZ domain of Sdt is not available for binding to the C terminus of Crb. Upon phosphorylation of S980 of Baz by *D*aPKC, the binding between Baz and Sdt becomes weaker, causing the dissociation of the Baz–Sdt complex and releasing Sdt for binding to Crb.
Therefore, the apical exclusion of Bazooka by *D*aPKC and the Crumbs complex restricts the extent of the AJ thus defining the border between the apical and lateral domains. Baz functions separately from *D*Par6 and *D*aPKC in epithelial cells, where its main function is

to stabilise and position the apical junction. This presumably depends on other activities of Bazooka, such as its binding to Armadillo and Echinoid and its recruitment of PTEN to regulate Phosphatidylinositide 4,5 P_2 (PIP2) levels (Pinal et al., 2006), (von Stein et al., 2005), (Wei et al., 2005); (Wu et al., 2007).

1.1.2. Crumbs Complex

The presence of the Crumbs complex in the subapical region (SAR) is key to the maintenance of the adhesion belt, since it provides a link to the apical spectrin membrane cytoskeleton, ultimately reinforcing the ZA (Medina et al., 2002). Embryos mutant for *crb* or *sdt* fail to maintain the ZA, thus resulting in the loss of apical identity, cell multilayering and cell death in some of the epithelia (Grawe et al., 1996); (Tepass and Knust, 1993). It has recently been reported that Crb is specifically required in epithelia that are undergoing morphogenetic movements (Harris and Tepass, 2008); (Campbell et al., 2009).

In the renal tubules of *Drosophila*, a tissue that undergoes dramatic morphogenetic changes, the Bazooka and Scribble protein groups are required for the establishment of tubule cell polarity, whereas Crumbs is required for cell polarity in the tubules only when morphogenetic movements start. If these movements are stalled, polarity persists even in the absence of Crumbs. The partial suppression of the ectodermal phenotype in *crumbs* mutant embryos, by a reduction in germband extension suggests that Crumbs has a specific, conserved function in stabilising cell polarity during tissue remodelling rather than in its initial stabilisation (Campbell et al., 2009). This and a previous report (Blankenship et al., 2007) also identified a requirement for the exocyst component Exo84 during tissue morphogenesis, which suggests that Crumbs-dependent stability of epithelial polarity is correlated with a requirement for membrane recycling and targeted vesicle delivery.

It remains to be determined whether Crb ensures ZA plasticity during cell rearrangements by restricting excessive endocytosis of apical proteins via apical exclusion of Bazooka (Morais-de-Sa et al., 2010) or in a more direct way by regulating the recycling of junctional proteins.

1.1.3. Scribble complex

The Scribble complex, located basally to the ZA, is key to properly define the localisation of the other complexes. Loss of Scribble in *Drosophila* embryos results in misdistribution of apical proteins and proteins of the adherens junctions to basolateral positions (Bilder and Perrimon, 2000). Scribble colocalises with Dlg and Lgl and their localisation mutually depends on each other. Removal of either of them in the imaginal disc epithelium leads to loss of adhesion and polarity, followed by dramatic overgrowth of the discs (Bilder et al., 2000).

All in all, this data suggests a regulatory hierarchy between the different polarity groups, where Bazooka/PAR3-*D*aPKC-*D*Par6 (establishment of polarity) is antagonized by Scribble-Dlg-Lgl (repression of apical identity) that in turn is antagonized by Crumbs-Stardust-*D*Patj (maintenance of polarity).
How these proteins contribute to junction formation and consequent membrane compartmentalisation is not entirely understood nor is their dynamics during active morphogenetic processes, e.g. *Drosophila* germband elongation (GBE).

1.2. Apical junctional complexes in vertebrates

In vertebrates, the location of the tight junction (TJ) corresponds to that of the *Drosophila* SAR. Tight junctions are intramembrane diffusion barriers and act as paracellular seals. They show a very similar protein composition to the SAR – Crb1, Pals1 (Stardust), PatJ, PAR3 (Bazooka), PAR6, aPKC and Cdc42 are present. However, Occludins, Claudins and Junction adhesion molecule (JAM) are exclusively present in TJs. It is the TJ that marks the boundary between the apical and basolateral membrane domains (Knust and Bossinger, 2002); (Figure A2).

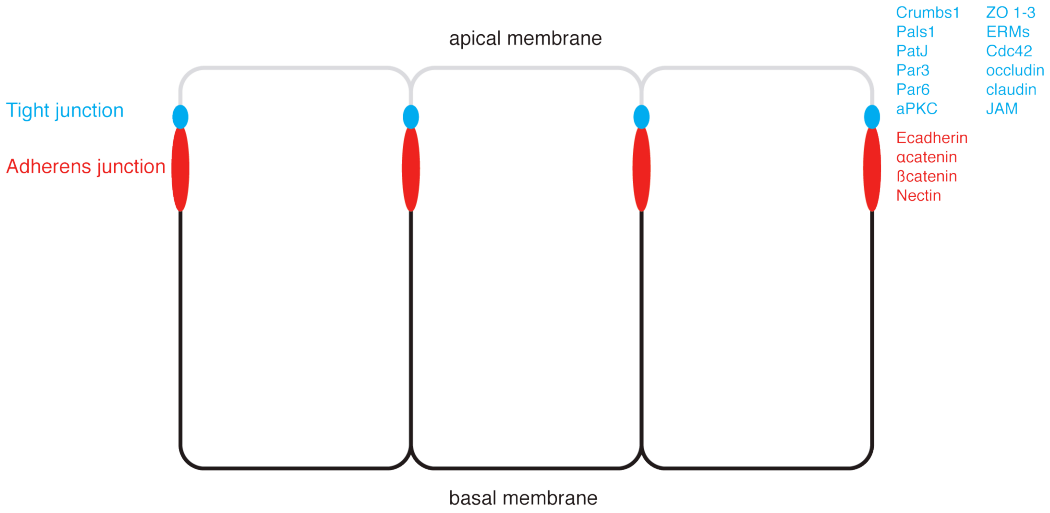

Figure A2 - Schematic representation of apical cell-cell junctions in vertebrates.

The type of junction is indicated on the left and the proteins localised in that subdomain are indicated on the right [adapted from (Knust and Bossinger, 2002)].

Tight junction assembly starts with the binding of ZO-1 to claudins and JAM. PAR3 also binds JAM and once this complex is assembled, PAR6, aPKC and Cdc42 can then be recruited to the TJ (Ebnet et al., 2001); (Itoh et al., 2001); (Kohjima et al., 2002); (Takekuni et al., 2003); (Drees et al., 2005). PAR3 directs tight junction formation, as overexpression of PAR3 increases the rate at which tight junctions form, whereas dominant negative PAR3 and PAR3 RNAi inhibit tight junction formation (Chen and Macara, 2005). Interestingly, PAR3 also localises beneath aPKC and PAR6 in mammalian epithelia, raising the possibility that, despite the different arrangement of junctions, the apical/lateral boundary might be positioned in the same way in mammals and *Drosophila* (Afonso and Henrique, 2006); (Martin-Belmonte et al., 2007); (Totong et al., 2007). Crb1 interacts with the PDZ domain of Pals1 via its cytoplasmic tail. In turn, Pals1 is recruited to PatJ, which interacts with ZO-3 and claudin-1. Therefore in mammalian TJs, both complexes (Par-aPKC-Cdc42 and Crb1-Pals1-PatJ) are anchored to the plasma membrane by claudins. Whether there is any crosstalk between them remains to be cleared (Itoh et al., 2001); (Lemmers et al., 2002); (Roh et al., 2002a); (Roh et al., 2002b).

2. Gastrulation and Germband extension

After blastoderm formation, it is required to define the three different embryonic germ layers – ectoderm, mesoderm and endoderm. Gastrulation is the stage of development where this takes place (Figure A3).

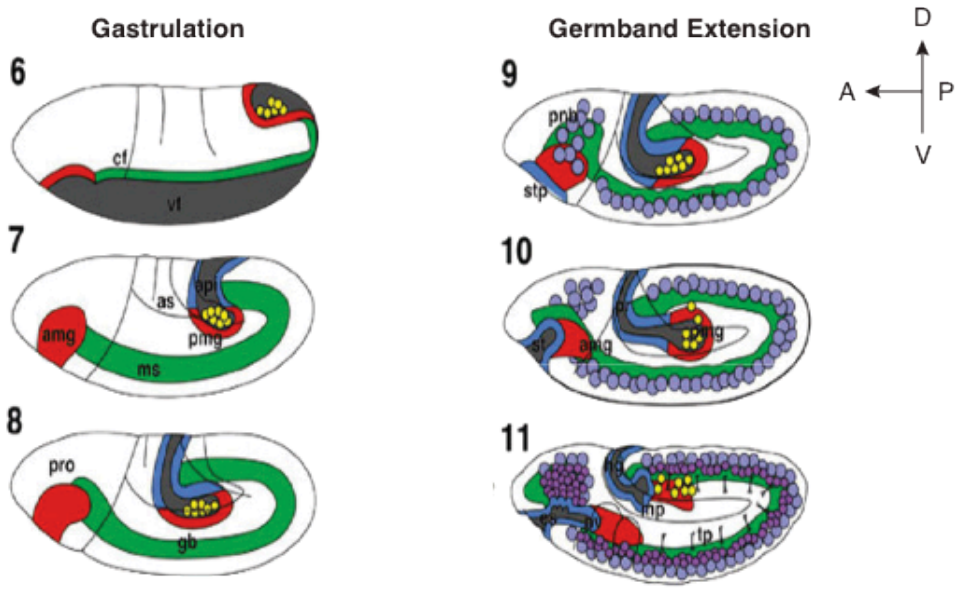

Figure A3 – Schematic lateral view of embryos undergoing Gastrulation and Germband Extension. Embryo orientation consists in anterior to the left and dorsal to the top. The numbers refer to the stage of development. Endoderm (red); mesoderm (green); central nervous system (purple); foregut and hindgut (blue) and pole cells (yellow). (*amg*) anterior midgut rudiment; (*api*) amnioproctodeal invagination; (*as*) amnioserosa; (*cf*) cephalic furrow; (*es*) esophagus; (*gb*) germ band; (*hg*) hindgut; (*mp*) Malpighian tubules; (*ms*) mesoderm; (*pmg*) posterior midgut rudiment; (*pnb*) procephalic neuroblasts; (*pr*) proctodeum; (*pro*) procephalon; (*pv*) proventriculus; (*st*) stomodeum; (*stp*) stomodeum primordium; (*tp*) tracheal pits; (*vf*) ventral furrow [from (Hartenstein, 1993)].

In *Drosophila*, gastrulation lasts approximately 1 hour and is a process characterised by highly reproducible patterns of cell movements and rearrangements (Pilot and Lecuit, 2005). As gastrulation occurs, the germband of the embryo, which will later give rise to the segmented trunk of the larva, starts to elongate in the anterior/posterior (AP) axis and narrowing in the dorso-ventral (DV) axis. Since the vitelline membrane (eggshell) encloses the embryo, the germband folds back dorsally at the posterior end, thus leading to minimal cell surface contacts and optimised packing. When it finishes, the germband posterior tip has moved over 70% of the embryo length towards the head region and the embryo length has almost doubled.

This extension occurs in two steps - a fast phase that lasts approximately 30 minutes followed by a slow phase, which lasts 90 minutes (Butler et al., 2009). Both phases require intensive cell intercalation movements (Figure A4); (GBE movies found in the attached DVD).

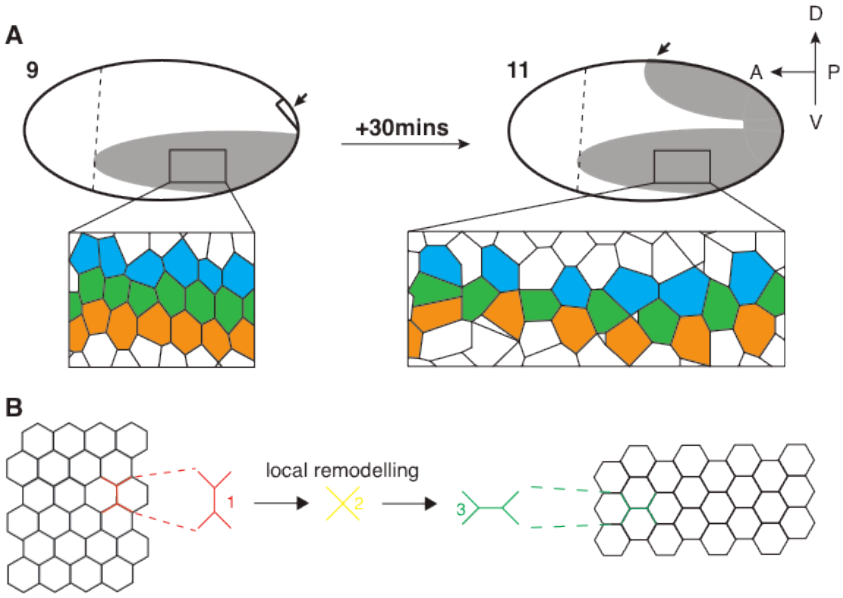

Figure A4 – Germband extension (GBE) and junctional remodelling.

(A) Embryo at the beginning of GBE and 30 mins later. Embryo orientation consists on anterior to the left and dorsal to the top. The germband (grey) is posterior to the cephalic furrow (dotted line) and folds back dorsally after cell intercalation in the ventral-lateral region. The arrow refers to the posterior end of the germband. Cells exchange neighbours and the tissue extends as a consequence [adapted from (Bertet et al., 2004)]. (B) Diagram highlighting cell junction transitions during GBE.

Oriented cell division and cell shape changes are also required for the fast phase of germband extension (GBE). This stage of development is ideal to analyse membrane and protein dynamics and the role polarity complex proteins play during GBE, since cells have to undergo extensive remodelling of their cell-cell junctions (Baum and Georgiou, 2011).

2.1 Junction remodelling during intercalation

At the onset of GBE, epithelial cells form a packed hexagonal array (type 1 configuration). When GBE begins, groups of four cells form characteristic tetrads around type 1 junctions. In this type 1 configuration, adjacent cells along the A/P axis are in contact but immediately dorsal and ventral cells are not in contact with each other. As GBE proceeds, type 1 junctions specifically shrink, leading to a configuration in which the four cells of the tetrad share equal contacts (type 2). Subsequently, new junctions of type 3 are built perpendicular to the old type 1 junction, resulting in effective intercalation of the cells that were dorsal and ventral (Figure A4B). This polarised pattern of junction remodelling shows that cells can distinguish between its different cell boundaries and control a specific behaviour in each of them (shrinkage or extension) (Bertet et al., 2004). The transition type 1 to type 2 to type 3 is unidirectional and the reverse transition never occurs. As intercalation proceeds, a relative decrease in the number of type 1 junctions occurs with a corresponding increase in the number of type 3 junctions. Junction remodelling happens only in the intercalating region; that is, in the ventral and lateral ectoderm (Bertet et al., 2004); (Classen et al., 2005); (Langevin et al., 2005); (Zallen and Wieschaus, 2004); (Baum and Georgiou, 2011).

3. Crumbs Complex

Crumbs is the key protein of a complex responsible for the maintenance of apicobasal polarity. The other core components present in this complex are Stardust, *D*Patj and DLin-7 (Figure A5).

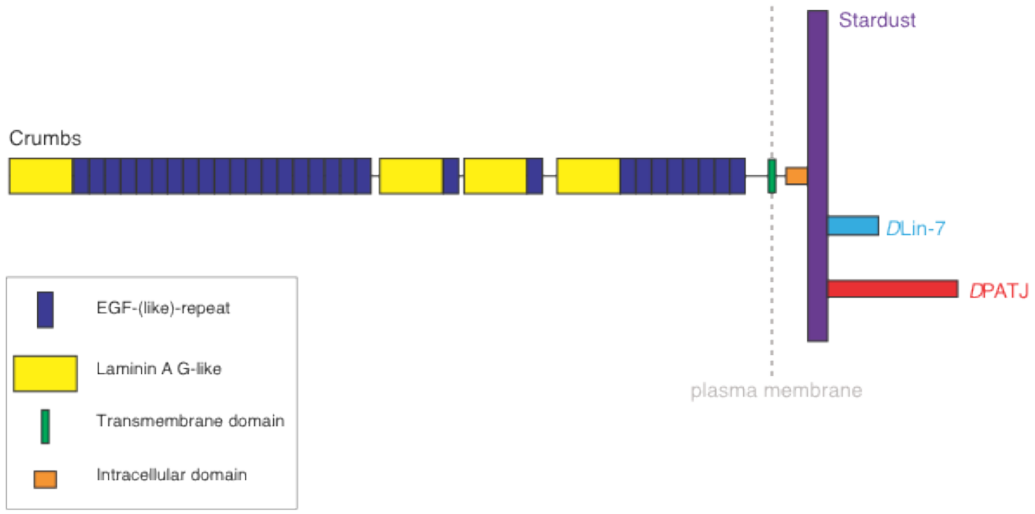

Figure A5 – The Crumbs complex.

Crumbs is a transmembrane protein with an extracellular domain composed by 29 to 30 EGF-like repeats and 4 laminin A G-like domains. Intracellularly, it contains a FERM binding motif, a PDZ binding domain (ERLI motif) and it can bind the retromer (Pocha et al., 2011). It is expressed in all epithelia derived from the ectoderm. Via its ERLI motif it binds Stardust – a membrane-associated guanylate kinase (MAGUK) homologue protein - thus anchoring it close to the plasma membrane. In turn, it is this scaffolding protein (Stardust) that recruits *D*Lin-7 and *D*Patj, thus forming the so-called Crumbs complex. Crumbs can also bind *D*-Par6 (Hurd et al., 2003); (Lemmers et al., 2004); (Wang et al., 2004); (Kempkens et al., 2006); (Nam and Choi, 2006).

3.1 Mutations in Crumbs show different phenotypes

Crumbs was originally found in a genetic screen for mutations affecting cuticle patterning (Jurgens et al., 1984). Later on, during a genomic screen for genes encoding EGF-like proteins similar to Notch and Delta, Crumbs was found and further characterised (Knust et al., 1987); (Tepass et al., 1990); (Tepass and Knust, 1990); (Tepass and Knust, 1993).

In the embryo, the most striking phenotype of mutations affecting Crumbs (*crb*^{11A22} is the null allele most commonly used in studies regarding Crumbs' function) is the absence of

a properly formed cuticle due to the failure in maintaining a proper Zonula Adherens in the epidermis and consequent epithelial cell polarity defects (Figure A6A and A6B). These defects – cell multilayering, loss of adherens junctions and subsequent loss of apical identity – manifest themselves during germband extension and when observed at the ultrastructural level are preceded by misdistribution of Armadillo and *D*E-Cadherin, the homologues of β-catenin and E-cadherin, respectively (Grawe et al., 1996); (Tepass, 1996). This data combined with evidences from *Drosophila* renal tubules (Campbell et al., 2009) suggests a model wherein the Crb complex is dispensable for the establishment of cell polarity in embryonic epithelia but as soon as morphogenetic cell rearrangements start, the complex acts both to stabilise apical proteins and to restrict the spread of basolateral proteins.

When overexpressed, Crumbs causes an enlargement of the apical domain (Figure A6C). This expansion of the apical membrane domain in epidermal cells also abolishes the formation of the Zonula Adherens and results in the disruption of tissue integrity, but without loss of membrane polarity (Grawe et al., 1996).

In *Drosophila* photoreceptor cells, Crumbs is localised in the stalk membrane and it is this subdomain that supports the morphogenesis and orientation of the photosensitive membrane organelles: the rhabdomeres. Crumbs is required to maintain Zonula Adherens integrity during the rapid apical membrane expansion that builds the rhabdomere thus making it a central component of a molecular scaffold that controls ZA assembly and defines the stalk as an apical membrane subdomain (Izaddoost et al., 2002); (Johnson et al., 2002); (Pellikka et al., 2002); (Hong et al., 2003); (Richard et al., 2006); (Berger et al., 2007). These morphogenetic events require the targeted delivery and retention of large amounts of membrane. Here too, it is not yet clear whether Crb acts directly on the stability of ZA components or indirectly, by controlling other polarity proteins. Although *D*Par6 is delocalised in *crb* mutant photoreceptor cells (Berger et al., 2007), other data suggest that the Crb complex regulates ZA integrity and trafficking of apical membrane via stabilisation of the membrane-associated cytoskeleton, including β_H-spectrin (Pellikka et al., 2002).

Besides morphological defects, the patterning and integrity of the fly ommatidia once exposed to constant light is lost in a Crumbs mutant background (Johnson et al., 2002); (Figure A6D). The mechanisms by which this occurs are still not understood although recent evidence in the lab points to the involvement of MyosinV in this process (unpublished data from Shirin Pocha).

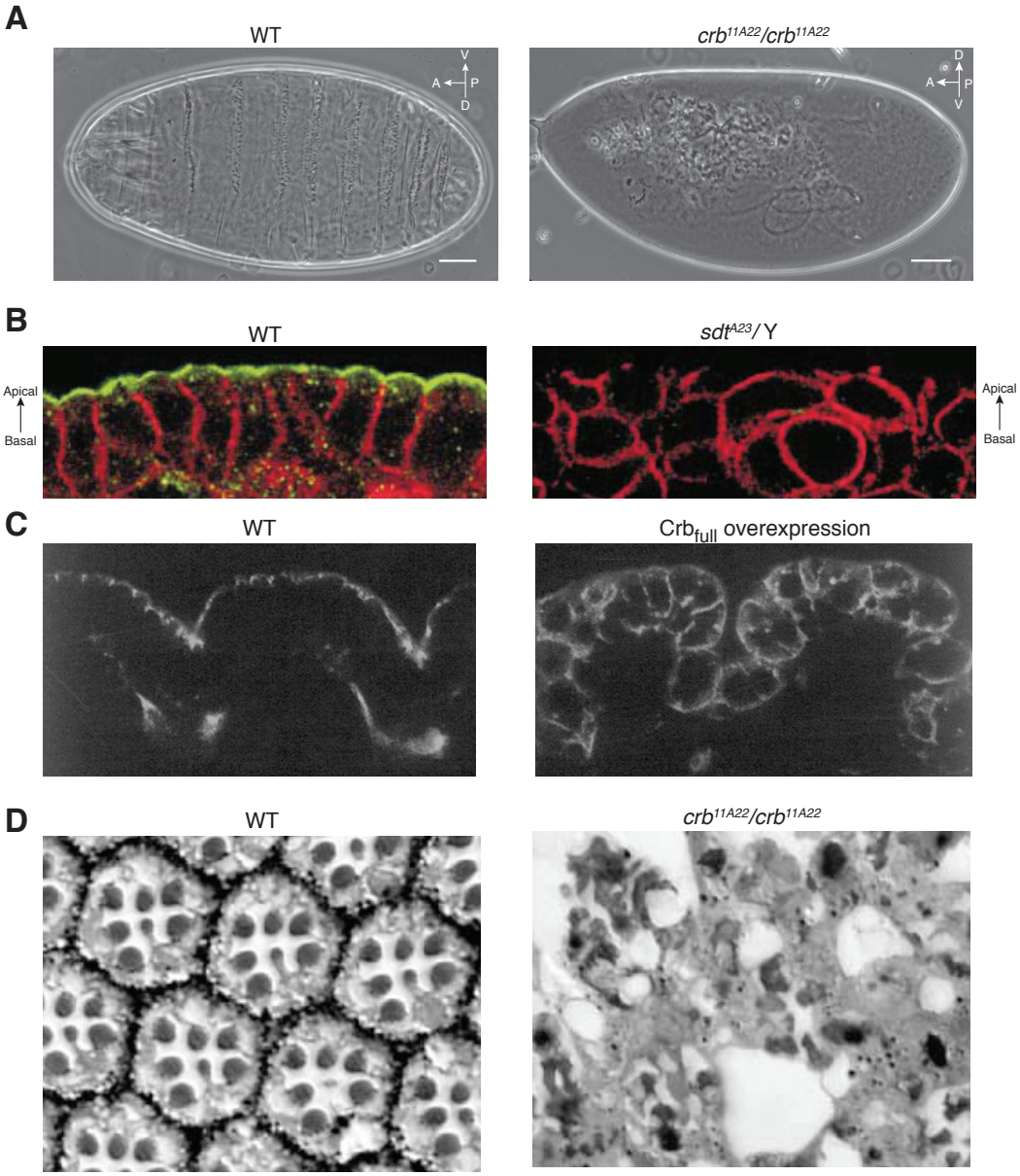

Figure A6 – Phenotypes of mutations in Crumbs and other complex components.

(A) Cuticle defects in *crb*^{11A22} embryos. Scale bar: 50μm (B) Antibody staining showing the disruption of epithelial cell polarity in *sdt*^{A23} embryos. The same phenotype occurs in *crb*^{11A22} embryos. Stranded at Second in green and Neurotactin in red (Bachmann et al., 2001). (C) Overexpression of full length Crumbs results in expansion of the apical domain labelled by Stranded at Second (Wodarz et al., 1995). (D) Light dependent degeneration of photoreceptor cells in *crb*^{11A22} ommatidia (Johnson et al., 2002).

4. Fluorescence Recovery After Photobleaching (FRAP)

Fluorescence Recovery After Photobleaching (FRAP) is a technique used for studying protein mobility in living cells by measuring the rate of fluorescence recovery at a bleached site. This recovery occurs by replenishment of intact fluorophore to the area previously bleached (Axelrod et al., 1976). The recent advent and availability of both fluorescent protein technology and confocal microscopy have made FRAP a common technique for studying almost all aspects of cell biology, including chromatin structure, transcription, mRNA mobility, protein recycling, signal transduction, cytoskeletal dynamics, vesicle transport, cell adhesion and mitosis (Sprague and McNally, 2005a).

Commonly, FRAP results are analyzed qualitatively to determine whether protein mobility is rapid or slow, whether binding interactions are present, whether an immobile fraction exists, or how a particular treatment (such as ATP depletion or a mutation in the protein of interest) affects these properties. Several mathematical models have been also developed to understand better the underlying processes, to ensure the accuracy of a qualitative interpretation, and to extract quantitative parameters from a FRAP curve (Sprague and McNally, 2005).

It is important to note that while FRAP is an extremely powerful technique, several factors affect its ability to describe protein kinetics in a 3D embryonic tissue over time. Time resolution over cell z-axis resolution is a conflicting conundrum that one has to consider whilst devising a FRAP experiment. Due to confocal imaging limitations, in order to achieve high temporal resolution of protein kinetics, cell z-axis resolution has to be sacrificed. Another problem deriving from performing FRAP in embryos is the fact that cells are not static throughout the duration of an experiment. Cell drift is a factor that has to be necessarily compensated when analysing the data from a FRAP experiment.

A FRAP experiment can be described by plotting fluorescence levels against time (Figure A7). Before exposure to an intense laser beam, the sample shows a certain level of fluorescence (F_{pre}). After the bleach (t_{post}), these levels drop to their lowest (F_{post}). Recovery then occurs by replenishment of fluorophores from areas that were not subject to photobleach. Eventually, fluorescence levels stabilise (F_{end}) and several physical parameters can be extracted from analysing the plot.

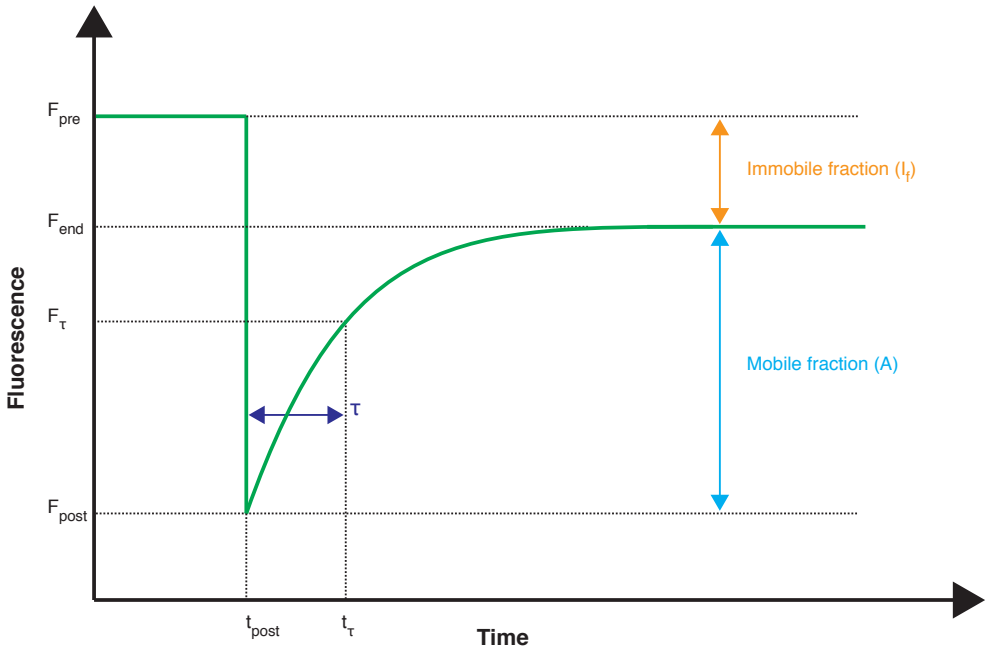

Figure A7 – FRAP recovery curve.

Protein fluorescence levels (y-axis) plotted against time (x-axis). Several physical parameters can be immediately ascertained from analysing the curve – mobile fraction, immobile fraction and τ. F_{end} (end fluorescence levels); F_{pre} (prebleach fluorescence levels); F_{post} (postbleach fluorescence levels); F_{τ} (67% of end fluorescence levels); t_{post} (bleach timepoint) and t_{τ} (timepoint where F_{τ} was achieved) [adapted from (Goldman and Spector, 2005)].

Whereas the mobile fraction parameter (A) refers to the amount of fluorophore used in the recovery of fluorescence, the immobile fraction refers to the amount of bleached fluorophore retained in the region analysed. These two parameters reflect protein mobility – a low mobile fraction value means that few nonbleached particles managed to replace the bleached protein during the experiment while high mobile fraction values mean that the nonbleached particles replaced most bleached ones. These parameters give an idea on how mobile or static a protein is.

As for τ, it marks the timepoint where 67% of final fluorescence levels were achieved. Therefore, this parameter reflects protein recovery kinetics – low values mean that the protein was faster in its recovery while high values mean the opposite. It is an essential parameter to determine how dynamic a protein is.

B. Scope of this thesis

The aim of this work was to describe and quantify polarised protein kinetics using FRAP (Fluorescence Recovery After Photobleaching) during specific stages of *Drosophila* embryogenesis (gastrulation and germband extension) in wild type embryos and compare them to crb^{11A22} embryos. These developmental stages were selected since a high level of morphogenetic activity is taking place, where epithelial cells necessarily have to remodel their plasma membranes whilst keeping their junctions intact. It should also be noted that the crb^{11A22} phenotype (epithelia disaggregation) only starts to manifest itself in the late stages of germband extension, thus allowing the FRAP assay to be done.

To achieve a proper characterisation of the recovery kinetics of the different plasma membrane compartments it was necessary not only to fluorescently tag an exclusively apical protein – Stranded At Second (SAS) – but also to develop an image acquisition method with a high temporal resolution for the FRAP assay.
Therefore, the polarised protein markers used were SpiderGFP (whole membrane), *D*E-cadherinGFP (Zonula Adherens), LachesinGFP (basolateral membrane) and SAS-Venus (apical membrane) – thus ensuring all cell compartments were labeled.

Live imaging of *D*E-CadGFP in crb^{11A22} background was also performed to test and reinforce the idea that Crb is required for adherens junction stabilisation and maintenance.

C. Summary

Apicobasal polarity is essential for epithelia formation and maintenance. Cell junctions, namely the zonula adherens in *Drosophila melanogaster*, are the morphological landmarks that define and distinguish the apical from the basal surface. This resulting compartmentalisation is key for the cell and consequently the epithelia. To maintain proper junctions, cells make use of several protein complexes and their interactions. Among these complexes, the Crumbs (Crb) network stands out. Mutations in Crumbs (*crb*^{11A22}) lead to zonula adherens collapse, consequent loss of apical surface and disaggregation of the epithelia. However, the mechanisms behind this are not known and haven't been addressed using modern techniques such as live imaging.

Several things came out of the dataset obtained from the FRAP experiments. Firstly, protein kinetics are better described when a double exponential fit curve is used, which raises the possibility that two cell processes might be involved in the recovery observed for the different markers.

Another finding was the fact that the kinetics of some polarised protein markers is not the same in every region of the embryo. Distinct areas of the embryo with different morphogenetic activity levels show different kinetics for the same compartment marker. That was the case with SpiderGFP (whole plasma membrane marker) and SASVenus (apical plasma membrane marker) where τ_2 was lower in the posterior region of the embryo which is characterised by intense cell movements resulting from convergence extension. *D*E-CadGFP (zonula adherens marker) and lacGFP (basolateral marker) behaved similarly in the whole embryo. This indicates that convergence extension shows different trafficking needs for the apical surface.

In *crb*^{11A22}, SpiderGFP kinetic spatial differences were not observed. τ_2 in the anterior (low level of morphogenesis) is affected and similar to wild type τ_2 levels in the posterior. This could pinpoint the fact that the epithelia disaggregation is a result of trafficking failure of apical components. Live imaging of *D*E-CadGFP in *crb*^{11A22} background revealed initial disaggregation in the anterior part of the embryo, which strengthens the idea that Crb is required for adherens junction stabilisation and maintenance.

D. Results

1. Generating transgenic flies with an exclusively apical marker for live imaging

1.1 Tagging Stranded at Second

Although several protein markers were available amongst the *Drosophila* community, an exclusively apical protein marker was lacking. Therefore, one of the initial goals was to tag such a protein with a fluorophore appropriate for live cell imaging. Stranded at Second (SAS) and Knickkopf (Knk) were selected after literature browsing. However, only the SAS transgenic flies were successful in expressing and giving a fluorescent signal, therefore only the rationale behind its tagging will be explained in this section. A more detailed description of the cloning protocols can be found in the materials and methods section of this thesis.

Stranded at Second is a type I transmembrane protein composed of 1693 aminoacids and it is expressed during germband retraction in ectodermally derived tissues. Its sequence suggests it to be a cell surface protein functioning as a receptor. Mutations in this gene cause the larvae to arrest at second instar and eventually die. Its extracellular region contains 4 tandem repeats of cysteine-rich motifs (von Willebrand factor type C) usually found in procollagen and thrombospondin and 3 copies of fibronectin type III repeats. Its short intracellular domain contains a sequence (NPXY) suggested to be involved in endocytosis via coated pits (Schonbaum et al., 1992); (Figure D1).

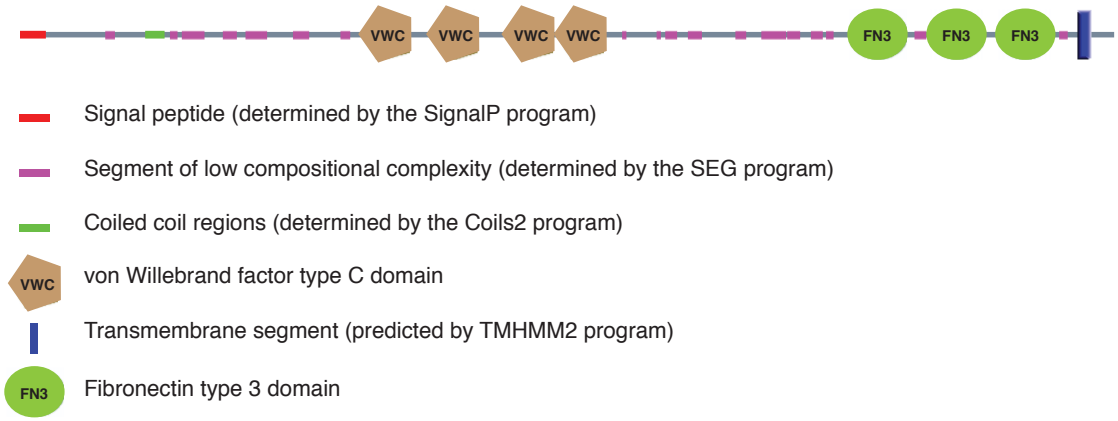

Figure D1 - Protein domains of Stranded at Second (SAS) as determined by SMART (http://smart.embl-heidelberg.de/).

Immunohistochemistry analysis revealed it to be localised strictly in the apical side of embryonic epithelial cells, thus covering the whole apical surface of the epidermis (Wodarz et al., 1995) (Figure D2).

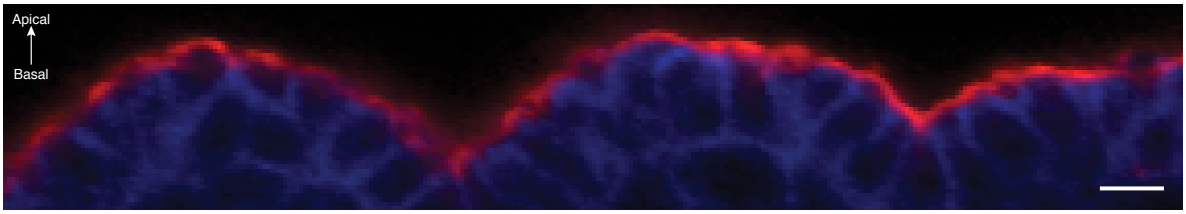

Stranded at Second

Discs Large

Figure D2 – Antibody staining against Stranded at Second and Discs Large of a late stage *Drosophila* embryo. SAS is localised apically whereas Discs Large is basolateral. Scale bar: 5μm.

In order to not affect its structure nor its trafficking sequence signals, a low complexity region of the protein (Figure D3) was replaced by a fluorophore surrounded by linkers composed of 8 glycine residues and 2 serine residues not only to increase protein solubility but to also minimise interferences with the native protein secondary structure, thus allowing for proper folding of the fluorophore (Goldman and Spector, 2005).

Figure D3 – Scheme of Stranded at Second protein. The arrows highlight the low complexity regions of SAS replaced by a suitable fluorophore (green box).

Four different fluorophores were selected - Venus (a derivative from YFP), mCherry (a derivative from RFP), Eos (a green-to-red photoconvertible fluorophore) and PA-GFP (photoactivatable GFP) (Table D1).

Fluorophore	Excitation maximum (nm)	Emission maximum (nm)	*In vivo* structure	Relative brightness (% of EGFP)
mCherry	587	610	Monomer	47
mEos (nonexcited)	505	516	Monomer	128
mEos (excited)	569	581	Monomer	68
PA-GFP	504	517	Monomer	41
Venus	515	528	Monomer	156

Table D1 – Properties of the fluorophores used for cloning SAS. Data retrieved from http://www.microscopyu.com/articles/livecellimaging/fpintro.html.

After tagging Stranded at Second (Figure F7), the gene was placed in two expression vectors suitable for *Drosophila* transgenesis – one with a tubulin promoter for ubiquitous embryonic expression and another with a UAS promoter which allows protein expression in specific tissues and in a specific time window depending on the GAL4 driver used (Brand and Perrimon, 1993) (Figure F8); (Figure F9).

1.2 Analysis of SAS transgenic flies

1.2.1. Antibody stainings of SAS transgenic flies

Antibody stainings were conducted with embryos expressing SAS-Venus. SAS-Venus localised just above *D*E-Cadherin, which proves its exclusively apical localisation. Overexpressing UAS SAS-Venus with an ubiquitous and strong GAL4 driver (DaGAL4) did not cause any morphological or viability defects in the embryos, therefore making it ideal for imaging the apical domain of cells (Figure D4A). Regarding the SAS-Eos transgenic lines, after excitation with a 405 nm laserbeam, a very fast photoconversion of the fluorophore was observed (Figure D4B).

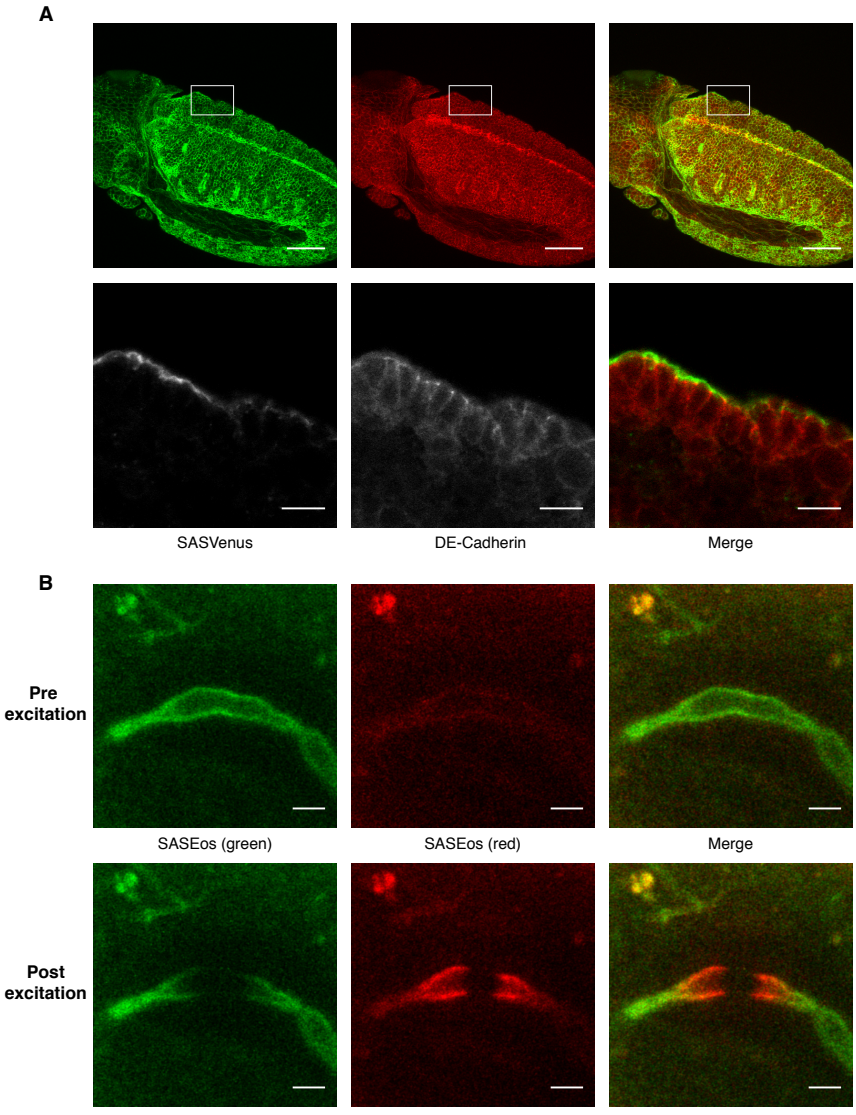

Figure D4 – SAS transgenic lines. (A) *D*E-Cadherin staining in a late GBE DaGAL4 UAS SAS-Venus 2 embryo (Scalebar: 50μm) with corresponding closeups (Scalebar: 10μm). (B) Image stills of Casper SASEos 2 transgenic fly line salivary glands before excitation with 405nm laser and post excitation (Scalebar: 10μm). Note the green to red conversion of Eos around the excited area.

1.2.2. Cuticle preparations of SAS transgenic lines do not show polarity defects

In order to check for possible polarity defects caused by overexpression of SAS, cuticle preparations were done. In all transgenic lines, no polarity defects were detected. All cuticles were uniform without any gaps and had the typical presence of 8 denticle belts in the ventral area of the embryos (Figure D5). As for viability, all transgenic lines were viable even in homozygous conditions.

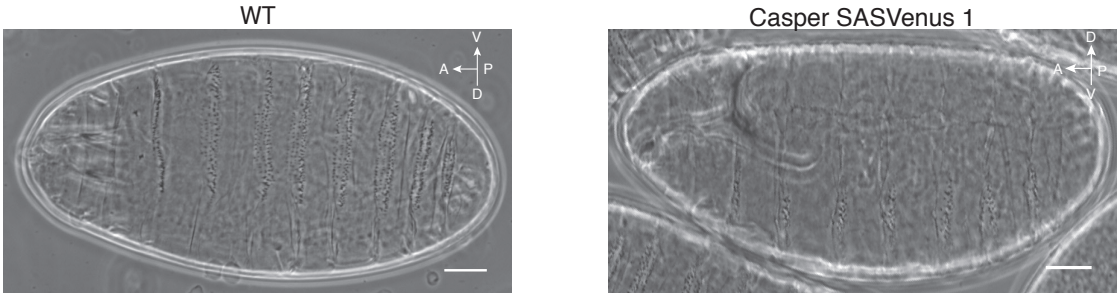

Figure D5 – Cuticle preparations of a wildtype embryo and a pCasper SAS-Venus 1 transgenic embryo. Anterior to the left and dorsal to the top. Scalebar: 50μm.

Together with the data from the antibody stainings, the overexpression of the fluorophore tagged SAS does not cause any embryonic defects and its localisation is strictly apical.

2. FRAP Assay

Initial FRAP experiments were done using a fixed image acquisition rate - every 5 seconds (Cliffe et al., 2004); (Cavey et al., 2008). However, analysis of the obtained FRAP curves showed that a good description of the initial part of the curve was lacking (Figure D6A and A').

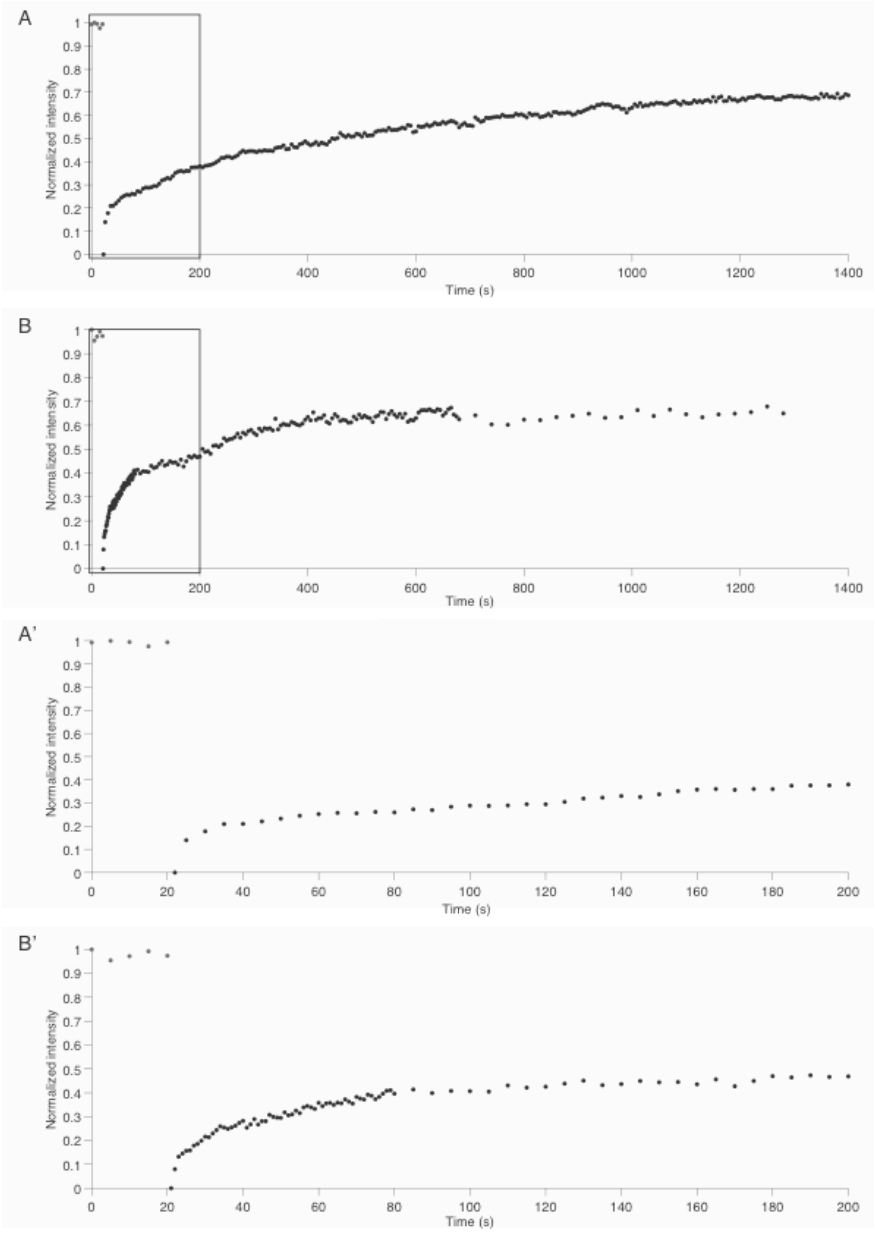

Figure D6 – FRAP recovery curves of two different *D*E-CadherinGFP experiments with different image acquisition rates. (A) Every 5 seconds. (B) Every second for 60 seconds; every 5 seconds for 600 seconds; every 30 seconds for 600 seconds. (A' and B') Closeup of the initial 200 seconds of each corresponding experiment.

2.1 Different image acquisition rates better describe fluorescence recovery

To circumvent this, a FRAP protocol with different image acquisition rates was developed (Figure D7). Initially, 5 images are taken and are interspersed by 5 seconds. Following that, a user defined region is bleached using a 405nm laser beam and immediately afterwards, an image is taken every second for 1 minute. Once this fast phase of acquisition is over, an image is taken every 5 seconds for 10 minutes - medium phase of acquisition - followed by the slow phase where an image is taken every 30 seconds for 10 more minutes. With this method, every experiment lasts 21 minutes and 25 seconds.

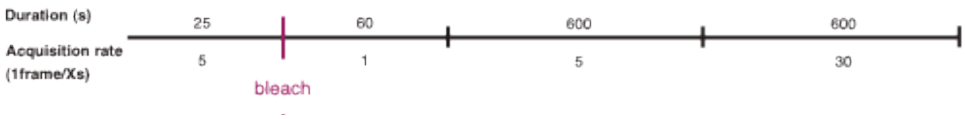

Figure D7 – Imaging protocol adopted for the FRAP assay. Four different image acquisition rates phases take place throughout the experiment – prebleach (1 frame every 5 seconds for 25 seconds); bleach of the user selected region; fast acquisition rate (1 frame every second for 60 seconds); medium acquisition rate (1 frame every 5 seconds for 600 seconds) and slow acquisition rate (1 frame every 30 seconds for 600 seconds).

With the new protocol, a higher time resolution was attained in the initial stages of the recovery thus allowing for a better description of the process (Figure D6B and B'). Another important factor for the usage of the protocol was the viability of the embryos throughout the experiment. They showed no major developmental defects during the duration of a typical experiment. It should also be mentioned, that whilst the bleach was most effective at the imaged optical section of 2µm, the remainder of the z-axis of the cell was equally affected by the bleaching laser, giving rise to partially bleached regions above and below the optical section.

Therefore, it was now possible to follow the fluorescence recovery of several membrane compartment proteins with high temporal resolution, for a determined duration (21minutes and 25 seconds) and without affecting the viability and normal development of the embryos.

2.2 Protein markers used in the FRAP assay

The protein markers used for reporting the behaviour of the different cell compartments were the following: SpiderGFP, which labels the whole membrane; *D*E-CadherinGFP, a marker for the Zonula Adherens; LachesinGFP, a basolateral marker and SAS-Venus, an exclusively apical marker (Figure D8).

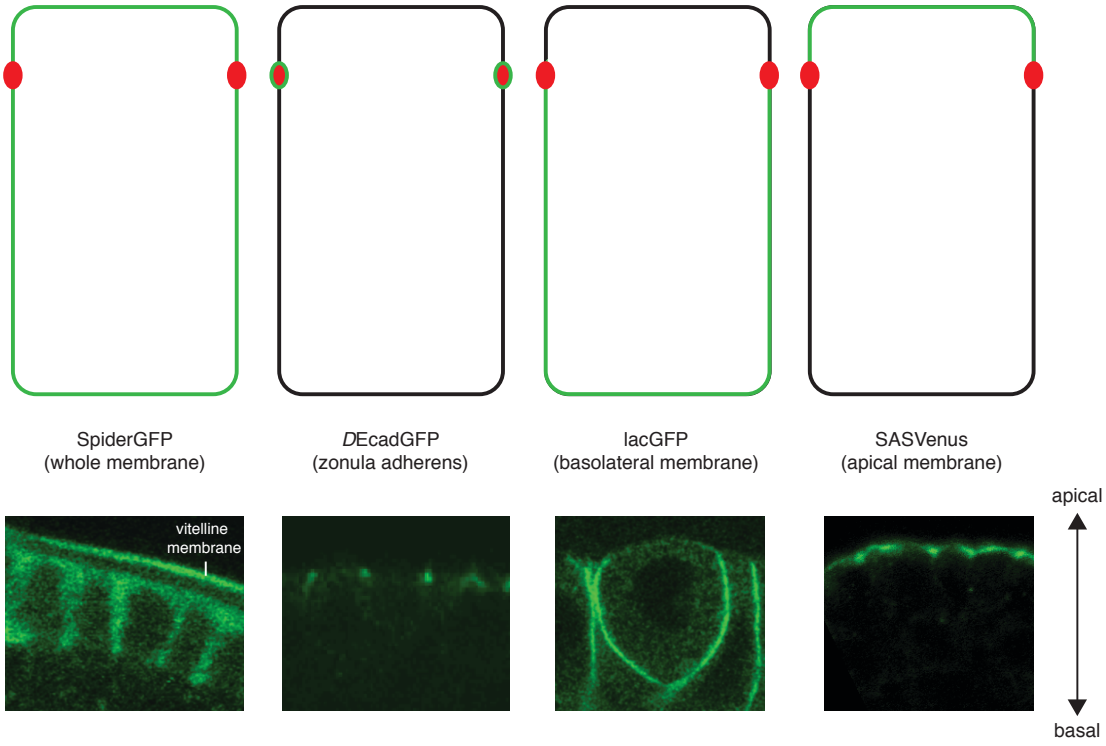

Figure D8 – Image stills of the protein markers used in the FRAP experiments and their schematic representation. The red dots in the schematic epithelia correspond to the Zonula Adherens whereas the green corresponds to the compartment where the marker is localised. All embryos were in early GBE stages of development. Scalebar: 5μm.

All protein markers were subject to the same experimental conditions (Figure D9); (see Example FRAP movies in the DVD).

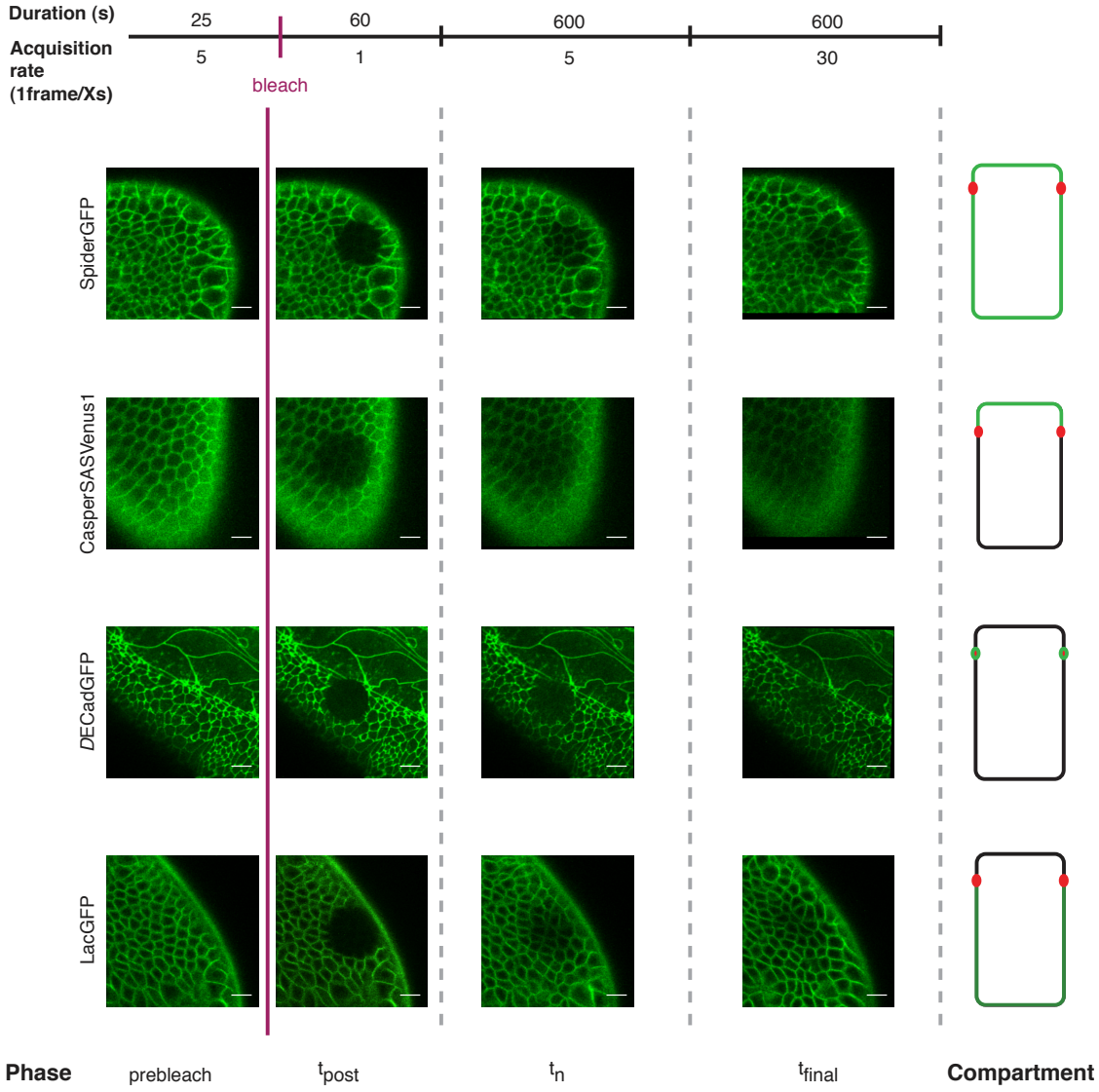

Figure D9 – Image stills of live imaging FRAP movies of all protein markers highlighting the different phases of acquisition during an experiment. Prebleach; first timepoint of the fast phase (t_{post}); medium phase (t_n) and slow phase (t_{final}) On the right side of the figure, a corresponding schematic representation of the cell compartment labeled by the depicted marker. The red dots in the schematic cells correspond to the Zonula Adherens whereas the green corresponds to the compartment where the marker is localised. Note that the markers are not showing the same embryonic regions and stages of development. Scalebar: 10μm.

2.3 Embryo regions imaged in the FRAP assay

In the assay, it was decided to describe the markers' behaviour in different regions of the embryo. This was done to analyse whether the different morphogenetic activities within the embryo would be affecting protein behaviour. If that would be the case, it would also be interesting to assess whether mutations in Crumbs would affect them. Therefore, every FRAP experiment consisted in 2 movies – one done in the anterior (where morphogenesis was not as intense as in the posterior) and the other one in the posterior region where GBE mostly takes place (Figure D10).

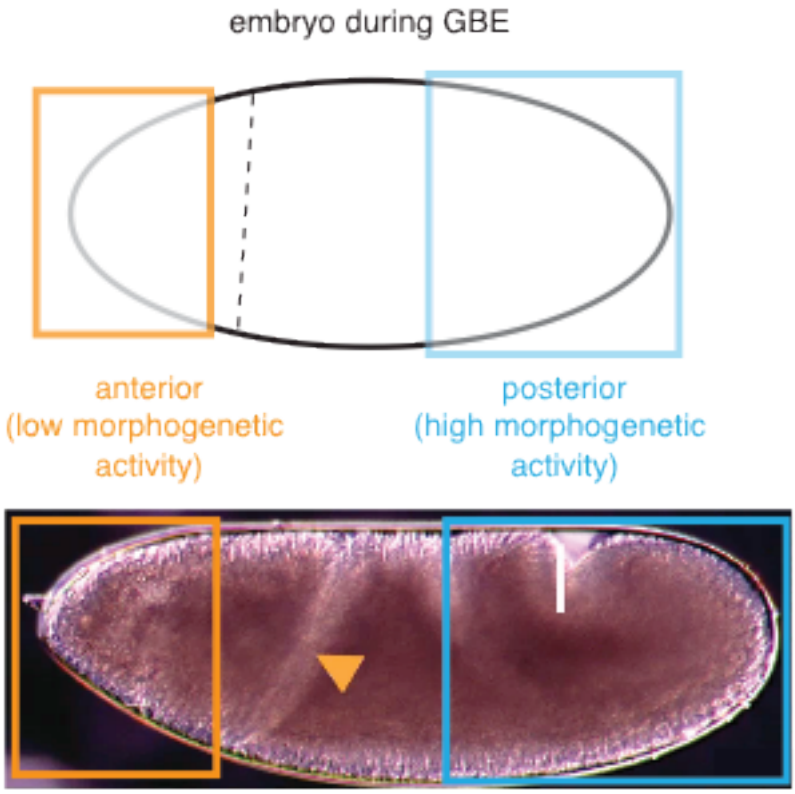

Figure D10 – Scheme highlighting the different regions of the embryo imaged in the FRAP assay with a corresponding image from a live embryo (image taken from FlyMove). The dotted line and arrowhead indicate the cephalic furrow. The anterior region (left) shows low levels of morphogenesis whereas the posterior (right) shows higher levels due to the intensive cell intercalation movements typical of GBE.

2.4 A double exponential fitting curve better describes the raw data

With the help of Dr. Jean-Yves Tinevez it was found that the raw data seemed to define an exponential recovery curve – therefore the initial fits were made using a single exponential equation: $y = A(1 - e^{[(t_0-t_x)/\tau]})$. Despite having high correlation factors (R^2) with the raw data, this fitting curve seemed to have certain problems in describing the initial steepness in recovery. Therefore, a double exponential equation:

$y = A_1(1 - e^{[(t_0-t_x)/\tau_1]}) + A_2(1 - e^{[(t_0-t_x)/\tau_2]})$ was employed to fit the data. This fit showed higher correlation factors and it coped much better with the initial steps of recovery (Figure D11).

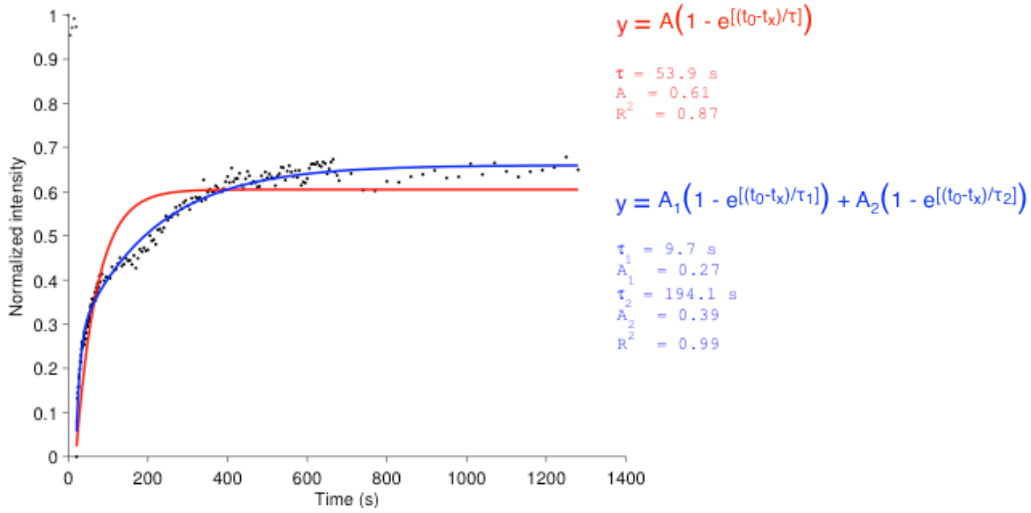

Figure D11 – FRAP recovery curve of a *D*E-CadherinGFP experiment with the newly developed imaging protocol with two different fitting curves and their parameters. Raw data (black); single exponential fitting curve (red) and double exponential fitting curve (blue).

The two components of the equation could indicate the presence of two independent cell processes responsible for fluorescence recovery. Regarding kinetics, the first component had a τ an order of magnitude smaller than the τ of the second component. This reflects the presence of a very fast process responsible for the initial steep increase in fluorescence (showing low kinetic values - τ_1) and a slower second process responsible for the later stages of recovery (showing higher kinetic values - τ_2) (Figure D11).

Once all double exponential fitting curves were obtained from all FRAP experiments, a statistical analysis of all parameters was performed with the use of a MATLAB script developed by Dr. Jean-Yves Tinevez (see attached DVD). This would allow not only for proper quantification of the parameters (A_1, A_2, τ_1 and τ_2) but also the identification of possible differences in the different areas of the embryos where the experiments were performed (anterior vs. posterior).

2.5 FRAP Assay Data

2.5.1. Mobile fraction values of the different markers in wildtype conditions

The mobile fraction parameter refers to the amount of fluorophore employed in the recovery of fluorescence.

2.5.1.1. SpiderGFP

A_1 and A_2 show no apparent difference between the anterior and posterior of the embryo. However, A_2 mean values tend to be higher when compared to A_1 Figure D12).

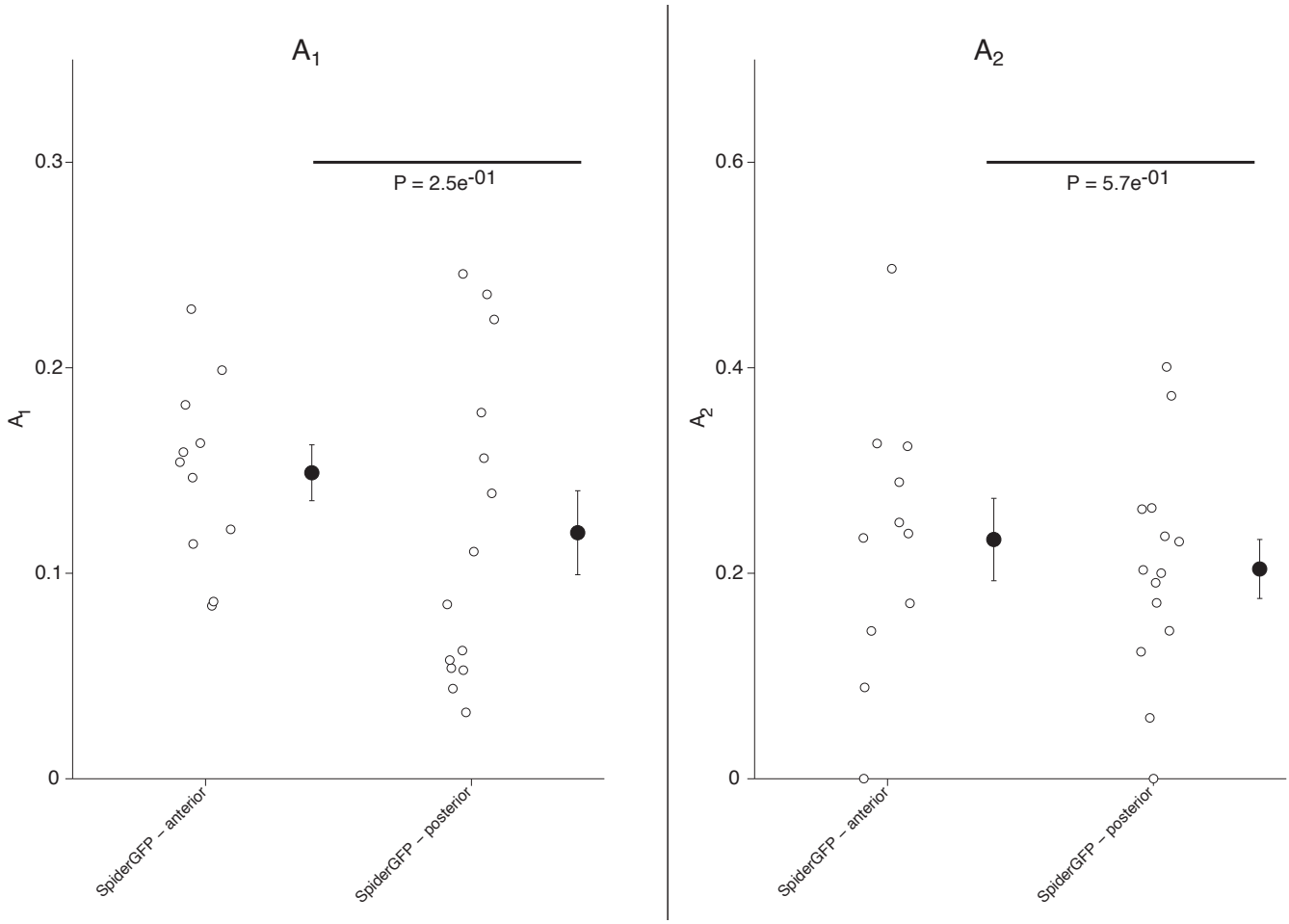

Figure D12 – Mobile fractions (A_1 and A_2) of anterior and posterior areas of SpiderGFP embryos. Open circles refer to the values obtained from the fitting curves. P-values and mean and error bars in black.

2.5.1.2. *D*E-CadherinGFP (homozygous and heterozygous conditions)

Experiments with *D*E-CadherinGFP were performed in two genetic conditions (homozygosity and heterozygosity) to test whether this would cause a recovery effect but also to be able to compare with future results obtained in the crb^{11A22} background.

Regarding A_1 mean values, there is no difference between the anterior and posterior of the embryo in both genetic conditions. A_2 mean values do show, however, a difference in homozygous conditions in the posterior. It should be noted, though, that this might not hold true once more movies in the posterior are performed and taken into account. As for their mean values, A_1 and A_2 seem to be comparable in heterozygous conditions whereas in homozygous conditions, A_2 mean values tend to be higher when compared to A_1 (Figure D13); (Figure D14).

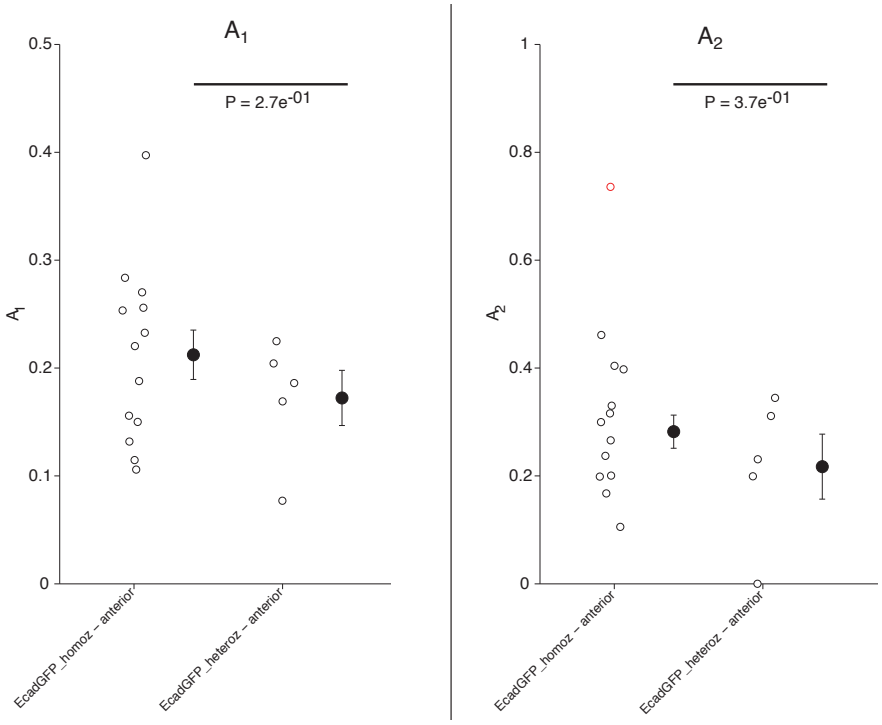

Figure D13 – Mobile fractions (A_1 and A_2) of anterior areas of *D*E-CadherinGFP embryos. Open circles refer to the values obtained from the fitting curves. P-values and mean and error bars in black. Open circles in red refer to outliers as determined by the MATLAB script.

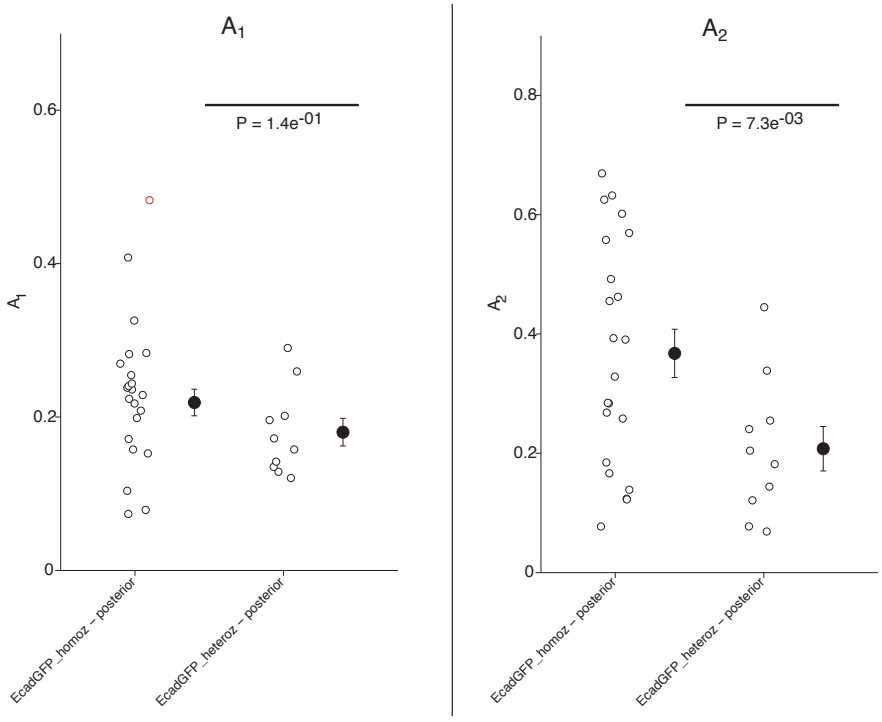

Figure D14– Mobile fractions (A_1 and A_2) of posterior areas of *D*E-CadherinGFP embryos Open circles refer to the values obtained from the fitting curves. P-values and mean and error bars in black. Open circles in red refer to outliers as determined by the MATLAB script.

2.5.1.3. LachesinGFP

There is no difference between the anterior and posterior of the embryo. As for their mean values, A_1 and A_2 seem to be comparable (Figure D15).

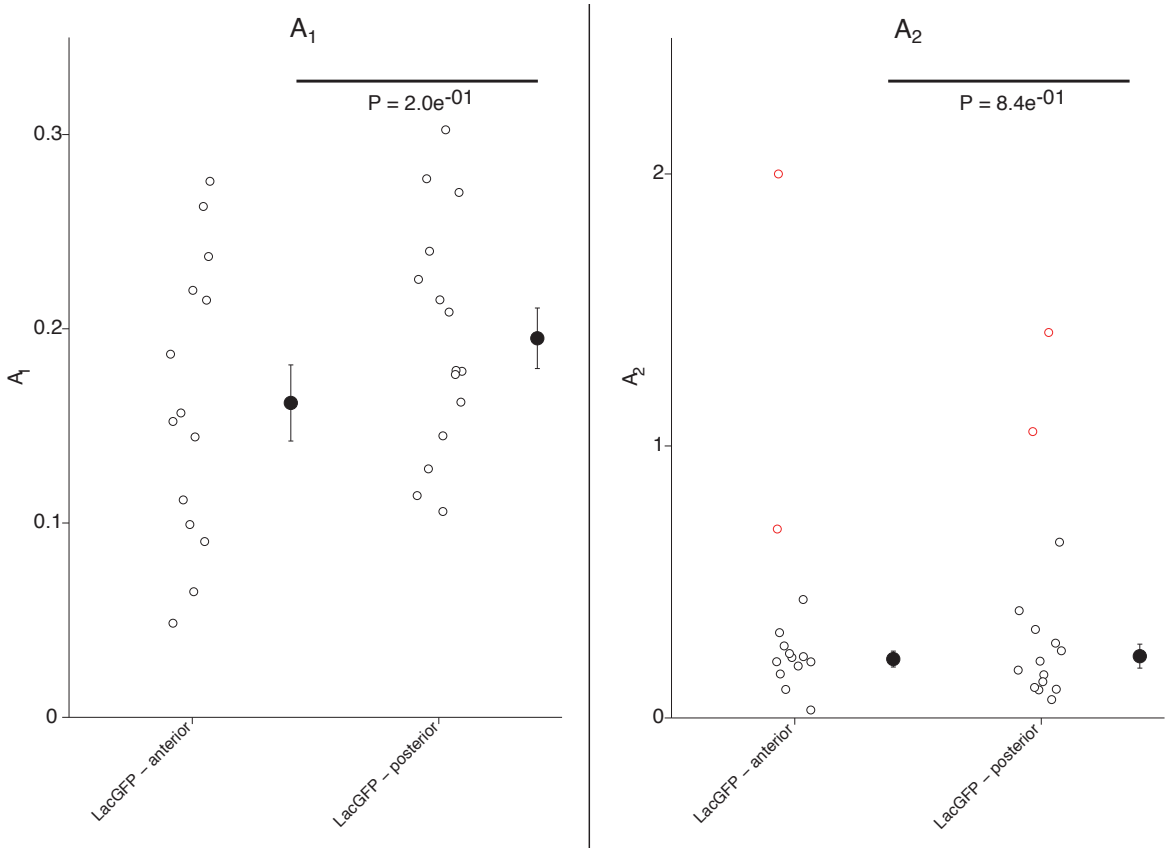

Figure D15 – Mobile fractions (A_1 and A_2) of anterior and posterior areas of LachesinGFP embryos. Open circles refer to the values obtained from the fitting curves. P-values and mean and error bars in black. Open circles in red refer to outliers as determined by the MATLAB script.

2.5.1.4. SAS-Venus

Experiments with SAS-Venus were performed using two different fly lines – pCasperSAS-Venus1 (where SAS-Venus expression is controlled by a tubulin promoter, thus making it expressed in all tissues but in low levels) and UAS SAS-Venus2 (where UAS SAS-Venus2 was crossed to DaGAL4, a driver that is strongly expressed early in embryogenesis and in every tissue). These two different fly lines were used to test the influence of SAS-Venus overexpression in the kinetics of recovery – whereas pCasperSAS-Venus was slightly overexpressed, UAS SAS-Venus2 crossed to DaGAL4 is much more overexpressed.

Regarding A_1, in both fly lines there appears to be no significant difference between the anterior and posterior of the embryo. However, A_2 mean values do show a difference between anterior and posterior. Interestingly, these differences seem to be the opposite in both fly lines – in pCasperSAS-Venus1, the posterior A_2 levels are higher than the anterior, whereas in DaGAL4 UAS SAS-Venus2, the anterior A_2 levels are higher than the posterior. It should be noted though, that the amount of movies in the pCasperSAS-Venus1 might not be sufficient to make a definite conclusion.

A_1 mean values are higher than A_2 mean values in pCasperSAS-Venus1. In DaGAL4 SAS-Venus2 that is not the case – A_1 is comparable to A_2 in the anterior whereas in the posterior we observe a difference: A_1 is higher than A_2 (Figure D16); (Figure D17).

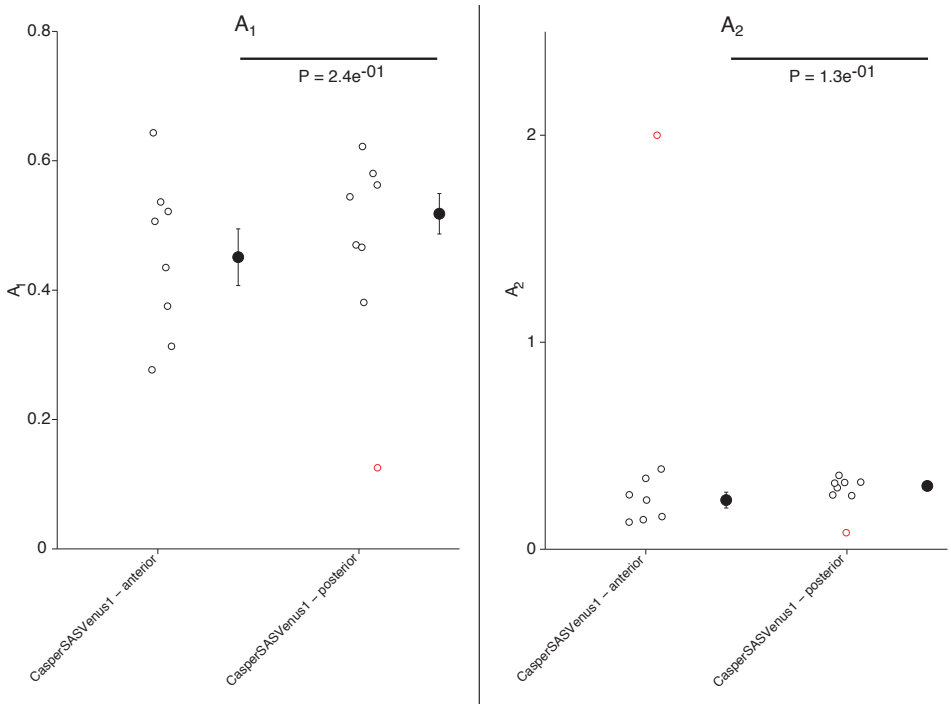

Figure D16 – Mobile fractions (A_1 and A_2) of anterior and posterior areas of pCasperSAS-Venus1 embryos. Open circles refer to the values obtained from the fitting curves. P-values and mean and error bars in black. Open circles in red refer to outliers as determined by the MATLAB script.

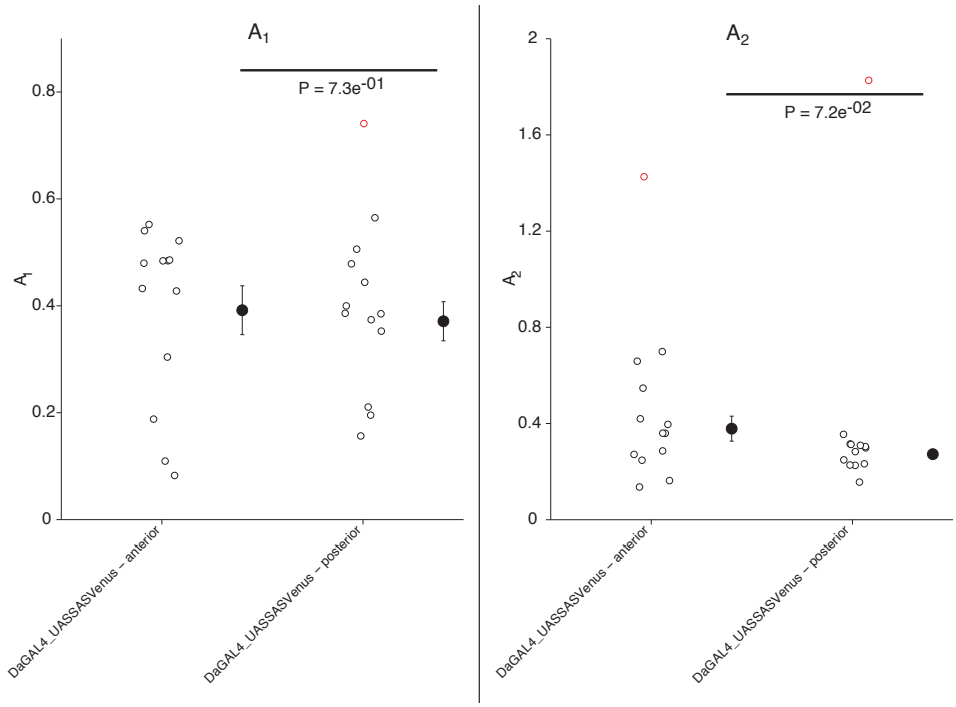

Figure D17 – Mobile fractions (A_1 and A_2) of anterior and posterior areas of DaGAL4 UAS SAS-Venus2 embryos. Open circles refer to the values obtained from the fitting curves. P-values and mean and error bars in black. Open circles in red refer to outliers as determined by the MATLAB script.

2.5.2. Mobile fraction values summary

Regarding differences in mobile fraction mean values in the anterior and posterior areas of the embryo, A_1 does not show any significant differences. A_2, however, seems to differ in *D*E-Cadherin homozygous conditions and in both SAS-Venus fly lines. In these cases, the posterior values are higher than the anterior values except in DaGAL4 SAS-Venus2 where the opposite occurs.

Regarding mobile fraction mean values, A_2 is higher than A_1 in SpiderGFP and *D*E-CadherinGFP homozygous whereas in pCasper SAS-Venus1 the reverse is observed. For LachesinGFP and *D*E-CadherinGFP heterozygous conditions, there appears to be no significant difference between both fractions. DaGAL4 SAS-Venus2 is a special case where, A_1 and A_2 are comparable in the anterior, however in the posterior, A_1 is higher than A_2 (Table D2); (Table D3); (Table D4); (Table D5).

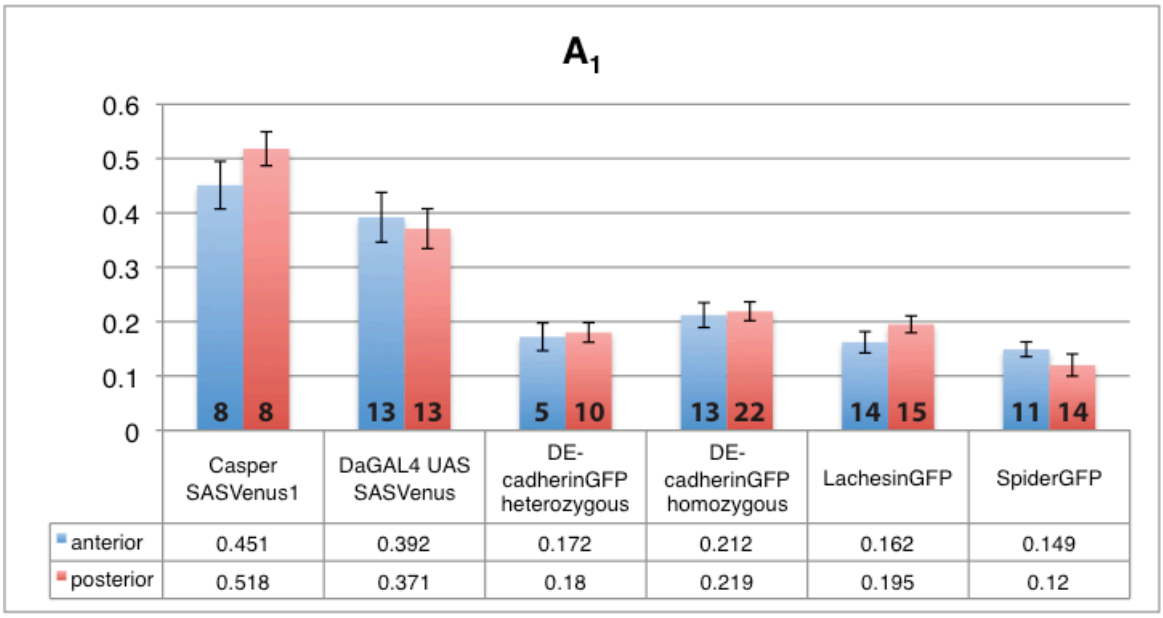

	Casper SASVenus1	DaGAL4 UAS SASVenus	DE-cadherinGFP heterozygous	DE-cadherinGFP homozygous	LachesinGFP	SpiderGFP
anterior	0.451	0.392	0.172	0.212	0.162	0.149
posterior	0.518	0.371	0.18	0.219	0.195	0.12

Table D2 –A_1 mean values with corresponding error bars in both anterior and posterior regions of the embryo. All membrane markers and their different conditions are shown. Numbers in the bottom of each bar refer to the number of movies analysed.

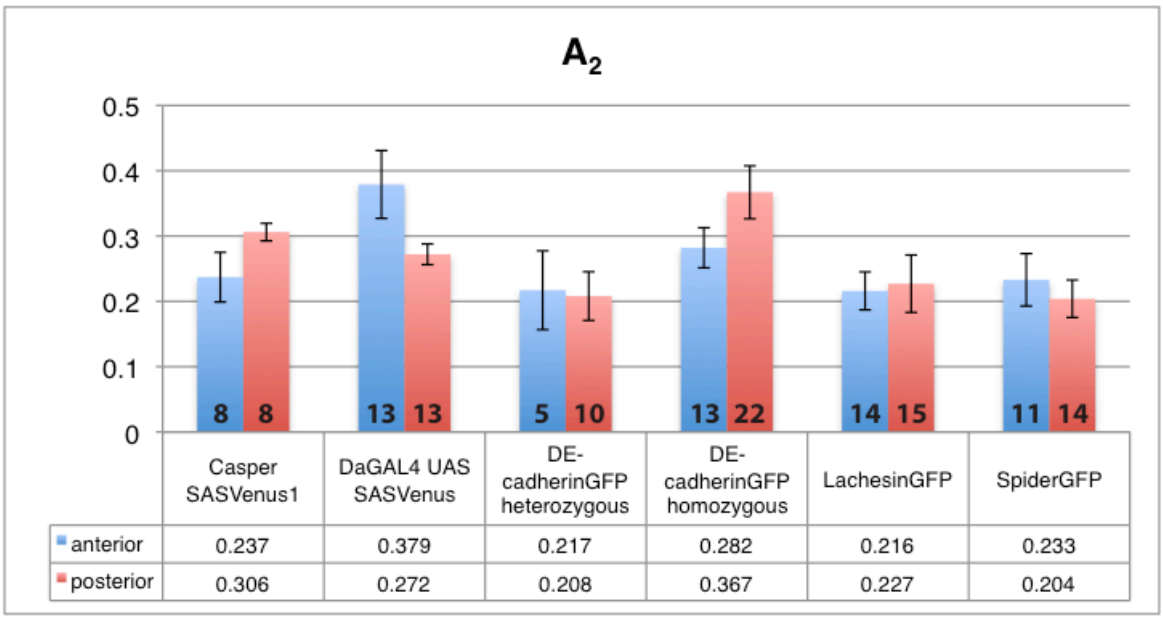

	Casper SASVenus1	DaGAL4 UAS SASVenus	DE-cadherinGFP heterozygous	DE-cadherinGFP homozygous	LachesinGFP	SpiderGFP
anterior	0.237	0.379	0.217	0.282	0.216	0.233
posterior	0.306	0.272	0.208	0.367	0.227	0.204

Table D3 –A_2 mean values with corresponding error bars in both anterior and posterior regions of the embryo. All membrane markers and their different conditions are shown. Numbers in the bottom of each bar refer to the number of movies analysed.

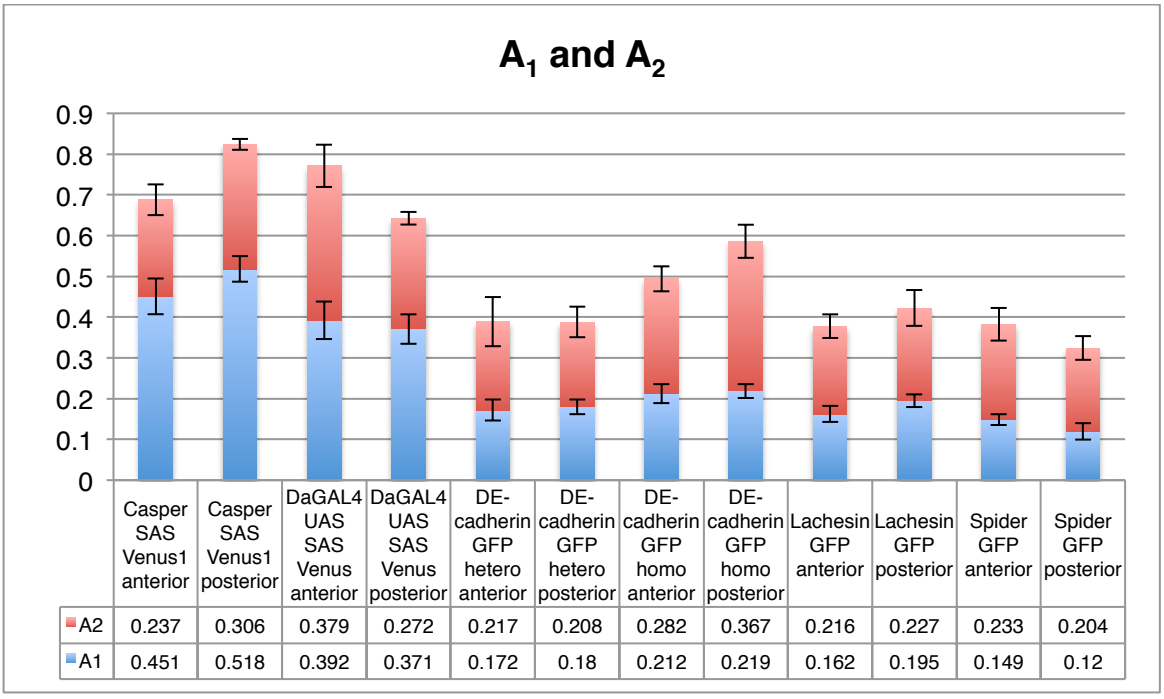

	Casper SAS Venus1 anterior	Casper SAS Venus1 posterior	DaGAL4 UAS SAS Venus anterior	DaGAL4 UAS SAS Venus posterior	DE-cadherin GFP hetero anterior	DE-cadherin GFP hetero posterior	DE-cadherin GFP homo anterior	DE-cadherin GFP homo posterior	Lachesin GFP anterior	Lachesin GFP posterior	Spider GFP anterior	Spider GFP posterior
A2	0.237	0.306	0.379	0.272	0.217	0.208	0.282	0.367	0.216	0.227	0.233	0.204
A1	0.451	0.518	0.392	0.371	0.172	0.18	0.212	0.219	0.162	0.195	0.149	0.12

Table D4 – A_1 and A_2 mean values combined with corresponding error bars in both anterior and posterior regions of the embryo. All membrane markers and their different conditions are shown.

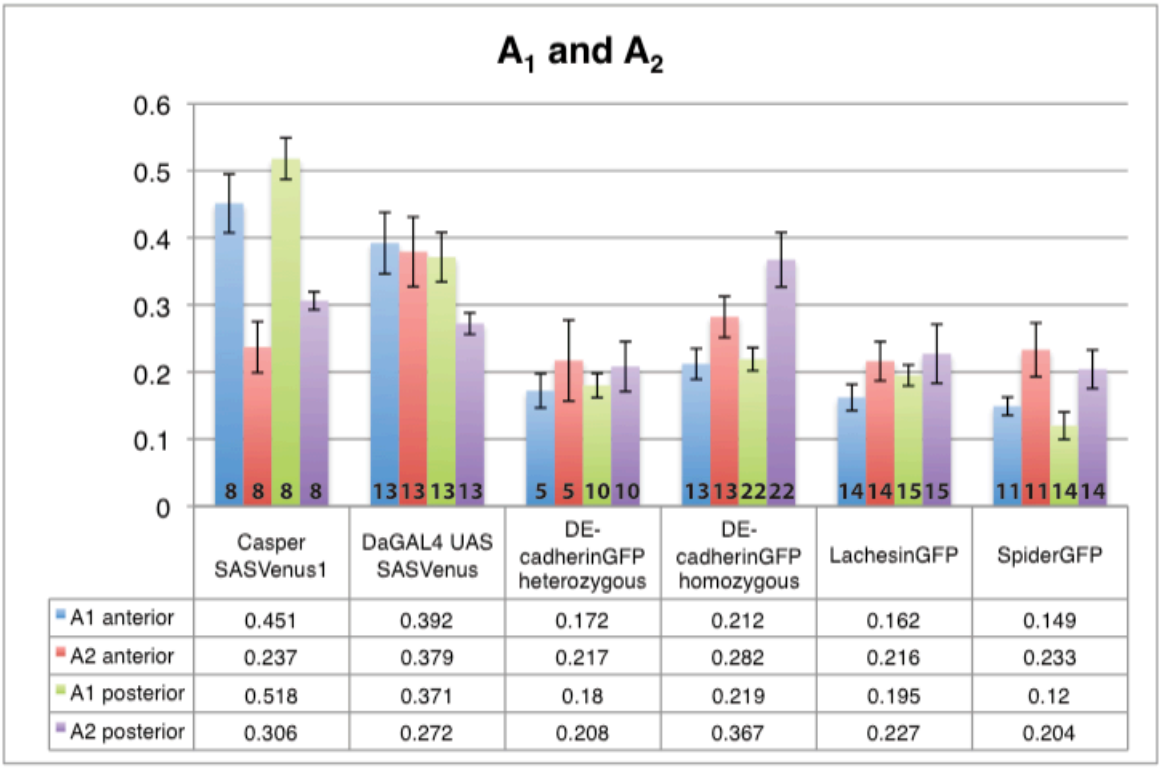

	Casper SASVenus1	DaGAL4 UAS SASVenus	DE-cadherinGFP heterozygous	DE-cadherinGFP homozygous	LachesinGFP	SpiderGFP
A1 anterior	0.451	0.392	0.172	0.212	0.162	0.149
A2 anterior	0.237	0.379	0.217	0.282	0.216	0.233
A1 posterior	0.518	0.371	0.18	0.219	0.195	0.12
A2 posterior	0.306	0.272	0.208	0.367	0.227	0.204

Table D5 –A_1 and A_2 mean values with corresponding error bars in both anterior and posterior regions of the embryo. All membrane markers and their different conditions are shown. Numbers in the bottom of each bar refer to the number of movies analysed.

2.5.3. Kinetic (τ_1 and τ_2) values of the different markers in wildtype conditions

These parameters reflect the 2-step protein recovery kinetics – low values mean that the protein was faster in its recovery while high values mean the opposite. It is an essential parameter to determine how dynamic a protein is. It should be noted that for all markers the mean values of τ_2 are an order of magnitude higher that of τ_1.

2.5.3.1. SpiderGFP

There is a clear difference in the mean values of τ_1 and τ_2 in the anterior and posterior of the embryos - the recovery is faster in the posterior since its τ mean values are lower (Figure D18).

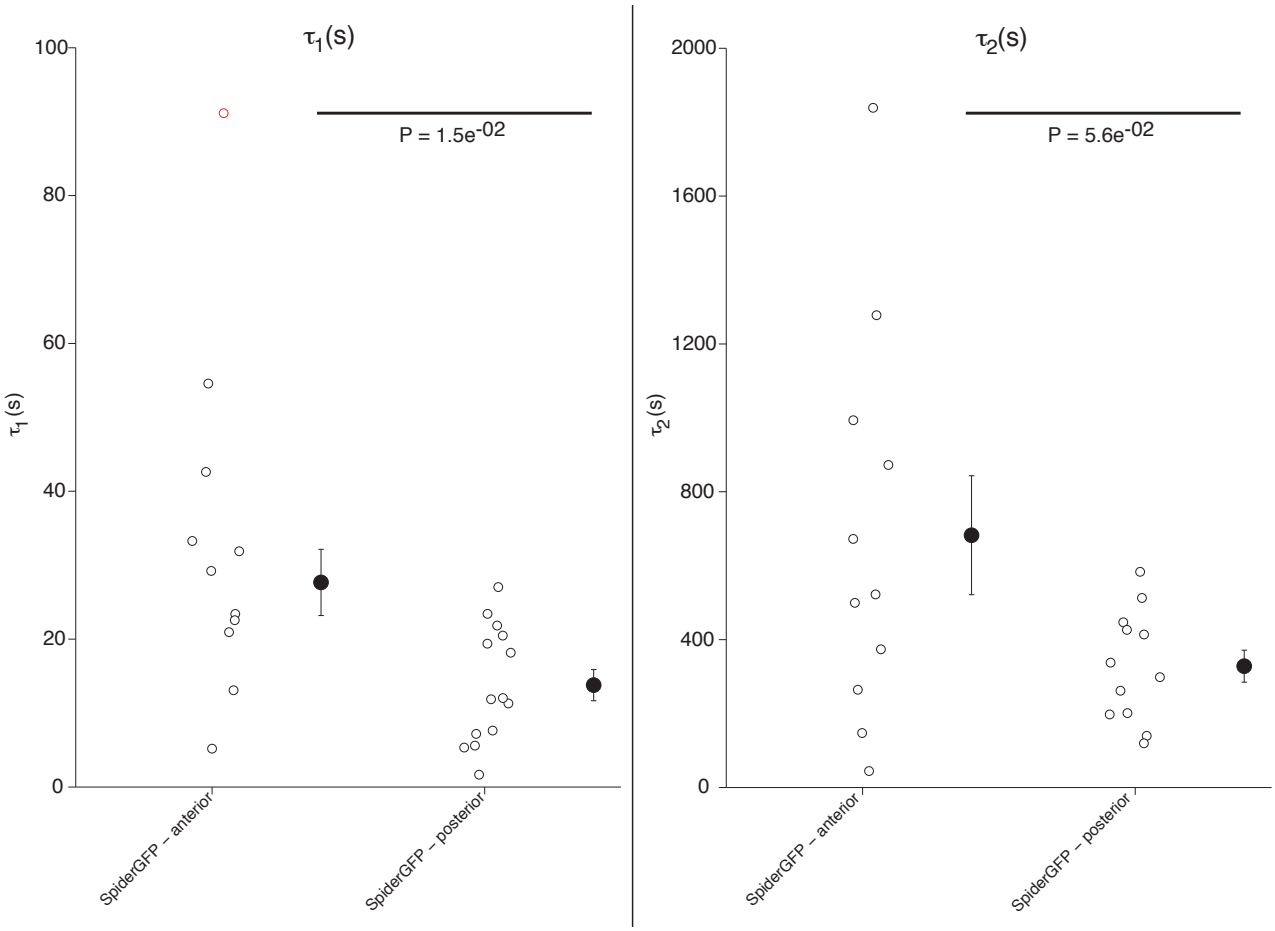

Figure D18 – Kinetic parameters (τ_1 and τ_2) of anterior and posterior areas of SpiderGFP embryos. Open circles refer to the values obtained from the fitting curves. P-values and mean and error bars in black. Open circles in red refer to outliers as determined by the MATLAB script.

2.5.3.2. *D*E-CadherinGFP (homozygous)

There is no difference between the mean values of τ_1 and τ_2 in the anterior and posterior of the embryo (Figure D19).

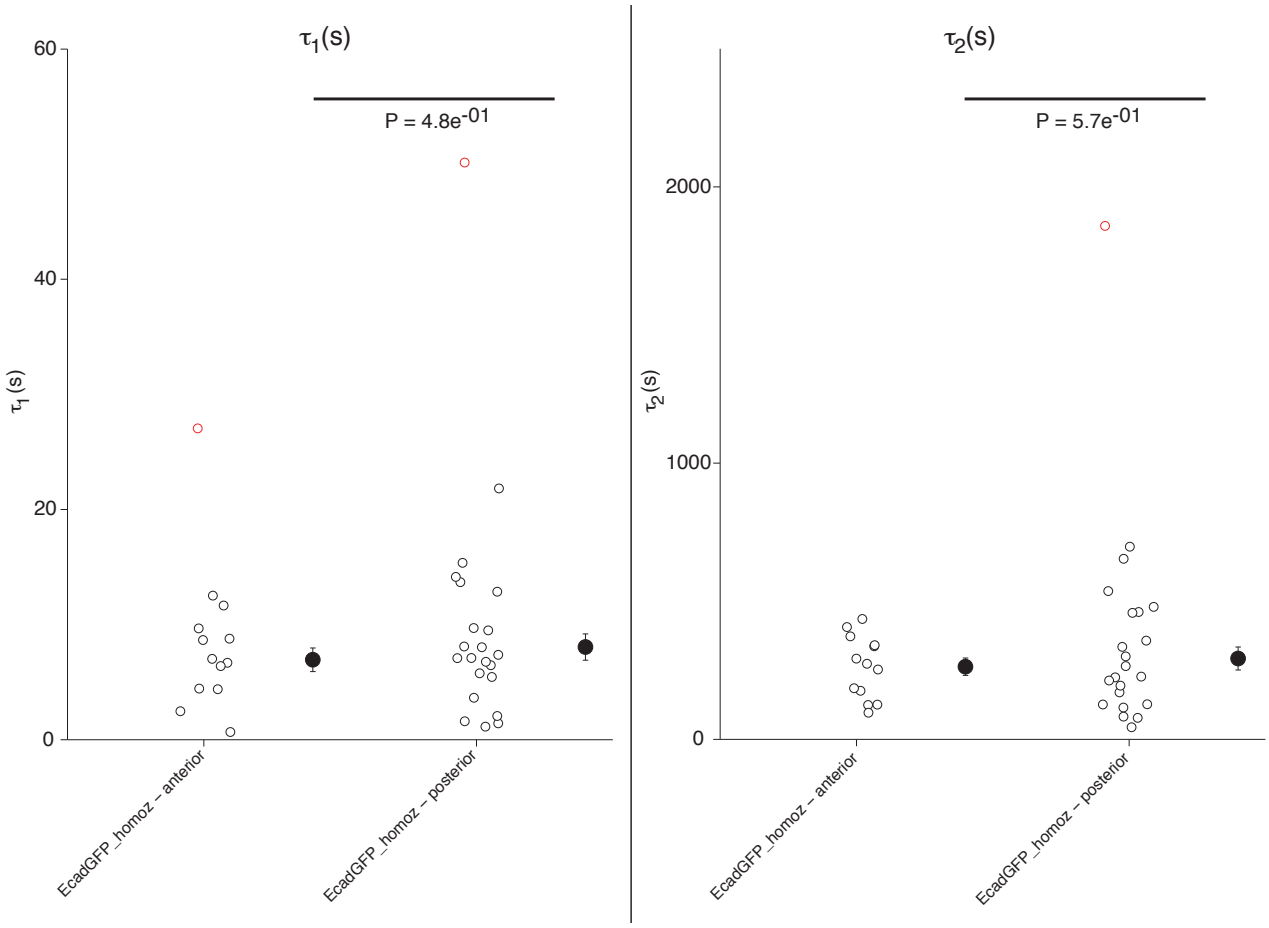

Figure D19 – Kinetic parameters (τ_1 and τ_2) of anterior and posterior areas of *D*E-CadherinGFP homozygous embryos. Open circles refer to the values obtained from the fitting curves. P-values and mean and error bars in black. Open circles in red refer to outliers as determined by the MATLAB script.

2.5.3.3. *D*E-CadherinGFP (heterozygous)

The mean values of τ_1 seem to be higher in the anterior of the embryo when compared to the posterior. However, it should be noted that the amount of data in the anterior might not be enough to draw significant conclusions and may lead to erroneous findings. With more movies it might be possible that this difference disappears since two of the datapoints in the τ_1 are clearly higher than the others, thus affecting the spread of the data. There is no difference between the mean values of τ_2 in the anterior and posterior of the embryo (Figure D20).

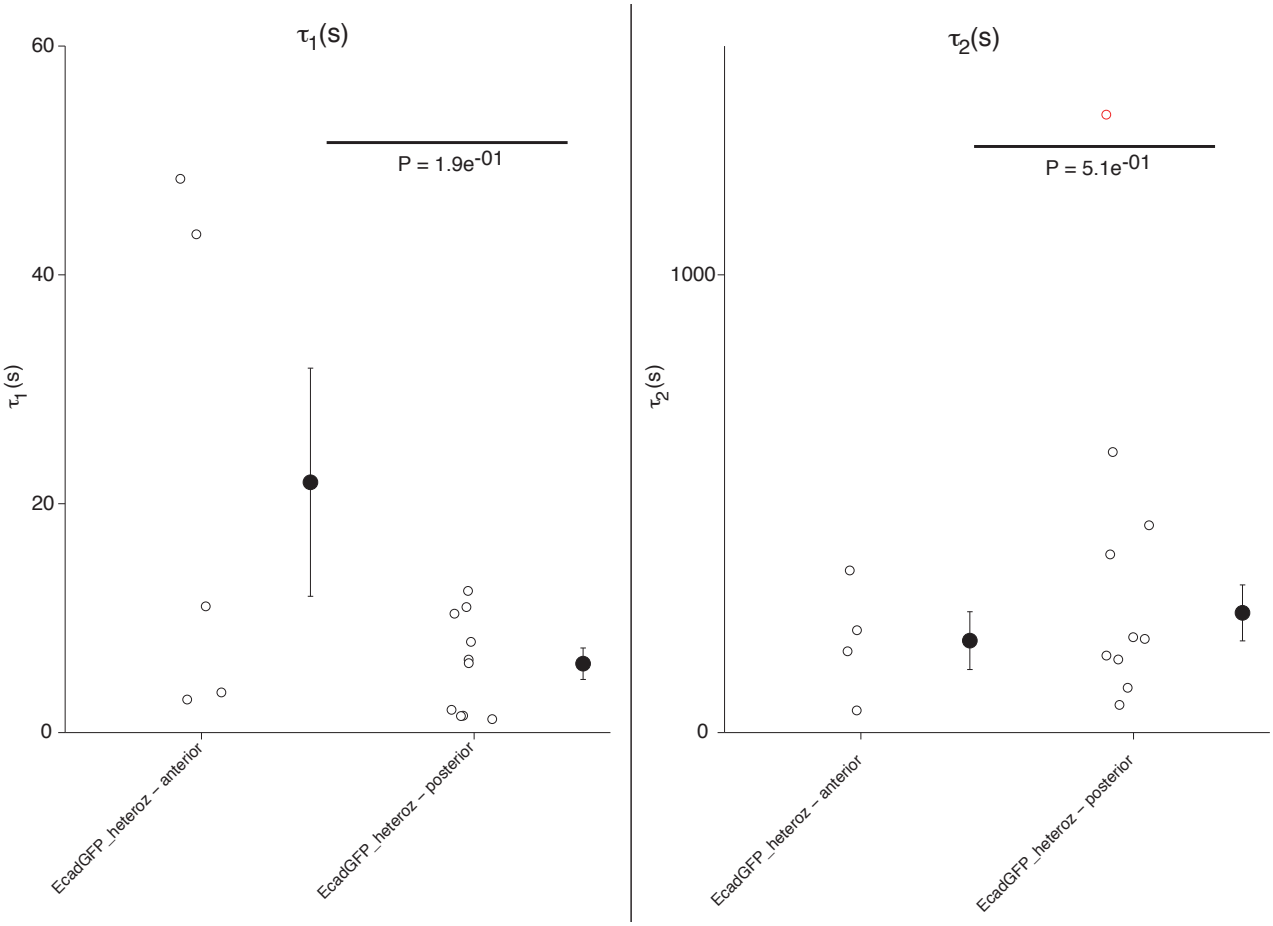

Figure D20 – Kinetic parameters (τ_1 and τ_2) of anterior and posterior areas of *D*E-CadherinGFP heterozygous embryos. Open circles refer to the values obtained from the fitting curves. P-values and mean and error bars in black. Open circles in red refer to outliers as determined by the MATLAB script.

2.5.3.4. LachesinGFP

There is no difference between the mean values of τ_1 and τ_2 in the anterior and posterior of the embryo (Figure D21).

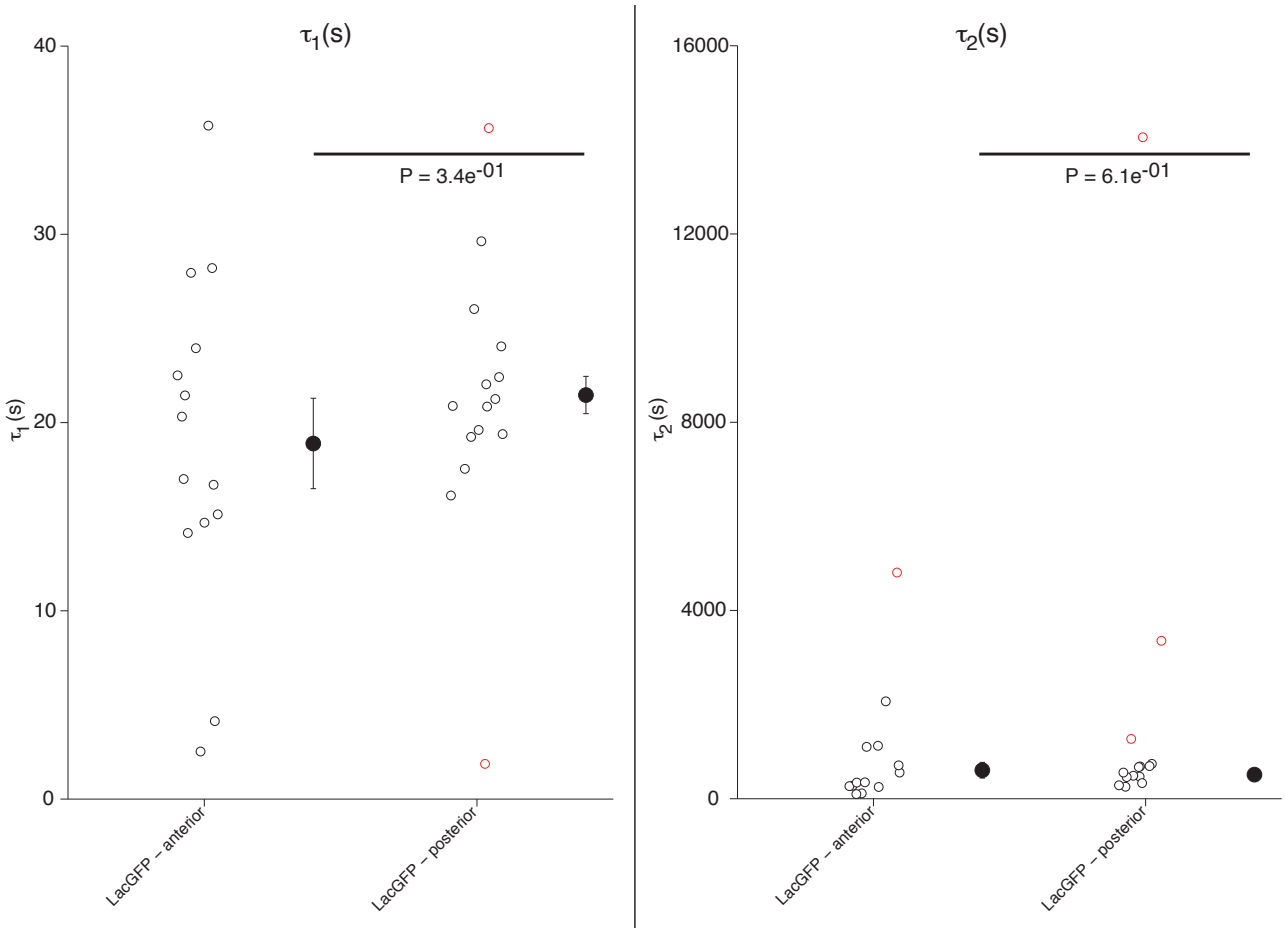

Figure D21 – Kinetic parameters (τ_1 and τ_2) of anterior and posterior areas of LachesinGFP embryos. Open circles refer to the values obtained from the fitting curves. P-values and mean and error bars in black. Open circles in red refer to outliers as determined by the MATLAB script.

2.5.3.5. pCasper SAS-Venus1

There is no difference between the mean values of τ_1 and τ_2 in the anterior and posterior of the embryo (Figure D22).

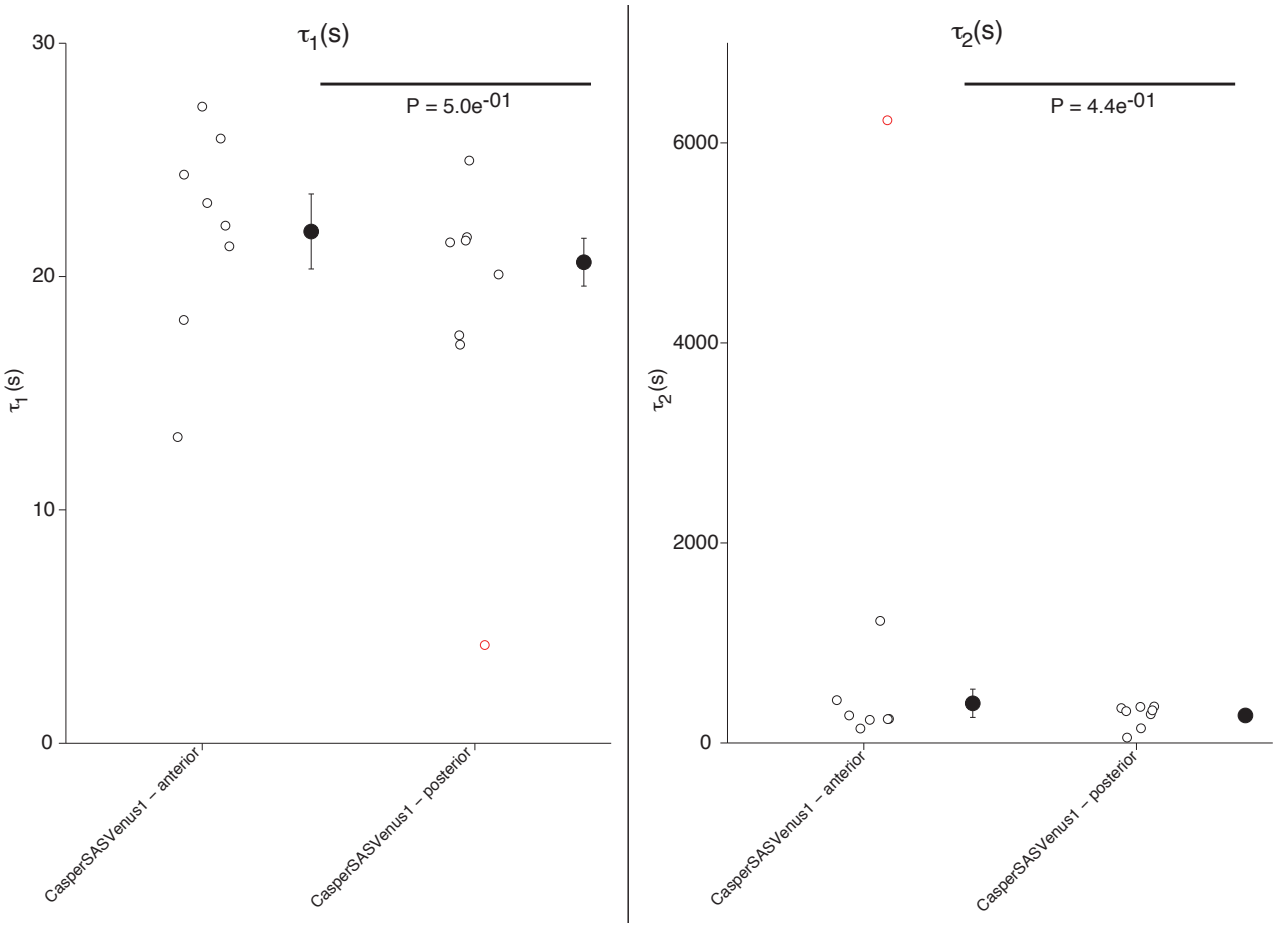

Figure D22 – Kinetic parameters (τ_1 and τ_2) of anterior and posterior areas of pCasper SAS-Venus1 embryos. Open circles refer to the values obtained from the fitting curves. P-values and mean and error bars in black. Open circles in red refer to outliers as determined by the MATLAB script.

2.5.3.6. DaGAL4 UAS SAS-Venus2

There is no difference between the mean values of τ_1 in the anterior and posterior of the embryo. The mean values of τ_2 seem to be higher in the anterior of the embryo when compared to the posterior (Figure D23).

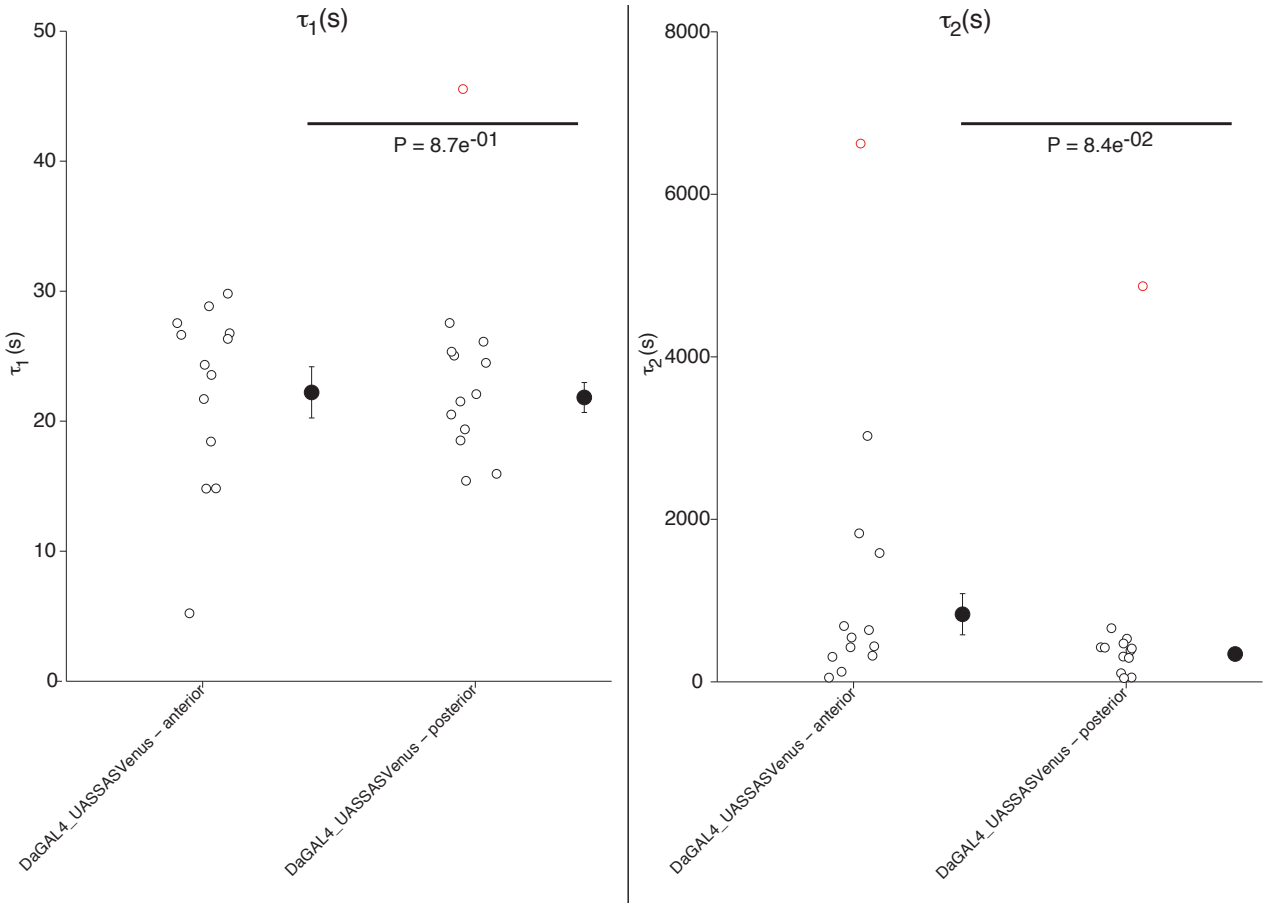

Figure D23 – Kinetic parameters (τ_1 and τ_2) of anterior and posterior areas of DaGAL4 UAS SAS-Venus2 embryos. Open circles refer to the values obtained from the fitting curves. P-values and mean and error bars in black. Open circles in red refer to outliers as determined by the MATLAB script.

2.5.4. Kinetic values summary

Regarding differences between anterior and posterior regions of the embryo, τ_1 does not differ in all markers except SpiderGFP and *D*E-Cadherin heterozygous, though in the latter, the number of movies analysed in the anterior might not be enough for a definitive conclusion. In these cases, the anterior values are higher than the posterior values. As for τ_2, SpiderGFP and DaGAL4 UAS SAS-Venus2 show higher values in the anterior.

For all conditions, τ_2 mean values are an order of magnitude higher than τ_1 (Table D6); (Table D7); (Table D8).

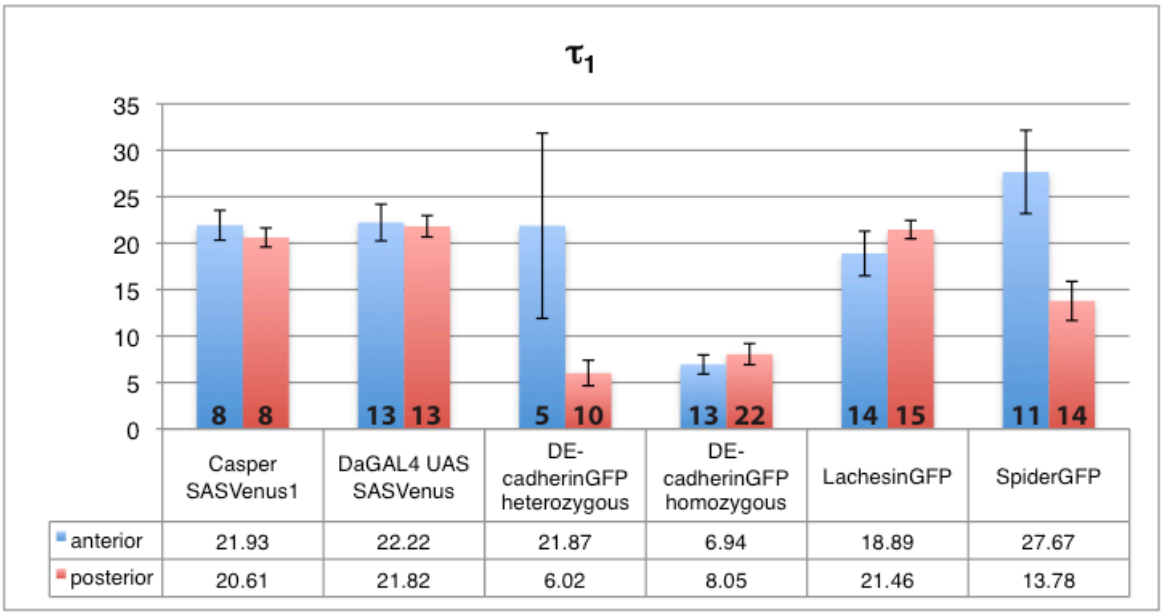

	Casper SASVenus1	DaGAL4 UAS SASVenus	DE-cadherinGFP heterozygous	DE-cadherinGFP homozygous	LachesinGFP	SpiderGFP
anterior	21.93	22.22	21.87	6.94	18.89	27.67
posterior	20.61	21.82	6.02	8.05	21.46	13.78

Table D6 – τ_1 mean values with corresponding error bars in both anterior and posterior regions of the embryo. All membrane markers and their different conditions are shown. Numbers in the bottom of each bar refer to the number of movies analysed.

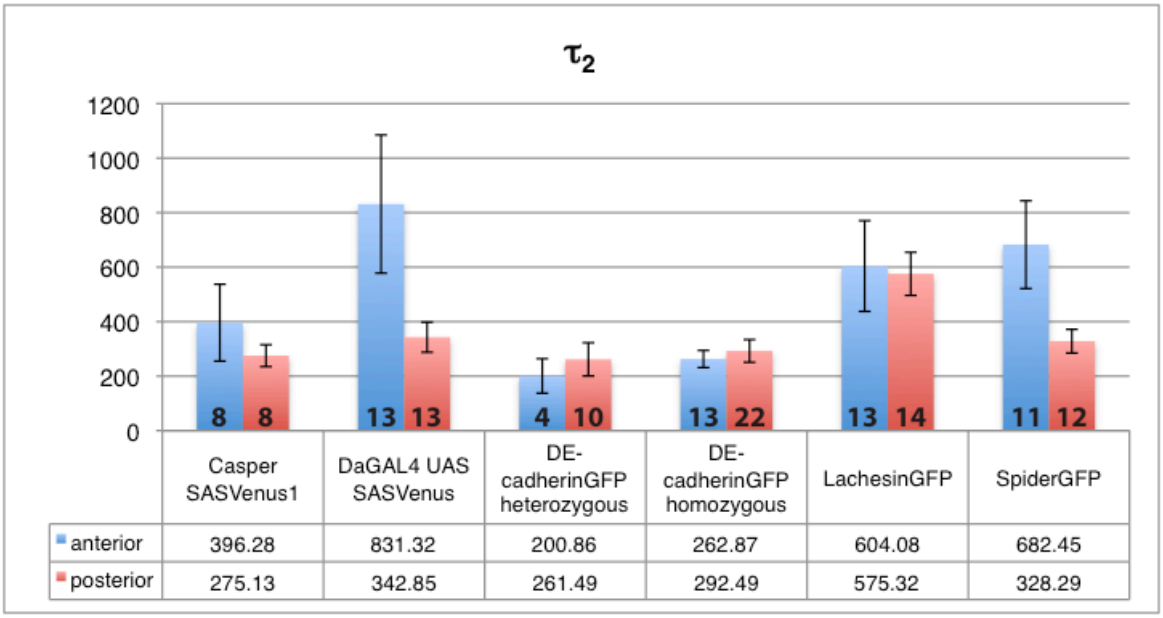

	Casper SASVenus1	DaGAL4 UAS SASVenus	DE-cadherinGFP heterozygous	DE-cadherinGFP homozygous	LachesinGFP	SpiderGFP
anterior	396.28	831.32	200.86	262.87	604.08	682.45
posterior	275.13	342.85	261.49	292.49	575.32	328.29

Table D7 – τ_2 mean values with corresponding error bars in both anterior and posterior regions of the embryo. All membrane markers and their different conditions are shown. Numbers in the bottom of each bar refer to the number of movies analysed.

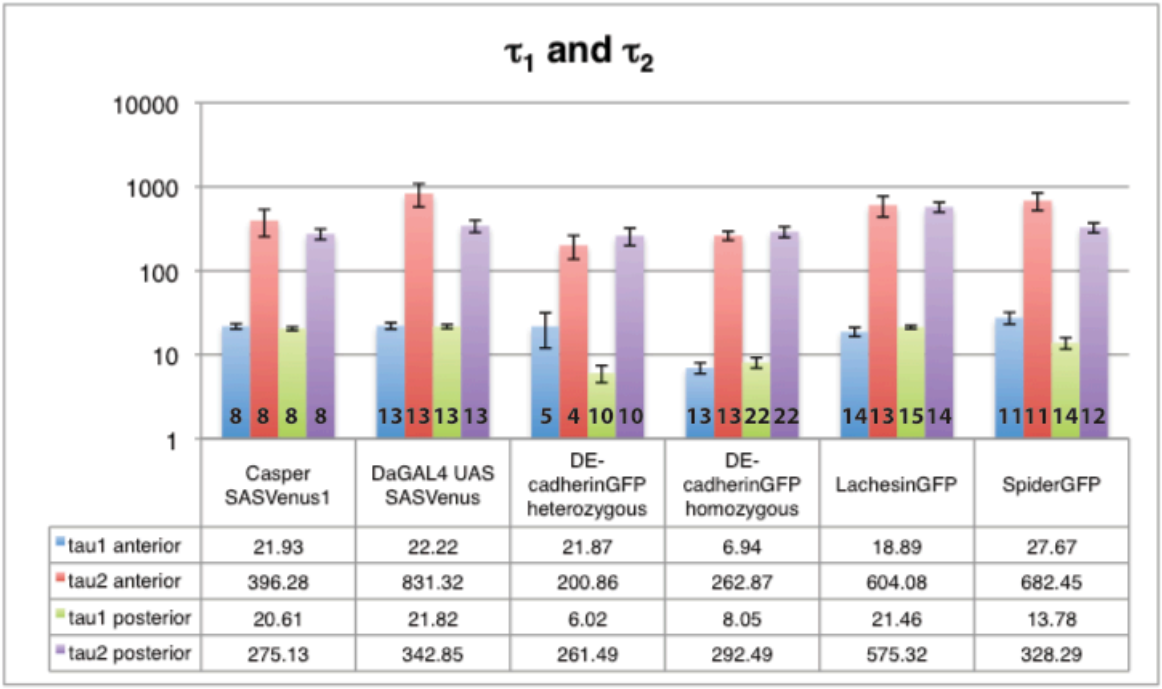

	Casper SASVenus1	DaGAL4 UAS SASVenus	DE-cadherinGFP heterozygous	DE-cadherinGFP homozygous	LachesinGFP	SpiderGFP
tau1 anterior	21.93	22.22	21.87	6.94	18.89	27.67
tau2 anterior	396.28	831.32	200.86	262.87	604.08	682.45
tau1 posterior	20.61	21.82	6.02	8.05	21.46	13.78
tau2 posterior	275.13	342.85	261.49	292.49	575.32	328.29

Table D8 – τ_1 and τ_2 mean values with corresponding error bars in both anterior and posterior regions of the embryo. For a better representation of the data, the y-axis is in logarithmic scale. All membrane markers and their different conditions are shown. Numbers in the bottom of each bar refer to the number of movies analysed.

2.5.5. SpiderGFP and SAS-Venus behaviour in *crb*^{11A22}

From all the data extracted from wildtype movies, it was striking that there were differences in the kinetic behaviour of SpiderGFP (whole membrane marker) and SAS-Venus (apical membrane marker) in the embryo. Could mutations in Crumbs affect this?

To answer this question it was necessary to genetically recombine both markers with a mutant allele of crumbs: *crb*^{11A22} (see Materials and Methods section).

The obtained recombinant lines used for the FRAP experiments were named *crb*^{11A22}SpiderGFP and *crb*^{11A22}Casper SAS-Venus C for the recombination between *crb*^{11A22} and pCasper SAS-Venus1.

It should be noted beforehand, that the amount of *crb*^{11A22} Casper SAS-Venus C movies is not sufficient to draw definitive conclusions at this stage. However, these initial movies are suggestive of a possible role of Crumbs in apical membrane behaviour.

Movies of *D*E-cadherinGFP in the *crb*^{11A22} background were not included in the statistical analysis because of their small sample. Such movies were extremely hard to obtain from a technical point of view thanks to the small region of the cell being imaged whilst the tissue integrity was being severely compromised.

2.5.5.1. Mobile fraction values of SpiderGFP and *crb*^{11A22}SpiderGFP

The differences observed between the anterior and posterior of the embryo regarding A_1 and A_2 values of SpiderGFP in the wildtype are not observed in *crb*^{11A22} (Figure D24); (Figure D25). However the mobile fraction mean values are higher in *crb*^{11A22}SpiderGFP embryos. This increase is more evident in the posterior regions of the embryo, though the anterior also registers slight increases.

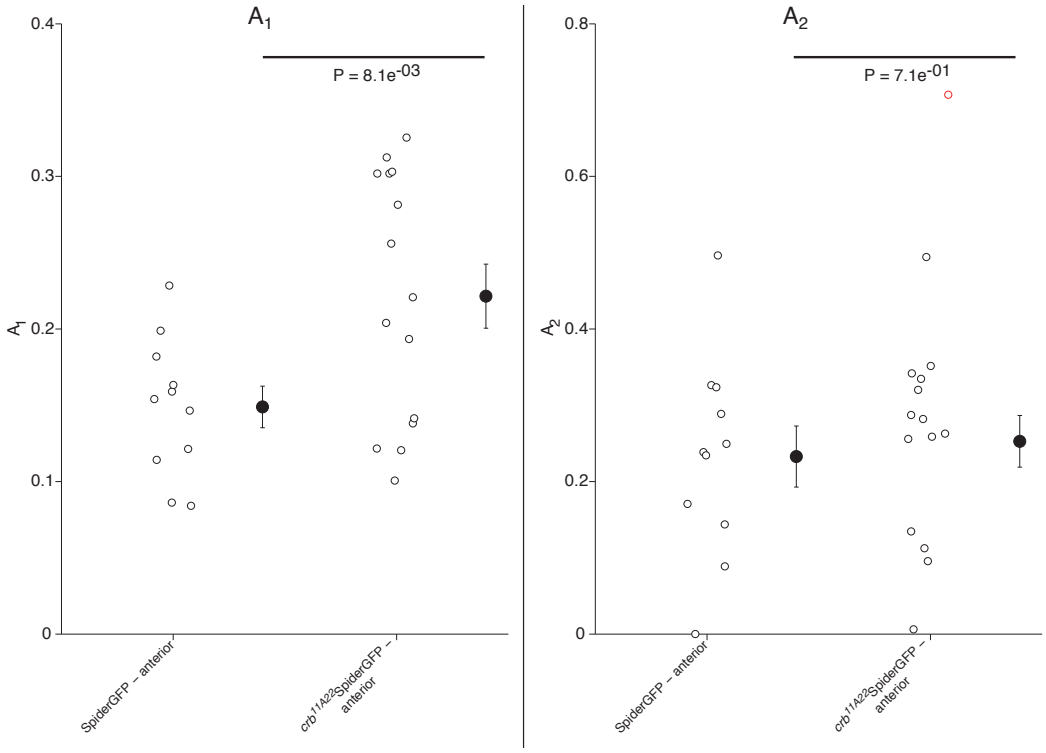

Figure D24 – Mobile fractions (A_1 and A_2) of the anterior area of SpiderGFP and *crb*^{11A22}SpiderGFP embryos. Open circles refer to values obtained from fitting curves. P-values and mean and error bars in black. Open circles in red refer to outliers as determined by the MATLAB script.

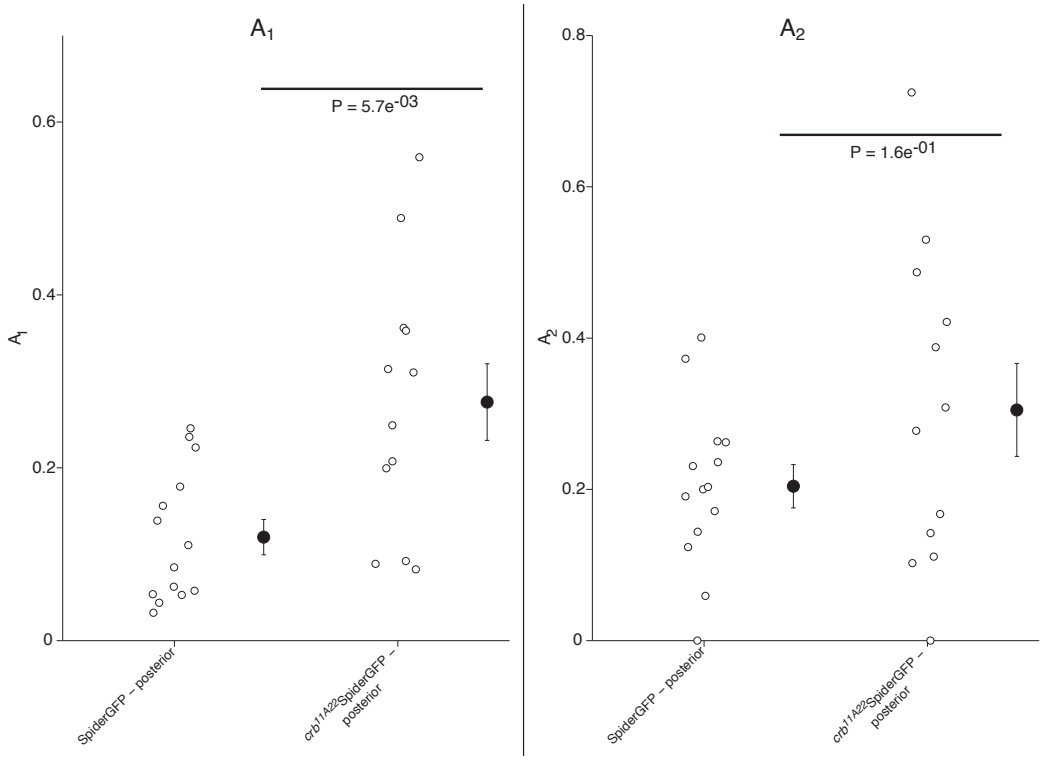

Figure D25 – Mobile fractions (A_1 and A_2) of the posterior area of SpiderGFP and *crb*^{11A22}SpiderGFP embryos. Open circles refer to the values obtained from the fitting curves. P-values and mean and error bars in black. Open circles in red refer to outliers as determined by the MATLAB script.

2.5.5.2. Kinetic values of SpiderGFP and *crb*^{11A22}SpiderGFP

The differences observed in τ_2 wildtype behaviour between anterior and posterior are abolished in *crb*^{11A22}SpiderGFP embryos. This is due to a huge decrease in the values of τ_2 in the anterior region, which brings them to the levels registered in the posterior.

Regarding τ_1 the difference is still present in *crb*^{11A22}SpiderGFP but it is reversed. A decrease in the anterior τ_1 values coupled to an increase in the posterior values leads to this behaviour (Figure D26); (Figure D27).

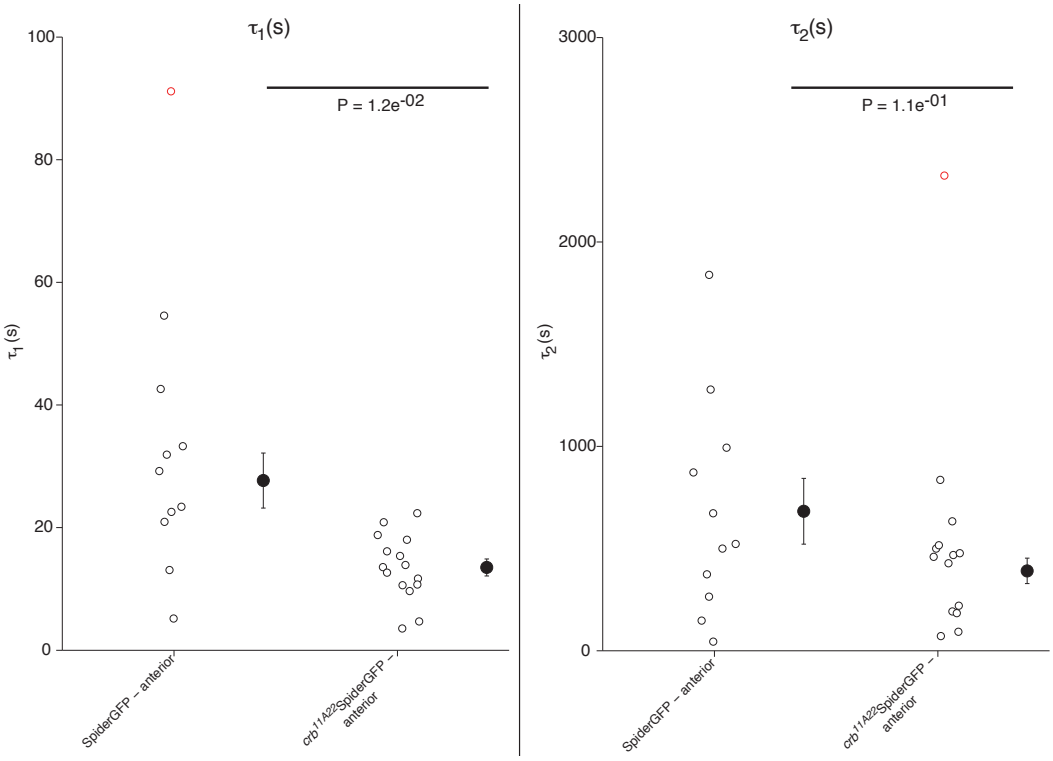

Figure D26 – Kinetic parameters (τ_1 and τ_2) of the anterior area of SpiderGFP and *crb*^{11A22}SpiderGFP embryos. Open circles refer to values obtained from fitting curves. P-values and mean and error bars in black. Open circles in red refer to outliers as determined by the MATLAB script.

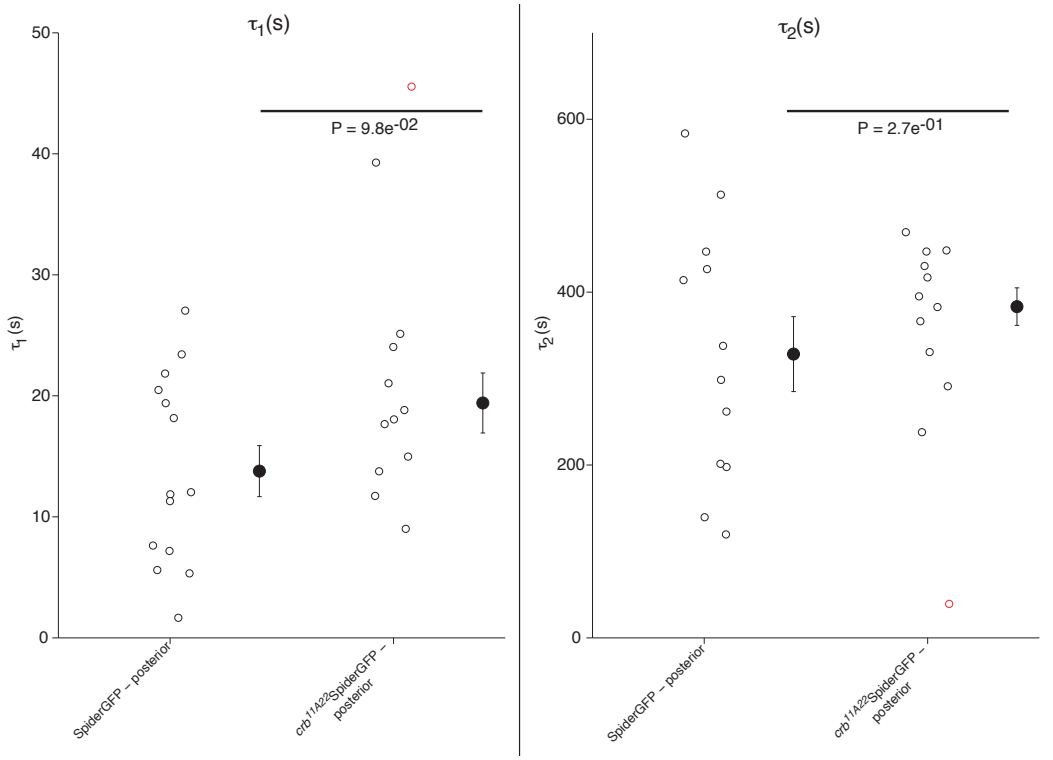

Figure D27 – Kinetic parameters (τ_1 and τ_2) of the posterior area of SpiderGFP and *crb*^{11A22}SpiderGFP embryos. Open circles refer to the values obtained from the fitting curves. P-values and mean and error bars in black. Open circles in red refer to outliers as determined by the MATLAB script.

2.5.5.3. Mobile fraction values of pCasper SAS-Venus 1 and *crb*^{11A22}CasperSAS-Venus C

Once again, it should be noted that the amount of data for *crb*^{11A22}CasperSAS-VenusC is not sufficient to draw definitive conclusions and that this data should be regarded as indications of the possible effect of *crb*^{11A22} in the behaviour of SAS-Venus.

Unlike the wildtype situation, A_1 levels in *crb*^{11A22} embryos are higher in the posterior of the embryo when compared to the anterior. However, for A_2 the situation is reversed – whereas in the wildtype, the posterior shows higher levels than the anterior; in *crb*^{11A22}, such difference is not observed. It should be stated that in *crb*^{11A22}, amongst the posterior A_2 datapoints, there is one that clearly affects the spread of the data, and consequently the mean value – however, since there are not enough movies, the MATLAB script could not correctly identify it as an outlier. With more movies, this should be rectified.

Finally, the differences between the levels of A_1 and A_2 in both the anterior and posterior in the wildtype are not present in *crb*^{11A22}CasperSAS-VenusC embryos due to a decrease in A_1 levels (Figure D28); (Figure D29).

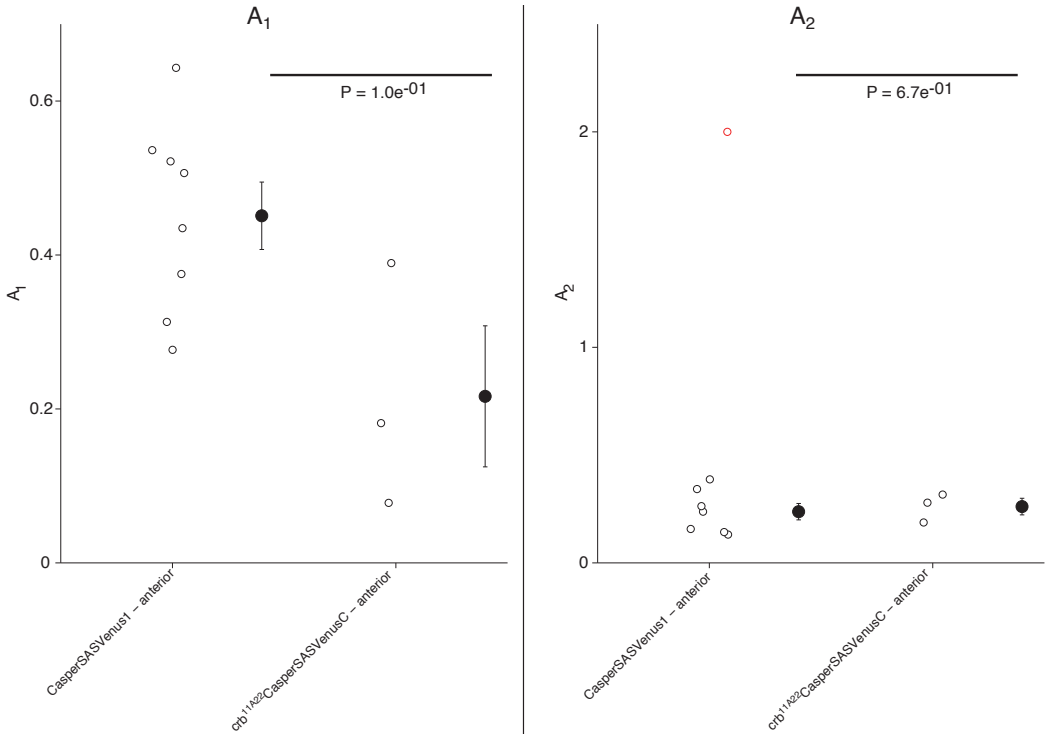

Figure D28 – Mobile fractions (A_1 and A_2) of the anterior area of pCasperSAS-Venus1 and *crb*^{11A22}CasperSAS-VenusC embryos. Open circles refer to the values obtained from the fitting curves. P-values and mean and error bars in black. Open circles in red refer to outliers as determined by the MATLAB script.

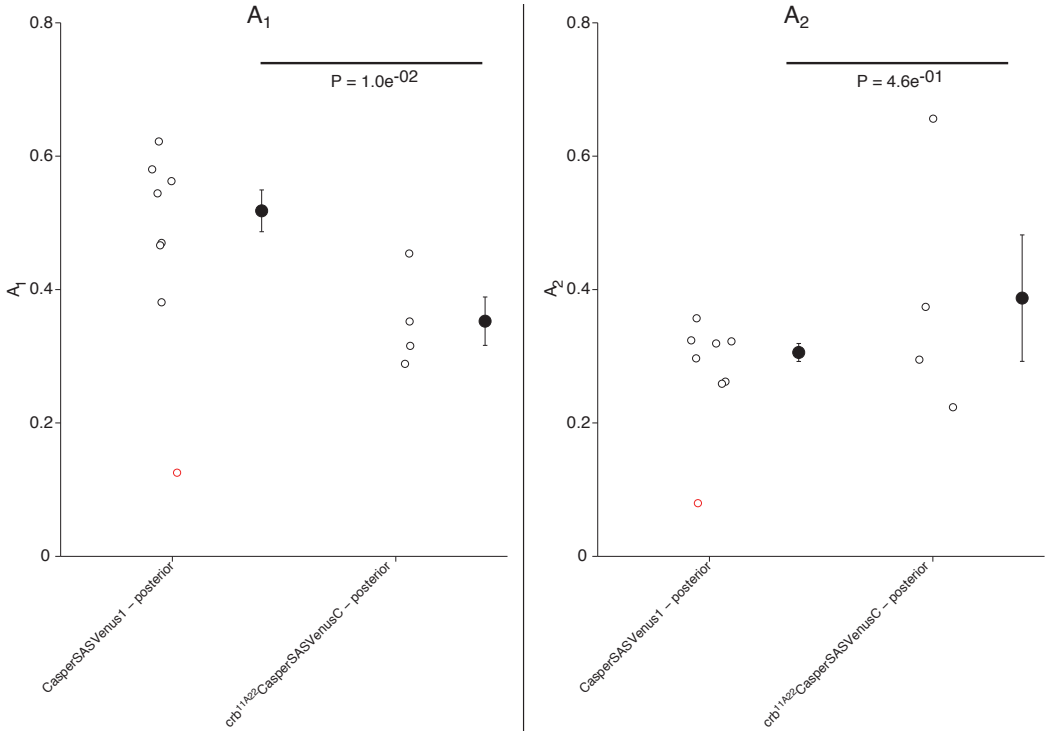

Figure D29 – Mobile fractions (A_1 and A_2) of the posterior area of pCasperSAS-Venus1 and *crb*^{11A22}CasperSAS-VenusC embryos. Open circles refer to the values obtained from the fitting curves. P-values and mean and error bars in black. Open circles in red refer to outliers as determined by the MATLAB script.

2.5.5.4. Kinetic values of CasperSAS-Venus1 and *crb*^{11A22}CasperSAS-VenusC

As in the wildtype, there seems to be no difference in both kinetic parameters in the anterior or posterior of the embryo (Figure D30); (Figure D31). It should be stated that regarding the posterior values of τ_2 in *crb*^{11A22}CasperSAS-VenusC, there is a datapoint clearly affecting the spread of the data and consequently the mean value – however, since there are not enough movies, the MATLAB script could not correctly identify it as an outlier. With more movies, this should be rectified.

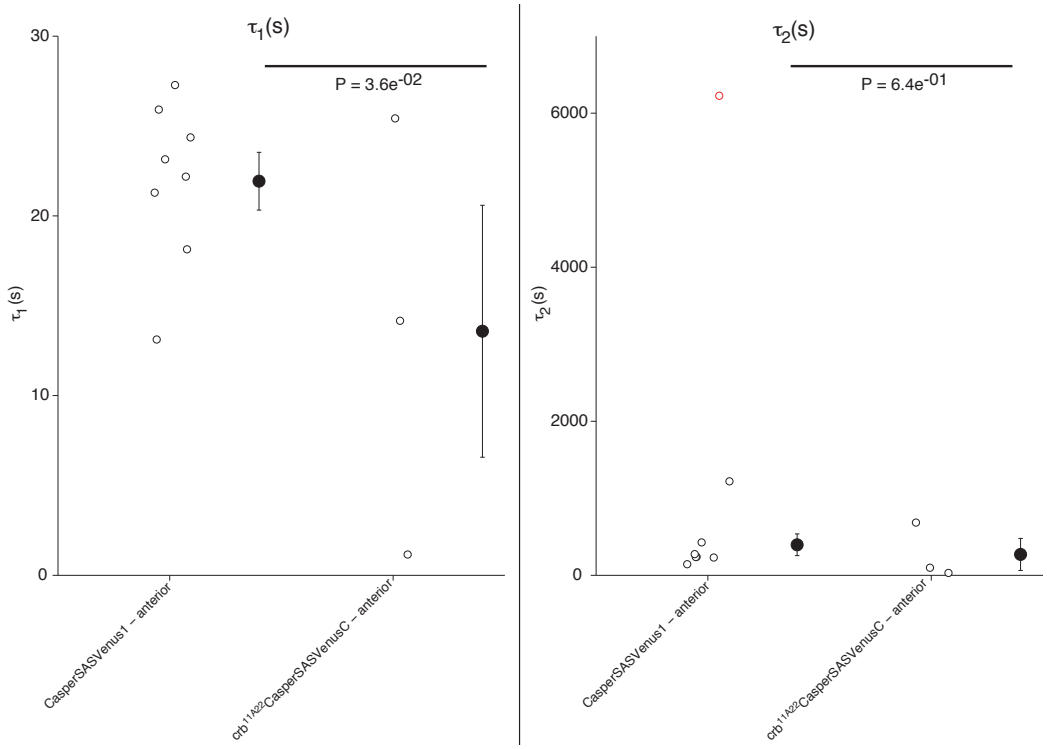

Figure D30 – Kinetic parameters (τ_1 and τ_2) of the anterior area of pCasperSAS-Venus1 and *crb*^{11A22}CasperSAS-VenusC embryos. Open circles refer to the values obtained from the fitting curves. P-values and mean and error bars in black. Open circles in red refer to outliers as determined by the MATLAB script.

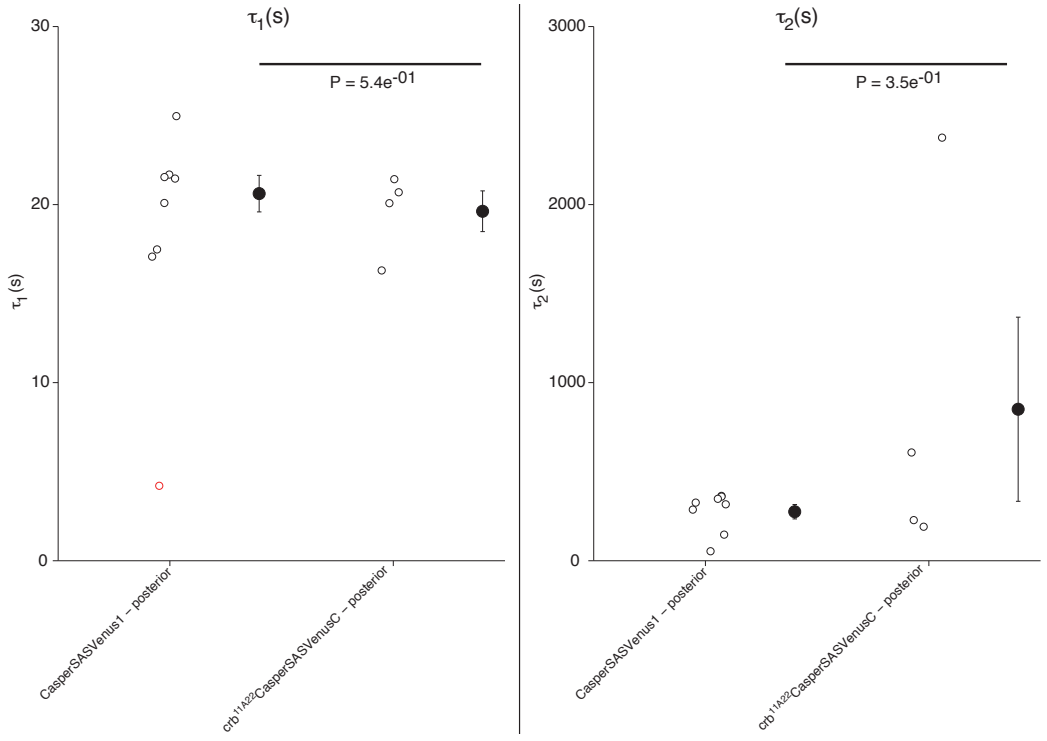

Figure D31 – Kinetic parameters (τ_1 and τ_2) of the posterior area of pCasperSAS-Venus1 and *crb*^{11A22}CasperSAS-VenusC embryos. Open circles refer to the values obtained from the fitting curves. P-values and mean and error bars in black. Open circles in red refer to outliers as determined by the MATLAB script.

2.5.5.5. SpiderGFP and SAS-Venus behaviour in *crb*^{11A22} summary

2.5.5.5.1. Mobile fractions

As in the wildtype situation of SpiderGFP, there appears to be no difference between anterior and posterior for both A_1 and A_2 in *crb*^{11A22} embryos. However, the levels are higher in *crb*^{11A22}SpiderGFP embryos, when compared to the wildtype, especially the posterior A_1 levels.

Regarding the differences between A_1 and A_2 observed in the wildtype for each region, they are not present in *crb*^{11A22}SpiderGFP due to a significant increase in A_1 levels (Table D9); (Table D10); (Table D11); (Table D12).

The behaviour of the mobile fractions of CasperSAS-Venus seems to be affected by the absence of Crumbs. In *crb*^{11A22}, A_1 levels are higher in the posterior and as for A_2 there seems to be no difference in both compartments. This behaviour is completely opposite to the one registered in the wildtype, where there are no differences for A_1 levels and A_2 levels are higher in the posterior. When comparing A_1 to A_2 levels, there are no differences in *crb*^{11A22}CasperSAS-VenusC whereas in the wildtype, A_1 is always higher both in the anterior and in the posterior (Table D9); (Table D10); (Table D11); (Table D12).

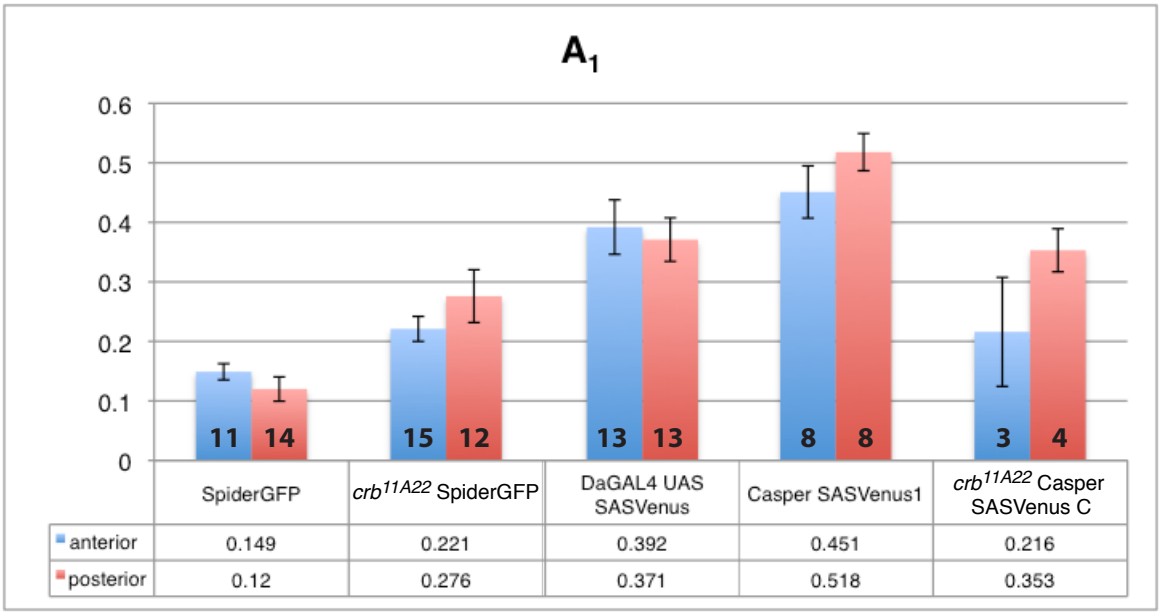

	SpiderGFP	*crb*^{11A22} SpiderGFP	DaGAL4 UAS SASVenus	Casper SASVenus1	*crb*^{11A22} Casper SASVenus C
anterior	0.149	0.221	0.392	0.451	0.216
posterior	0.12	0.276	0.371	0.518	0.353

Table D9 – A_1 mean values with corresponding error bars in both anterior and posterior regions of the embryo. Numbers in the bottom of each bar refer to the number of movies analysed.

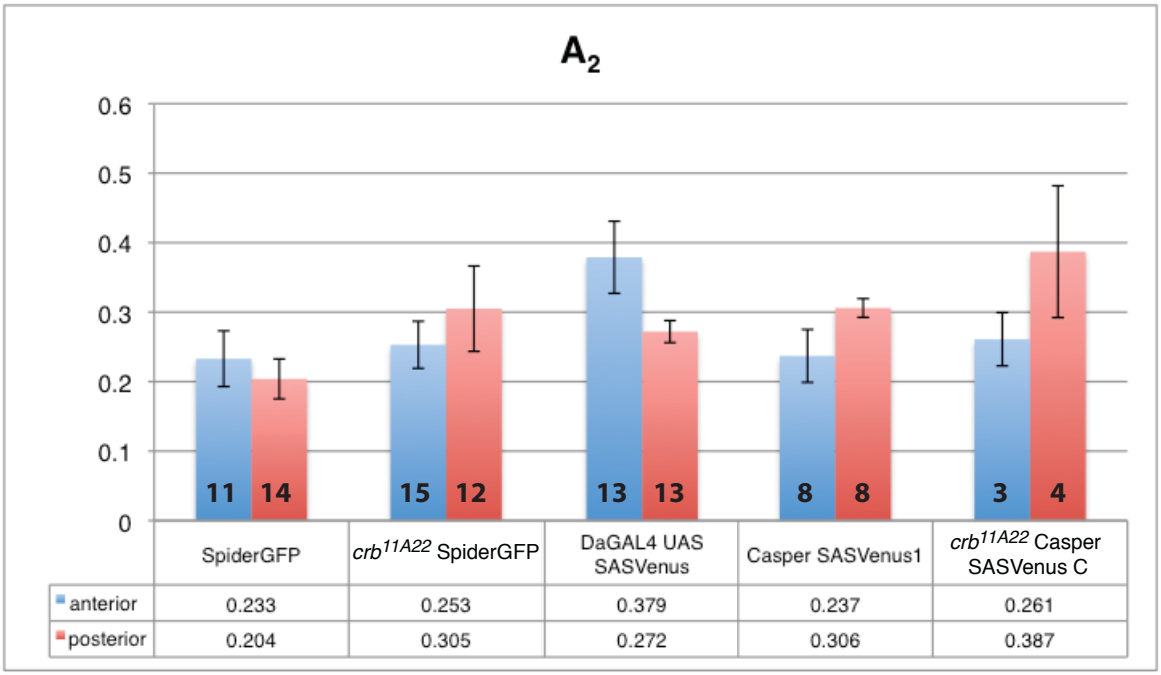

	SpiderGFP	*crb*^{11A22} SpiderGFP	DaGAL4 UAS SASVenus	Casper SASVenus1	*crb*^{11A22} Casper SASVenus C
anterior	0.233	0.253	0.379	0.237	0.261
posterior	0.204	0.305	0.272	0.306	0.387

Table D10 – A_2 mean values with corresponding error bars in both anterior and posterior regions of the embryo. Numbers in the bottom of each bar refer to the number of movies analysed.

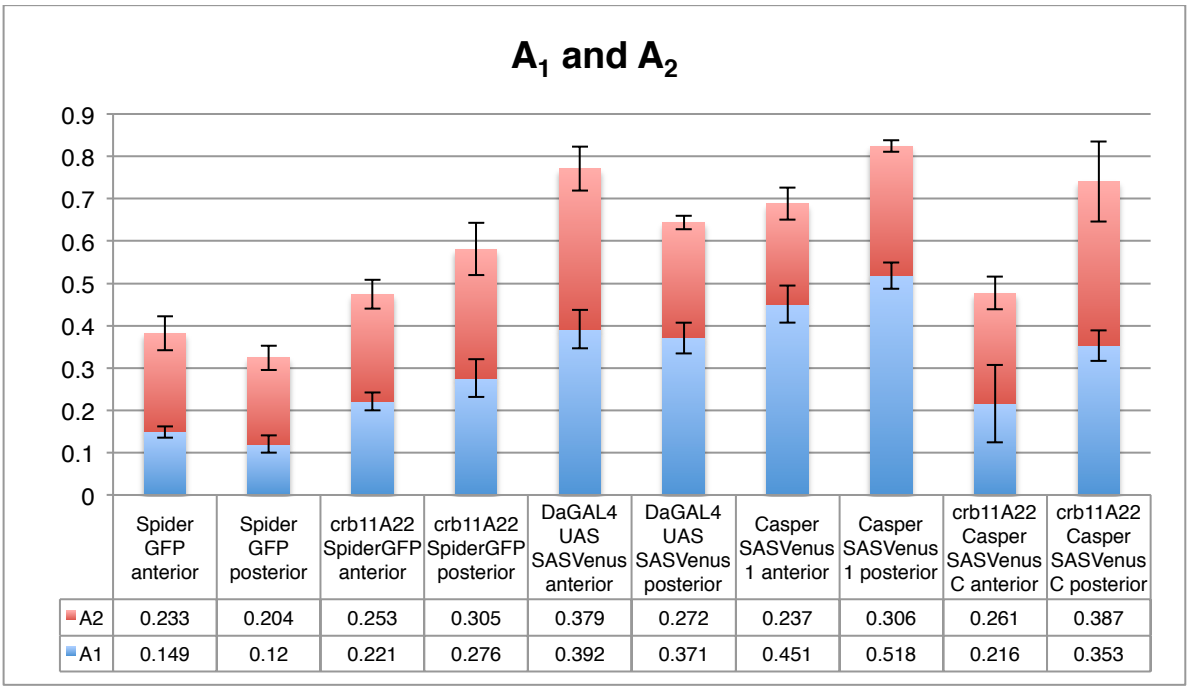

	Spider GFP anterior	Spider GFP posterior	crb11A22 SpiderGFP anterior	crb11A22 SpiderGFP posterior	DaGAL4 UAS SASVenus anterior	DaGAL4 UAS SASVenus posterior	Casper SASVenus 1 anterior	Casper SASVenus 1 posterior	crb11A22 Casper SASVenus C anterior	crb11A22 Casper SASVenus C posterior
A2	0.233	0.204	0.253	0.305	0.379	0.272	0.237	0.306	0.261	0.387
A1	0.149	0.12	0.221	0.276	0.392	0.371	0.451	0.518	0.216	0.353

Table D11 – A_1 and A_2 mean values combined with corresponding error bars in both anterior and posterior regions of the embryo.

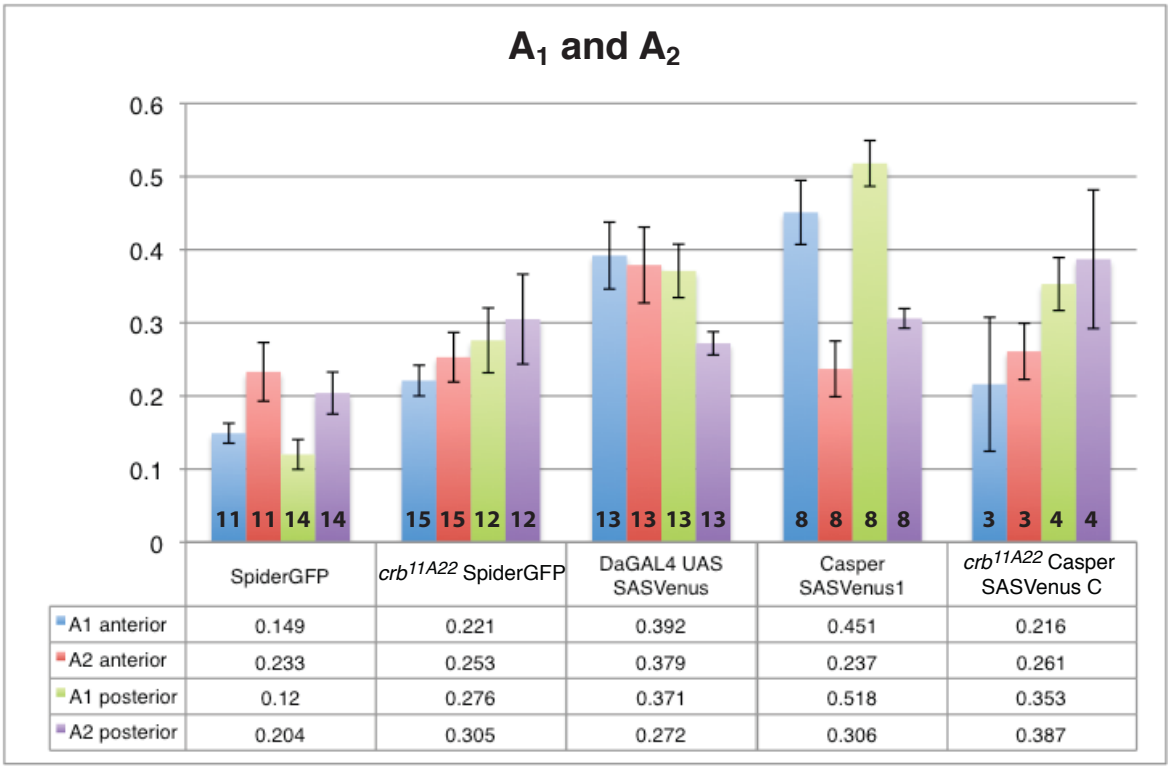

	SpiderGFP	*crb*^{11A22} SpiderGFP	DaGAL4 UAS SASVenus	Casper SASVenus1	*crb*^{11A22} Casper SASVenus C
A1 anterior	0.149	0.221	0.392	0.451	0.216
A2 anterior	0.233	0.253	0.379	0.237	0.261
A1 posterior	0.12	0.276	0.371	0.518	0.353
A2 posterior	0.204	0.305	0.272	0.306	0.387

Table D12 – A_1 and A_2 mean values with corresponding error bars in both anterior and posterior regions of the embryo. Numbers in the bottom of each bar refer to the number of movies analysed.

2.5.5.5.2. Kinetic values

The kinetic parameters behaviour of SpiderGFP seems to be affected by the presence of the *crb*^{11A22} allele. Regarding τ_1, there seems an inversion of the behaviour – whereas in wildtype, the anterior shows higher values than the posterior, in *crb*^{11A22}SpiderGFP embryos, the posterior levels are higher. As for τ_2, the difference observed between anterior and posterior is abolished in *crb*^{11A22}SpiderGFP embryos (Table D13); (Table D14); (Table D15).

When comparing CasperSAS-Venus 1 to *crb*^{11A22}CasperSAS-Venus C, the behaviour of both τ_1 and τ_2 does not seem to be affected by *crb*^{11A22}. It would be interesting though, to investigate whether the difference in τ_2 in DaGAL4 UAS SAS-Venus2 would be affected by the presence of *crb*^{11A22} (Table D13); (Table D14); (Table D15).

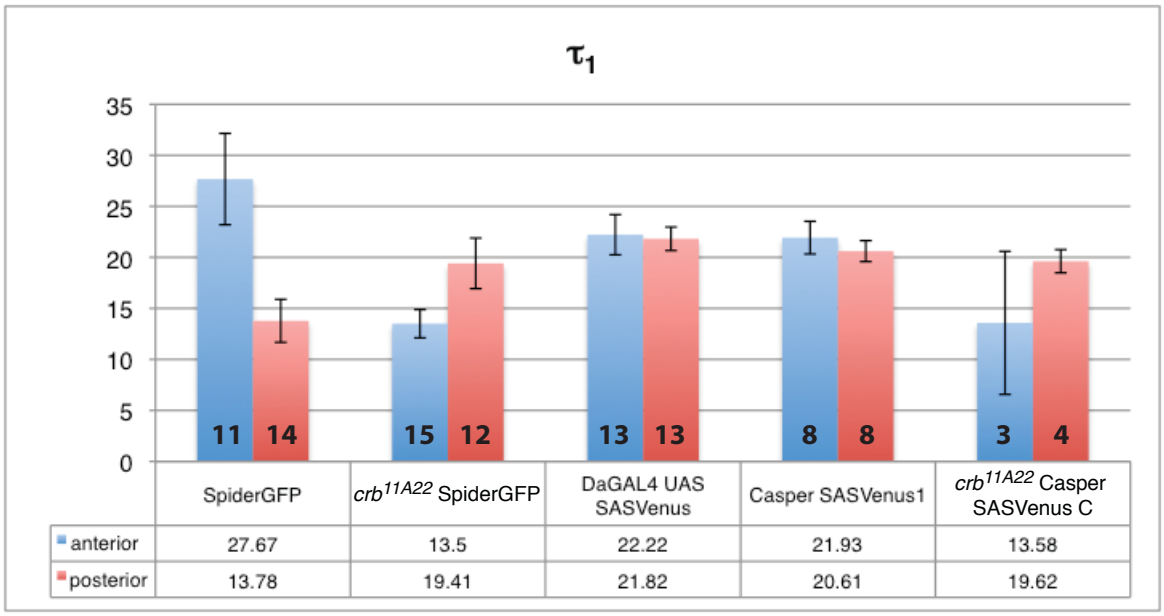

	SpiderGFP	*crb*^{11A22} SpiderGFP	DaGAL4 UAS SASVenus	Casper SASVenus1	*crb*^{11A22} Casper SASVenus C
anterior	27.67	13.5	22.22	21.93	13.58
posterior	13.78	19.41	21.82	20.61	19.62

Table D13 – τ_1 mean values with corresponding error bars in both anterior and posterior regions of the embryo. Numbers in the bottom of each bar refer to the number of movies analysed.

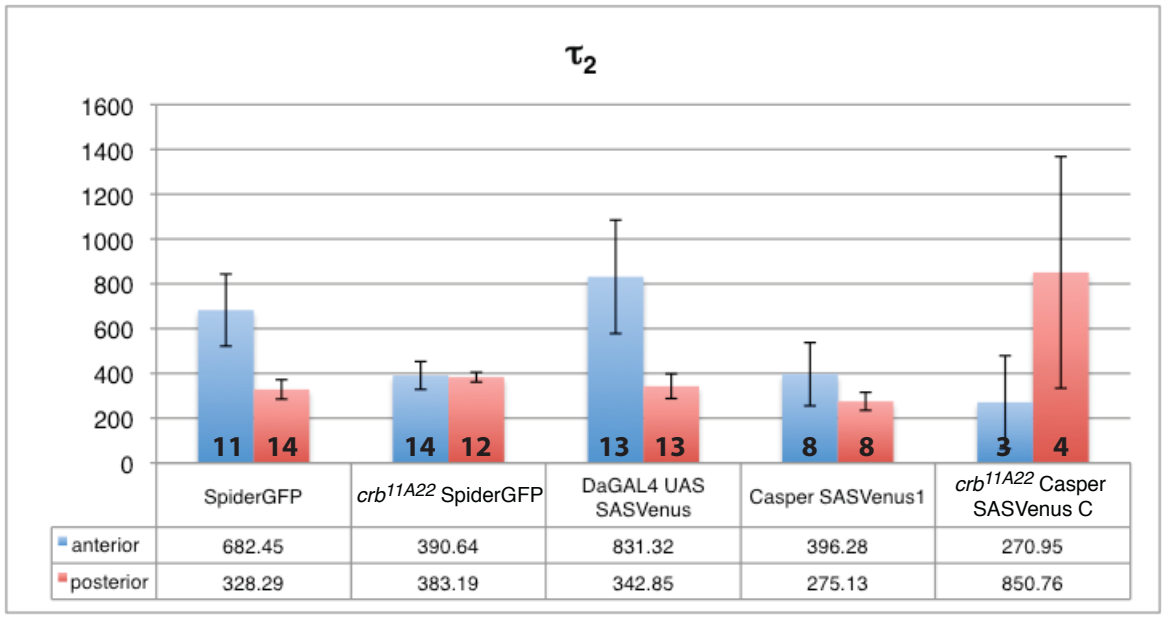

	SpiderGFP	*crb*^{11A22} SpiderGFP	DaGAL4 UAS SASVenus	Casper SASVenus1	*crb*^{11A22} Casper SASVenus C
anterior	682.45	390.64	831.32	396.28	270.95
posterior	328.29	383.19	342.85	275.13	850.76

Table D14 – τ_2 mean values with corresponding error bars in both anterior and posterior regions of the embryo. Numbers in the bottom of each bar refer to the number of movies analysed.

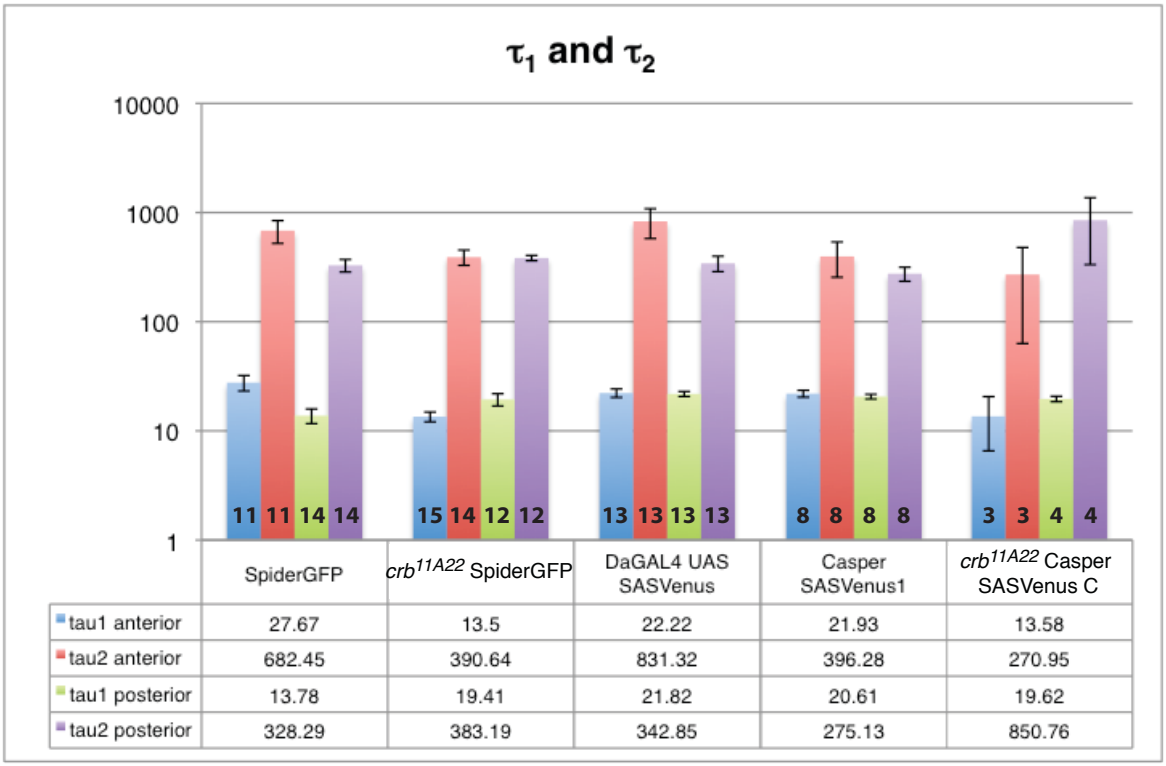

	SpiderGFP	*crb*^{11A22} SpiderGFP	DaGAL4 UAS SASVenus	Casper SASVenus1	*crb*^{11A22} Casper SASVenus C
tau1 anterior	27.67	13.5	22.22	21.93	13.58
tau2 anterior	682.45	390.64	831.32	396.28	270.95
tau1 posterior	13.78	19.41	21.82	20.61	19.62
tau2 posterior	328.29	383.19	342.85	275.13	850.76

Table D15 – τ_1 and τ_2 mean values with corresponding error bars in both anterior and posterior regions of the embryo. For a better representation of the data, the y-axis is in logarithmic scale. Numbers in the bottom of each bar refer to the number of movies analysed.

3. Live imaging of *D*E-CadGFP in *crb*^{11A22} embryos

Since Crumbs had an effect on the recovery kinetics of some protein markers in the anterior region of the embryo, long term imaging experiments of *D*E-CadherinGFP in wildtype and *crb*^{11A22} backgrounds were performed to describe adherens junctions behaviour during germband extension. Interestingly enough, it was observed that in *crb*^{11A22} embryos, the epithelia in the anterior region started to collapse and lose their structure during early to mid stages of GBE whereas the posterior epithelia showed only minor defects (Figure D32). Eventually, the posterior epithelia would collapse but at a later stage of GBE, thus recapitulating the already known phenotype of *crb*^{11A22}.

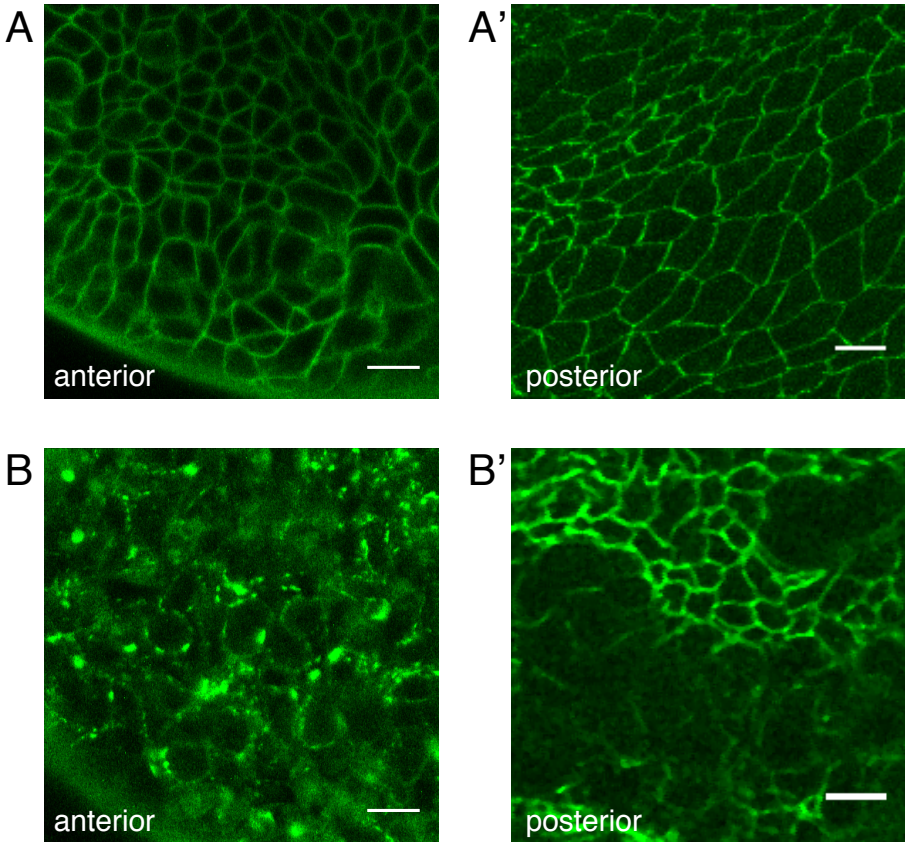

Figure D32 – Image stills of timelapse microscopy movies of *D*E-CadherinGFP. (A) Anterior and (B) posterior of a wildtype embryo during early GBE and anterior (A') and posterior (B') of a *crb*^{11A22} embryo at mid GBE development. Scalebar: 10μm.

E. Discussion

1. FRAP recovery plots are better defined by double exponential fits

Most FRAP experiments are done using fixed image acquisition rates (Cliffe et al., 2004); (Braga et al., 2007); (Cavey et al., 2008). When starting this project, together with Dr. Jean-Yves Tinevez, it was found that the initial stages of fluorescence recovery were not properly described if a rate of 1 frame/5 seconds was used (Figure D6A). To circumvent that, experimental conditions were modified in order obtain a better temporal description. By using different rates of image acquisition during the FRAP assay (1f/5s (25s) – bleach – 1f/s (60s) – 1f/5s (600s) – 1f/30s (600s)) (Figure D7), the initial steepness of the FRAP recovery curve was now much better described (Figure D6B).

It became obvious that although a single exponential fit gave high correlation values (R^2) with the data, when a double exponential was used, the correlation value was much higher, thus better describing the fluorescence recovery (Figure D11). This could mean that two cell processes are involved in the recovery – whereas the faster component (with low values of τ - τ_1) is probably diffusion-related due to the measured kinetic values, the second, slower process (with high values of τ - τ_2), might be vesicle trafficking-related since the kinetic values are an order of magnitude higher than the ones measured in the first component (Sprague and McNally, 2005). In order to perturb this supposed second component of recovery, attempts at disrupting vesicle fission events with the plasma membrane via use of the *shibire*^{ts} mutation were tried but technical difficulties did not allow for a definite answer to this question. As for the fast component of recovery, Fluorescence Correlation Spectroscopy (Yu et al., 2009); (Petrasek et al., 2010) was considered but due to lack of time from our collaborating group in Düsseldorf, assessment of our protein markers' diffusion rates via this technique was not performed.

2. *D*E-Cadherin kinetics are similar to the ones found in the literature

The methods used in (Cliffe et al., 2004) for FRAP were different to the ones used in this work. In their work, the bleach regions of interest (ROIs) used did not encompass the whole cell membrane but only certain parts of the plasma membrane. Also, their image acquisition conditions were different (1z-stack every 15 seconds) to the ones used in this project as well as the time duration of the experiments (5 minutes).
Nevertheless, our data, when fitted using a single exponential, shows very similar kinetic values to the ones proposed in the aforementioned paper (~100 seconds). This confirms that our imaging conditions did not cause any aberrant behaviour of the imaged protein marker – *D*E-CadherinGFP.
As for mobile fraction comparisons, it is hard to do so, since a stable plateau in the levels of fluorescence was not reached in the plots shown in (Cliffe et al., 2004).

3. During GBE, wildtype embryos show spatial differences regarding some marker parameters

One very interesting observation that came from this work is that embryos do not show the same kinetic values for SpiderGFP and DaGAL4 UAS SAS-Venus2 in the anterior and posterior regions, during morphogenetic events such as GBE (Figure D10); (Table D15) in wildtype conditions. It is very tempting to assume that this reflects a difference in membrane compartment behaviour, although that cannot be said in all certainty since only protein kinetics are being measured and not lipid kinetics - such tools are not yet available.
Nonetheless, when analysing germband extension, it is obvious that differences in morphogenetic activities in different regions of the embryos are present. Posterior cells, in order to undergo cell intercalation, need to remodel their junctions and membranes (Bertet et al., 2004); (Butler et al., 2009) much more actively than cells in the anterior region of the embryo which are less morphogenetically active (see GBE movies in the attached DVD).
SpiderGFP, a protein marker that labels the entire plasma membrane, shows lower τ values in posterior cells (Table D15). As for mobile fraction values, they appear to be the same in both the anterior and posterior regions of the embryo (Table D12). This

means that posterior cells replace the same amount of protein faster than anterior cells, thus reflecting the different morphogenetic activities of these two cell populations.

Since Spider (*gish*) is a casein kinase Iγ homolog and it associates with the plasma membrane due to a prenylation site (Tan et al., 2010), its higher turnover in the posterior region of the embryo could mean that its substrates are differently localised in the embryo, thus requiring different levels of activity from Spider. Casein kinases are known to regulate Wnt signalling (Cheong and Virshup, 2011) and studies in *Tribolium castaneum* have shown that several *Wnt* genes are required for posterior patterning and germband elongation (Bolognesi et al., 2008). One could envision then, that a higher level of activity of Spider in the posterior would lead to the activation of the *Wnt* genes necessary for the posterior patterning of the embryo. Though *Tribolium* is a short-germ insect, it would be interesting to assess if this would occur in the long-germ embryo of *Drosophila*. All in all, this could imply a more direct role of *gish* in GBE; however no GBE-related phenotype has been described for mutations in *gish* in *Drosophila*.

Nonetheless, both kinetic components (τ_1 and τ_2) of SpiderGFP are lower in the posterior (Table D15). Based on our assumption that the fast component of recovery (τ_1) is diffusion-related and the second, slower, component of recovery (τ_2) is membrane trafficking-related, it is hard to envision how τ_1 would show any differences between cells. Limitations to our FRAP assay imaging conditions could be a possible explanation for this, however only proper measurements of diffusion rates via FCS would clarify this question. Nevertheless, the fact that SpiderGFP's τ_2 shows spatial differences in behaviour raises interesting biological questions. Could Spider be more stabilised at the membrane by other proteins in the anterior? Could different membrane delivery requirements be causing the difference in morphogenetic activities of these two cell populations? Are all cell membrane compartments reflecting this behaviour? If not, which one(s) could be causing such differences?

Although it is not possible to directly tackle these questions experimentally, as mentioned above, this work tried to give some insight by quantifying kinetics and mobile fractions of protein markers labelling different membrane compartments.

*D*E-CadherinGFP showed no significant spatial differences in mobile fraction values both in homozygous and heterozygous conditions (Table D5). It should be noted, though, that absolute values in homozygosity were higher than in heterozygosity,

which could be caused by different protein amounts of the marker in the cells. As for the kinetic parameters, they do not show any spatial differences in both conditions, though again, τ_1 in heterozygosity, did seem to be higher in the anterior cells of the embryo (Table D8). This could be explained, however by the reduced number of anterior movies deemed appropriate to be included in the analysis.

If SpiderGFP truly reflects different spatial membrane delivery requirements for morphogenesis, it is very interesting to note that *D*E-Cadherin behaves similarly in both regions of the embryo. This could mean that despite all the different morphogenetic activities taking place within the embryo, all cells require the same trafficking kinetics to their adherens junctions. *D*E-CadherinGFP protein delivery is not altered, whether cells are intercalating, actively remodelling their membranes or just not undergoing any significant morphogenetic events.

LachesinGFP, much like *D*E-CadherinGFP, did not show any significant spatial differences both in mobile fraction values and in kinetic parameters (Table D5); (Table D8). Therefore, both the zonula adherens marker and basolateral marker do not mimic the different spatial behaviour found in SpiderGFP embryos.

The last compartment marker to be analysed was SAS-Venus. This marker was expressed using a basal ubiquitous tubulin promoter – pCasperSAS-Venus 1 - and by driving its expression with DaGAL4 (a strong and early driver used in the UAS/GAL4 expression system). A_1 levels did not show any significant spatial difference for both expression conditions. However, when analysing A_2 levels, it was found that such spatial differences were present (Table D5). Whereas in pCasperSAS-Venus1, the posterior had higher values, in DaGAL4 UASVenus2, it was the anterior showing higher values. Such discrepancy could be explained by the small amount of movies taken into account for the analysis of pCasperSAS-Venus1. Performing the FRAP assay in the small apical domain can be quite daunting since any cell movements occurring during the imaging lead to shifts in the z-axis which ultimately makes the movie unsuitable for analysis. Nevertheless, it would be interesting to see if this behaviour would still be present when more movies are taken into account. If that is the case, it could mean that the protein delivery machinery might have limitations regarding the amount of apical protein it can carry to the plasma membrane in different cells, or that the apical surface where vesicles are delivered has different sizes in the anterior and posterior of the embryo. Live imaging movies of SAS-Venus embryos undergoing GBE in both expression vectors could answer this question.

It should be stressed that for SAS-Venus, overexpression was employed in order to drive its expression early in development (under tubulin promoter and under UAS/GAL4 control) whereas SpiderGFP and LachesinGFP expression is under control of their endogenous promoter. This fact could lead to the observed differences in the behaviour of the markers but technically this was the only way to drive expression of SAS-Venus during gastrulation and GBE.

As for τ_2, DaGAL4 SAS-Venus2 shows the same behaviour found in SpiderGFP. However, the pCasper SAS-Venus1 line does not show such spatial difference (Table D8). Again, the small sample of movies could be the reason for that. However, if the different behaviour between the expression conditions would persist, one possible explanation could be an "overload" of the protein delivery machinery due to the sheer amount of protein present within the cells.

4. In *crb*^{11A22} embryos, the spatial differences in SpiderGFP kinetics are not present

Strikingly, in *crb*^{11A22} embryos expressing SpiderGFP, the anterior values of τ_1 and τ_2 are extremely reduced. Their levels strongly resemble the values found in the posterior region of the embryo, which are not that dissimilar from the wildtype values (Table D15).

Therefore, the spatial differences observed in the wildtype conditions could not be recapitulated. This is quite exciting, since it could mean that Crumbs is affecting somehow the delivery of proteins to the plasma membrane in a specific region of the embryo. Although there is not a significant number of pCasperSAS-Venus1 movies in the *crb*^{11A22} background to draw definitive conclusions, it seems that only the anterior values of τ_1 and τ_2 are affected. If that is truly the case, this would be a strong evidence for the role of Crumbs in apical delivery of proteins.

5. In *crb*^{11A22} embryos, A_1 values of SpiderGFP are slightly higher

Another interesting aspect of *crb*^{11A22}, is the fact that A_1 values are slightly higher both in the anterior and posterior regions of the embryo. A_2 values are not significantly different from the wildtype situation (Table D12). This could mean that lateral diffusion of SpiderGFP in the plasma membrane is easier to accomplish in the absence of Crumbs. Though not a strong argument, this could imply that Crumbs

acts as a physical barrier within the subapical region of the cell. Without Crumbs, the cell membrane would be more susceptible to lateral diffusion movements of proteins. However, when analysing A_1 behaviour of pCasperSAS-Venus1 in *crb*^{11A22} embryos, it is evident that the protein is less mobile both in the anterior and posterior regions. A_2 values, on the other hand, behave similarly to the wildtype. Only with more movies of *crb*^{11A22}pCasperSAS-VenusC will it be possible to assess if this is indeed the case. Also, it would be very interesting to analyse the behaviour of DaGAL4 UAS SAS-Venus2 in the *crb*^{11A22} background, since this condition shows evident differences in A_2 values between anterior and posterior.
Another possible explanation for all these results could be the fact that *crb*^{11A22} affects the protein levels of all markers imaged – western blots will have to be performed to assess if that is the case.

6. Live imaging movies of *D*E-cadherinGFP in the *crb*^{11A22} background reveal earlier defects in the anterior region of the embryo

Based on the FRAP assay observations that Crumbs was affecting protein delivery specifically in the anterior region of the embryo, it was decided to image the adherens junction component *D*E-cadherinGFP in the *crumbs* mutant background. Interestingly, it was found that the anterior region of the embryo was showing the epithelial defects previously characterised for *sdt* (Bachmann et al., 2001) and *crb*, earlier than the posterior region. Although this reinforces the idea that Crumbs' function is more essential in the anterior cells during GBE, the fact that neuroblast delamination is occurring very actively in the head area of the embryo during the imaged developmental stages (Hartenstein and Campos-Ortega, 1984); (Hartenstein, 1993) should not be overlooked. Though the cells are not undergoing morphogenetic movements, the 'intrusion' of the neuroblasts within the epithelium causes the loss of its integrity. Nonetheless, this shows that the stability of the epithelia in the anterior depends heavily on the presence of Crumbs in the cell (Harris and Tepass, 2008).
As for the function of Crumbs in the posterior, these movies show that during the active cell intercalation events taking place in the posterior region of the embryo, the cells do not require Crumbs for morphogenesis to occur. Later on, the epithelium eventually collapses. A possible explanation could be that Crumbs function by stabilising the junctions once the cells composing the germband reach their final destination. More movies focused on the tip of the germband will need to be made to

test if that is really the case. It would also be very interesting to observe the behaviour of SAS-Venus during GBE to assess directly whether Crumbs is truly affecting apical membrane delivery or the surface area of this domain. Nonetheless, based on our data, a model for the role of Crumbs during GBE is proposed (Figure E1).

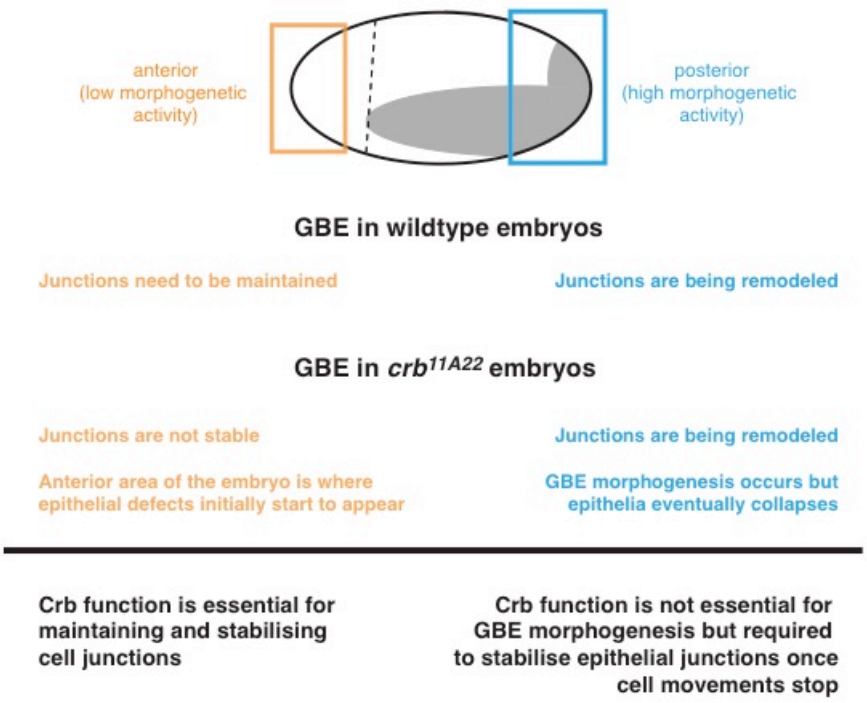

Figure E1 – Model for the role of Crumbs during GBE

In (Campbell et al., 2009) we find supporting evidence for our findings, despite the focus of this paper being on renal tubule formation in *Drosophila.*

*"…*It is tempting to speculate that Crb acts by targeting recycling vesicles of ZA components in order to maintain junctional integrity in the elongating renal tubules. Without Crb ZAs are lost and membrane domains no longer remain distinct, leading to the collapse of cell polarity. Alternatively, lack of Crb could result in loss of cell polarity in morphogenetically active tissues and, as a consequence, ZAs cannot be maintained. In this case the primary requirement for Crb during cell movement would be to maintain the apical localisation of Baz/Par-6/aPKC, thereby also ensuring the normal distribution of basolateral proteins (Bilder et al., 2003; Hutterer et al., 2004;Tanentzapf and Tepass, 2003).

The requirement for *D*E-cadherin in different tissues shows a similar dependence on the degree of morphogenetic activity (Tepass et al., 1996; Uemura et al., 1996). It was shown that the zygotic *Drosophila E-cadherin* mutant phenotype can be rescued in dynamic tissues, for example in the neurectoderm and Malpighian tubules, by suppressing morphogenetic cell movements (Tepass et al., 1996)…"

F. Materials and Methods

1. Experimental Procedures

1.1. Fly strains

The following table lists all fly lines used in this study:

Fly line	Description
*D*E-CadherinGFP	*D*E-Cadherin fused with GFP under control of ubiquitin promoter on 2nd chromosome; homozygous viable (Oda and Tsukita, 1999)
SpiderGFP	FlyTrap line: *gish* fused with GFP under endogenous promoter on 3rd chromosome; homozygous viable (Buszczak et al., 2007)
LachesinGFP	Protein trap line: *lachesin* fused with GFP under endogenous promoter on 2nd chromosome; homozygous viable (origin Knust lab)
UAS SAS-Eos 2	*Stranded at Second* fused with Eos under UAS binding region control on 3rd chromosome; homozygous viable (origin this study)
pCasper SAS-Venus 1	*Stranded at Second* fused with Venus under tubulin promoter on 3rd chromosome; homozygous viable (origin this study)
UAS SAS-Venus 2	*Stranded at Second* fused with Venus under UAS binding region control on 3rd chromosome; homozygous viable (origin this study)
DaGAL4	*daughterless*GAL4 - ubiquitous and strong driver line for expression of UAS constructs on 3rd chromosome; homozygous viable (Vincent and Girdham, 1997; Wodarz et al., 1995)
crb^{11A22} SpiderGFP/TTG	SpiderGFP recombined with crb^{11A22} with TTG balancer (TM3, P{GAL4-twi.G}2.3, P{UAS-2xEGFP}AH2.3, Sb^1 Ser^1) (origin this study)
crb^{11A22} pCasper SAS-Venus C/TTG	pCasper SAS-Venus 1 recombined with crb^{11A22} over TTG balancer (TM3, P{GAL4-twi.G}2.3, P{UAS-2xEGFP}AH2.3, Sb^1 Ser^1) (origin this study)
*D*E-CadherinGFP; crb^{11A22}/TTG	*D*E-CadherinGFP crossed to crb^{11A22} over TTG balancer (TM3, P{GAL4-twi.G}2.3, P{UAS-2xEGFP}AH2.3, Sb^1 Ser^1) (origin this study)
crb^{11A22}/TTG	crb^{11A22} over TTG balancer (TM3, P{GAL4-twi.G}2.3, P{UAS-2xEGFP}AH2.3, Sb^1 Ser^1) (origin this study)

1.2. Immunohistochemistry

The following primary antibodies were used: mouse anti-Dlg (1:500; Developmental Studies Hybridoma Bank); rabbit anti-SAS (1:500; a gift from D. Cavener) and rat anti-*D*E-Cadherin (1:10, DCAD2 concentrate; Developmental Studies Hybridoma Bank). Embryos were dechorionated by placing them in a 10% bleach solution for 3 minutes. Embryos were then fixed in 4% formaldehyde, using standard techniques (Wodarz et al., 1993). Primary incubations were performed overnight, followed by incubation with appropriate secondary antibodies (Alexa Fluor 488, Alexa Fluor 568 and Alexa Fluor 647; Molecular Probes, Invitrogen). Embryos were mounted in antibleach medium (Vectashield; Vector Laboratories).

1.3. Cuticle preparations

Embryos were dechorionated by placing them in a 10% bleach solution for 3 minutes. After thoroughly rinsing with water, embryos were placed in a scintillation vial containing a 1:1 solution of PBS pH 7.4/heptane. Embryos in the upper heptane solution were then transferred to an eppendorf tube and an equal amount of methanol was added. After vigorous shaking for 30 seconds and subsequent methanol washes, embryos were placed on a clean glass slide. A drop of Hoyer's mounting medium was added and the slide was carefully covered with a coverslip. The slide was then placed in a 65^{o}C oven overnight and afterwards allowed to air dry with its edges being sealed off with nail polish.

1.4. Hoyer's mounting medium recipe

Mix 30 g of gum arabic in 50 ml distilled water by stirring overnight. While stirring, add 200 g chloral hydrate in small quantities. Add 20 g glycerol. Centrifuge for at least 3hr at 12000 g to clear. Add lactate 1:4 to increase contrast and decrease clearing time.

1.5. Image acquisition and manipulation

For antibody stainings, samples were imaged using a single photon point scanning Zeiss LSM 510 confocal microscope (Carl Zeiss) with three PMTs using a C-Apochromat x40 NA 1.2 water immersion objective (Carl Zeiss). For every *z*-stack, each plane was separated by 1 µm.

Cuticle preparations were imaged using a widefield Zeiss microscope (Axio Imager Z1 stand with Apotome attachment) with a condenser set up for darkfield and DIC optics, an Axiocam MRm (monochrome CCD) and a Zeiss EC Plan-Neofluar 10x 0.3 objective.

2. FRAP Assay protocol

2.1. Embryo staging and mounting

Embryo staging consists of placing the desired flies in a cage for 2 hours, after which you collect the agar plate they were laying eggs (embryos) on. Afterwards you incubate the plate with the embryos at 25°C for 4 hours thus ensuring most embryos are undergoing germband extension.

For removal of the chorion (eggshell), embryos are placed in a 1:1 solution containing bleach and PBS pH 7.4 for 2 minutes and 40 seconds. Wash them thoroughly with water and place them in a vial containing PBS pH 7.4.

For mounting the embryos, a small drop of Halocarbon oil 700 is placed in the middle of the imaging slide. The tips of the slide contain coverslips (thickness 1 and size 25mmx25mm) so that when covering the slide an artificial bridge is created thus ensuring the embryos are not squashed or pressed too much.

The next step consists in picking the embryos from the PBS containing vial with a brush and spreading them in the Halocarbon oil drop. They are separated as much as possible and, if required, tungsten needles are used to orient them. The imaging slide is then covered with an appropriate coverslip (thickness 1,5 and size 25mmx60mm) and the sample is taken to the Zeiss LSM 510 DuoScan confocal (Carl Zeiss).

2.2. Image acquisition

Before starting the FRAP assay, it is essential to take an overview image of the embryo showing its developmental stage.

A 40x water objective (Zeiss C-Apochromat 40x 1.2 W) is used and the pinhole is set to an optical section of 2μm and the zoom to 3 – this ensures you can visualise a sufficient number of cells during the FRAP experiment.

2.3. VisualMacro Editor Macro

In order to acquire the images sequentially but with different acquisition rates, a VisualMacro Editor (from Zeiss) macro was developed (Figure F1).

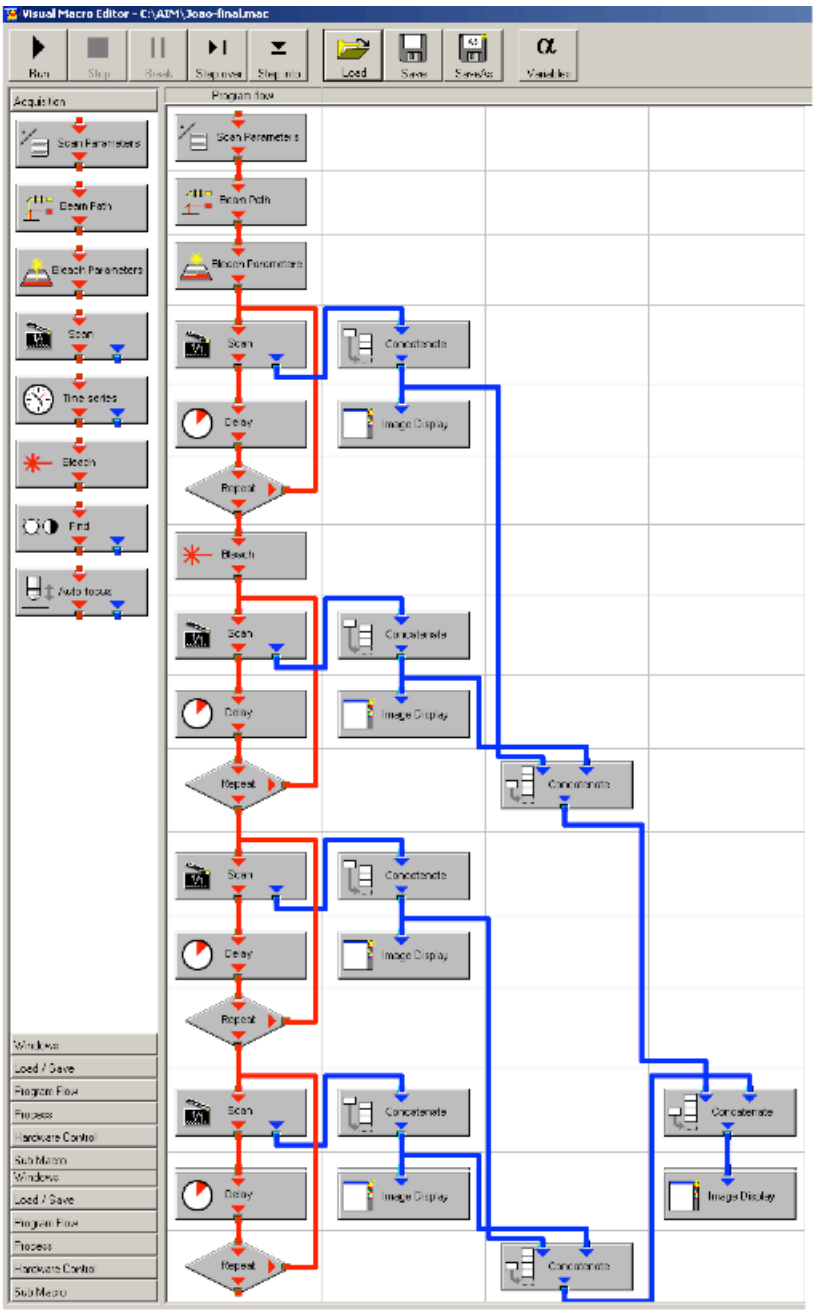

Figure F1 – VisualMacro Editor macro developed for image acquisition.

The first steps of this macro define the image scan conditions (pinhole size, channel gain, channel offset, zoom and objective used) and bleach conditions (number of iterations – 7, lasers used – 488nm and 489nm at 100% and the region of interest to be bleached) (Figure F2).

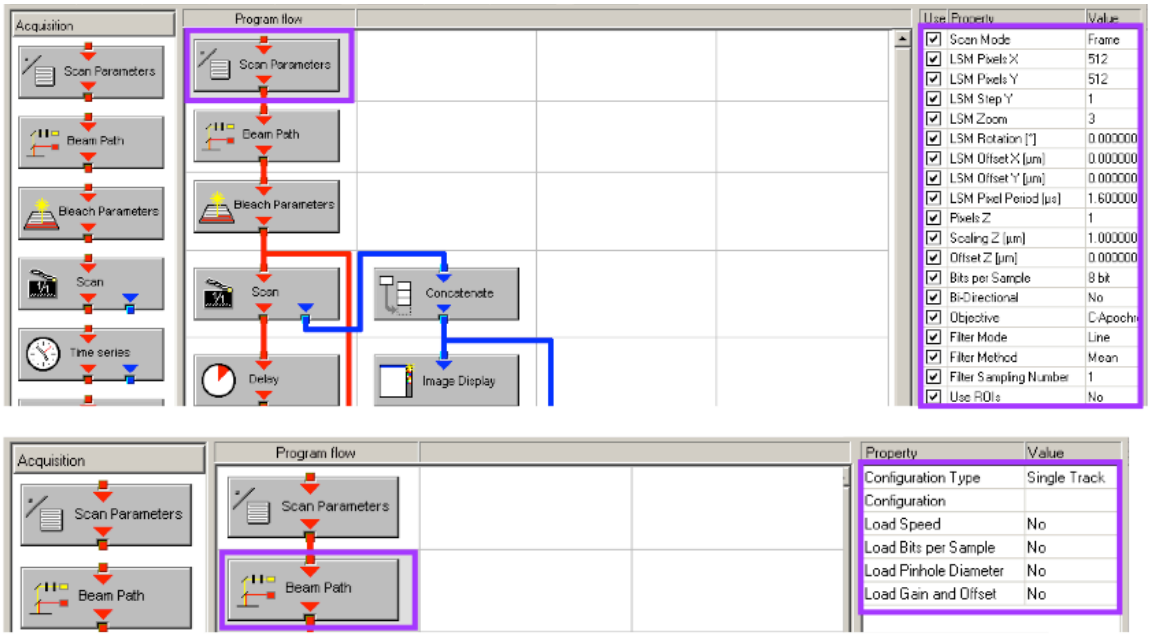

Figure F2 – Scan Parameters and Beam Path options used in the developed macro.

After defining these parameters, the macro is instructed to acquire 5 prebleach images interspersed by 5 seconds. Afterwards, the user-defined region of interest (ROI) is bleached.

Regarding the ROI, it is important to note that one should bleach the target cell as well as its surrounding cells so that when measuring fluorescence recovery from the target cell, the adjoining membranes' contribution is reduced considerably. With the current resolution limits in confocal imaging it is impossible to bleach only the membranes of a specific cell – by also bleaching its neighbours, one tries to minimise their contribution to the target cell fluorescence recovery (Sprague and McNally, 2005a).

Immediately after the crucial bleaching step, the program starts acquiring 60 images interspersed by 1second. This is the so-called fast acquisition step. Once this minute of intensive imaging is over, 120 images are taken with 5 seconds interval (10 minutes). This is the medium acquisition step. Finally, 60 images with 30 seconds interval are taken (10 minutes - slow acquisition). In the end, the macro has created 4 different movies (Figure D9); (several examples can be found in the attached DVD), which it then concatenates to create a single movie file. After this movie is complete, it is possible to select another area of the embryo (posterior or anterior) and follow the same procedure.

2.4. Image processing

In order to illustrate the methodological procedures for this section, a lacGFP embryo movie will be used as an example.

After image acquisition, it is required to process the obtained data. Since a highly dynamic developmental stage is being imaged, cells tend to move out of the ROI. In order to correct for such drift, or at least minimise it, a FIJI (http://pacific.mpi-cbg.de/wiki/index.php/Fiji) plugin is used – Linear Stack Alignment with SIFT (Figure F3).

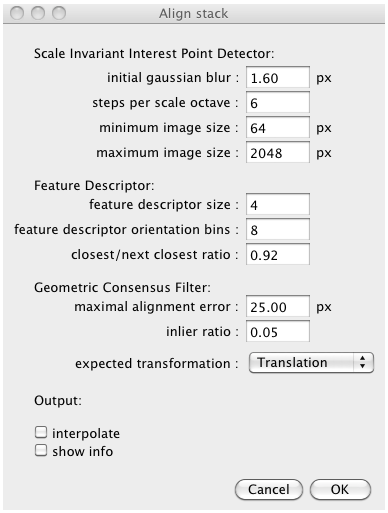

Figure F3 – Linear Stack Alignment with SIFT conditions used for cell drift compensation.

By comparing the raw data with the “aligned” images one can see that the target bleached cell drifts significantly less after applying this plugin (Figure F4).

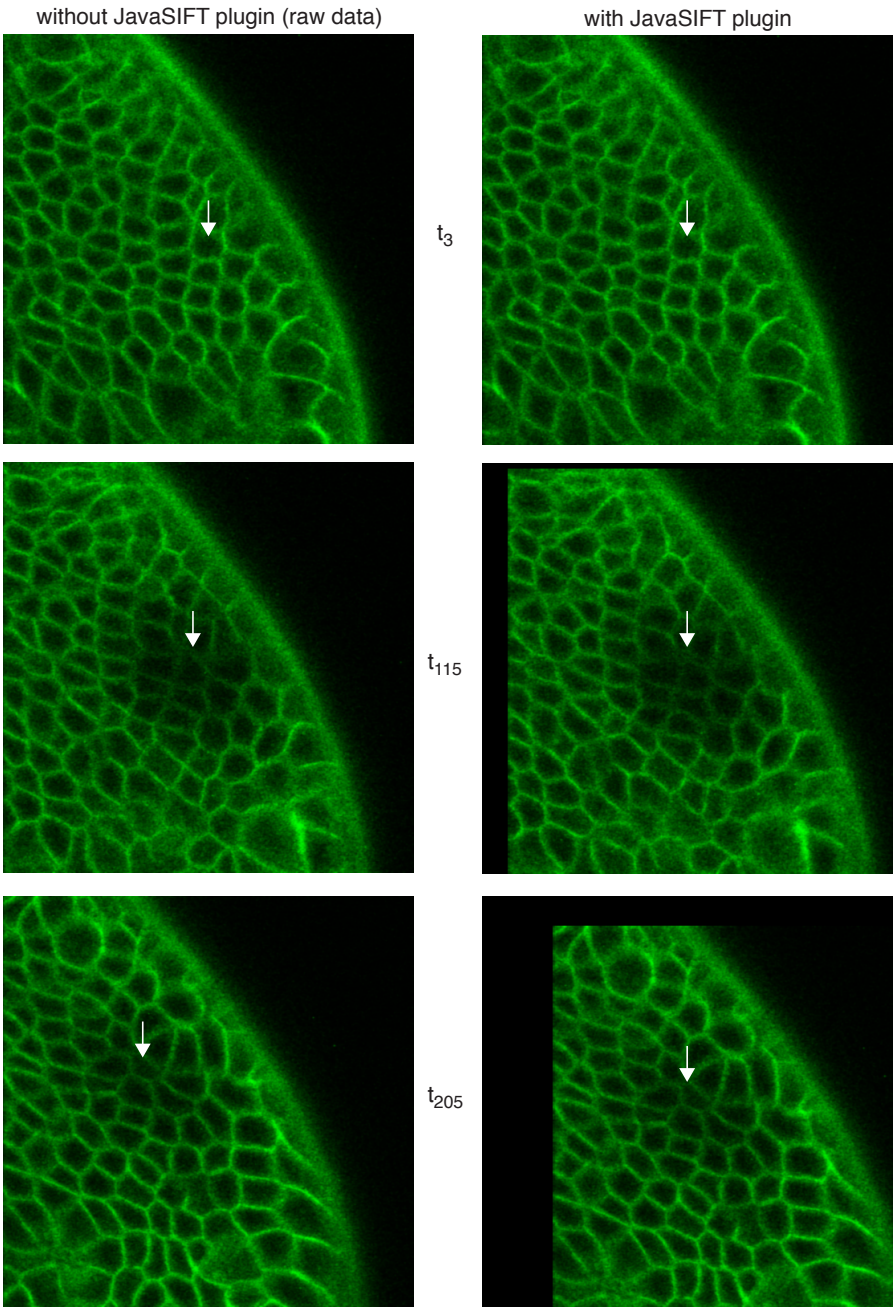

Figure F4 – LachesinGFP embryo movie stills before and after applying the Linear Stack Alignment with SIFT plugin. The arrow points to the position of the target bleach cell in the different timepoints.

2.5. Data extraction

After correcting for drift, the fluorescent mean values of the bleached target cell over all time points need to be retrieved. To do so, the cell is selected using FIJI basic tools such as oval selection. One should obtain something similar to the following image (Figure F5).

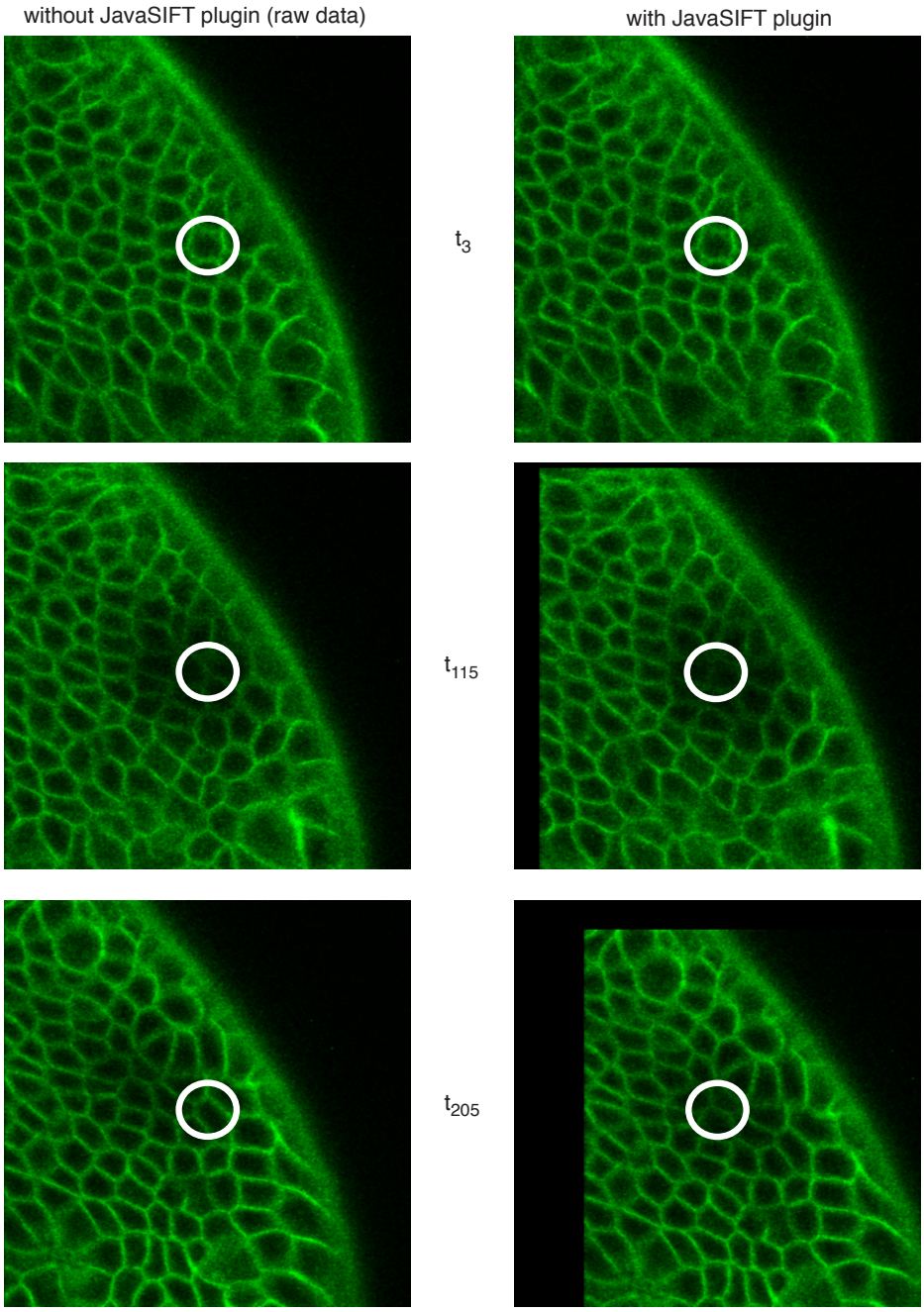

Figure F5 – LachesinGFP embryo movie stills before and after applying the Linear Stack Alignment with SIFT plugin. The circle highlights the target bleach area.

Though the Linear Stack Alignment with SIFT plugin does well in correcting for cell drift, towards the late images of the movie (t_{205}), it is possible to observe that a neighbouring cell has entered the selected area. A way to reduce the noise derived from this is by performing manual annotation of every movie – by carefully watching the movies, one establishes the precise timepoint when neighbouring cells entered the ROI or even the timepoint at which the target bleached cell has left the ROI. All subsequent values would then be excluded from the dataset.

Once the area of the bleached cell is defined, fluorescent values are extracted using the plot Z-axis profile function from FIJI. This measures a certain number of parameters (minimum value, maximum value, area, mean) over all 205 timepoints of the movie. The mean value parameter will be the one used for quantification since it reflects the total amount of fluorescence over the ROI and consequently of the bleached cell. However, since every image acquired with the 488nm laser implies a certain amount of photobleach, one needs to correct for that. Therefore, it is necessary to measure a nonbleached area of the embryo thus normalising all values. The bigger the nonbleached area the better, since occasional vesicles appearing in the imaging field could impose major noise interference if the selected area was small. By increasing the area, this effect is reduced (Figure F6).

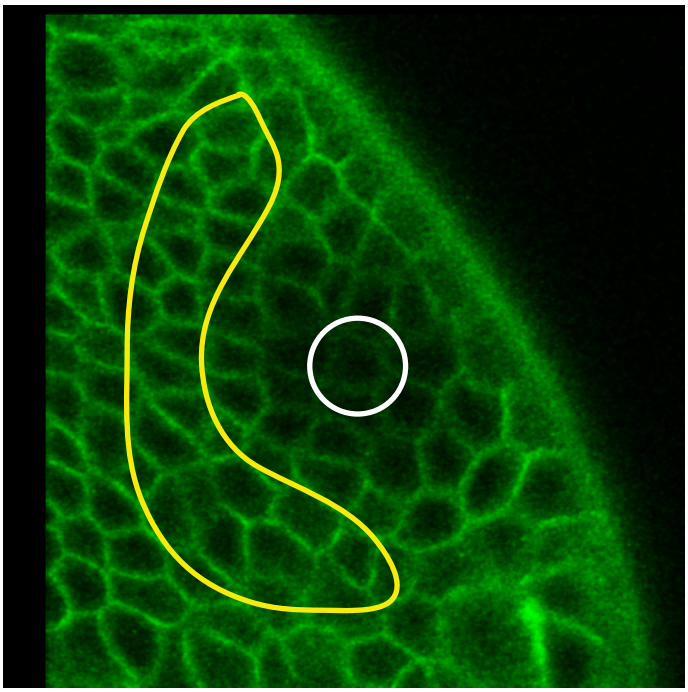

Figure F6 – ROIs used for data extraction. The white ROI reflects the bleched cell whereas the yellow ROI reflects the nonbleached area.

Once all raw mean values have been obtained for both areas (bleached vs nonbleached) for every timepoint, the next step consists in normalising the bleached area values. This shows how well the cell recovered from the bleach and reveals the dynamics of the imaged protein.

2.6. Data normalisation

The formula used for normalising the values is the following:

$$I_{norm} = \frac{\left[(I_{bleach} - I_{nonbleach})_n - \max(I_{bleach} - I_{nonbleach})\right]}{\left[\max(I_{bleach} - I_{nonbleach}) - \min(I_{bleach} - I_{nonbleach})\right]}$$

This formula normalises your bleached area mean values by comparing them with the nonbleached area mean values ($I_{bleach} - I_{nonbleach}$) and, at the same time, it scales them between 0 - $\max(I_{bleach} - I_{nonbleach})$ and 1 - $\min(I_{bleach} - I_{nonbleach})$.
The normalisation step is done using a template spreadsheet developed in Microsoft Excel (it can be found on an attached DVD). Every movie will have a corresponding Excel spreadsheet with the normalised values.

2.7. MATLAB script

Dr. Jean-Yves Tinevez developed the MATLAB script for curve fitting and statistical analysis and it can be found on a DVD attached to the hardcover of this thesis.
This script automatically retrieves the normalised values from all excel spreadsheets and organises them according to the specific genotype and region of the embryo. It then fits a single exponential recovery curve and a double exponential recovery curve for all movies. The next step consists in doing a statistical analysis of the obtained curve fitting parameters.
In the end, the script generates several files – a MATLAB figure regarding the curve fitting plot (Figure D11) and several MATLAB figures for the different parameter statistical analysis (examples of these can be found in the Results section of this thesis).

2.8. Figure preparation

Figures were prepared using Adobe Illustrator, Adobe Photoshop and FIJI. Movies were generated with FIJI. Normalisation of mean values was done with Microsoft Excel. Curve fitting and statistical analysis were obtained with MATLAB. Text was written using Microsoft Word and Endnote X2.

3. Stranded at Second cloning strategy

In order to clone Stranded at Second, its CDS was ordered from the *Drosophila* Genomics Resource Center (See Supplementary Data). Since it was decided to place four different fluorophore tags inside the protein (mCherry; Eos; paGFP and Venus) a common cloning strategy had to be devised (Figure F7). It would be a 5-step strategy in which, all 4 different fluorophores would be surrounded by 2 linker sequences rich in serine and glycine residues not only to improve protein solubility but also protein folding.

Since SAS is quite a large protein it was decided to replace a low complexity region of SAS by the fluorophore sequence (Figure D3), which happened to have a very similar size to the replaced region.

Once SAS-mCherry-SAS, SAS-Eos-SAS, SAS-paGFP-SAS and SAS-Venus-SAS were obtained, these 4 different proteins were placed in 2 different expression vectors (Figure F8A). Since it was not known whether the overexpression of SAS early in development could cause any phenotypes, by placing the tagged versions of SAS in two different expression vectors – one ubiquitous but with low level of overexpression (pCasper with tubulin promoter) and another under the UAS/GAL4 expression system (Figure F9) – such risks were expected to be minimized. If the ubiquitous expression granted by pCasper would give any phenotypes, one would hope that by using a low expression and localized GAL4 driver such phenotypes would not be present. Finally, in order to test the tagged proteins before sending the final constructs for *Drosophila* transgenesis, S2 cells were transiently transfected and analysed (Figure F8B). The protein not only localised to the plasma membrane but it also showed quite a strong fluorescent signal.

Ultimately, after sending all 8 different constructs for transgenesis, several fly lines were obtained (Table F1).

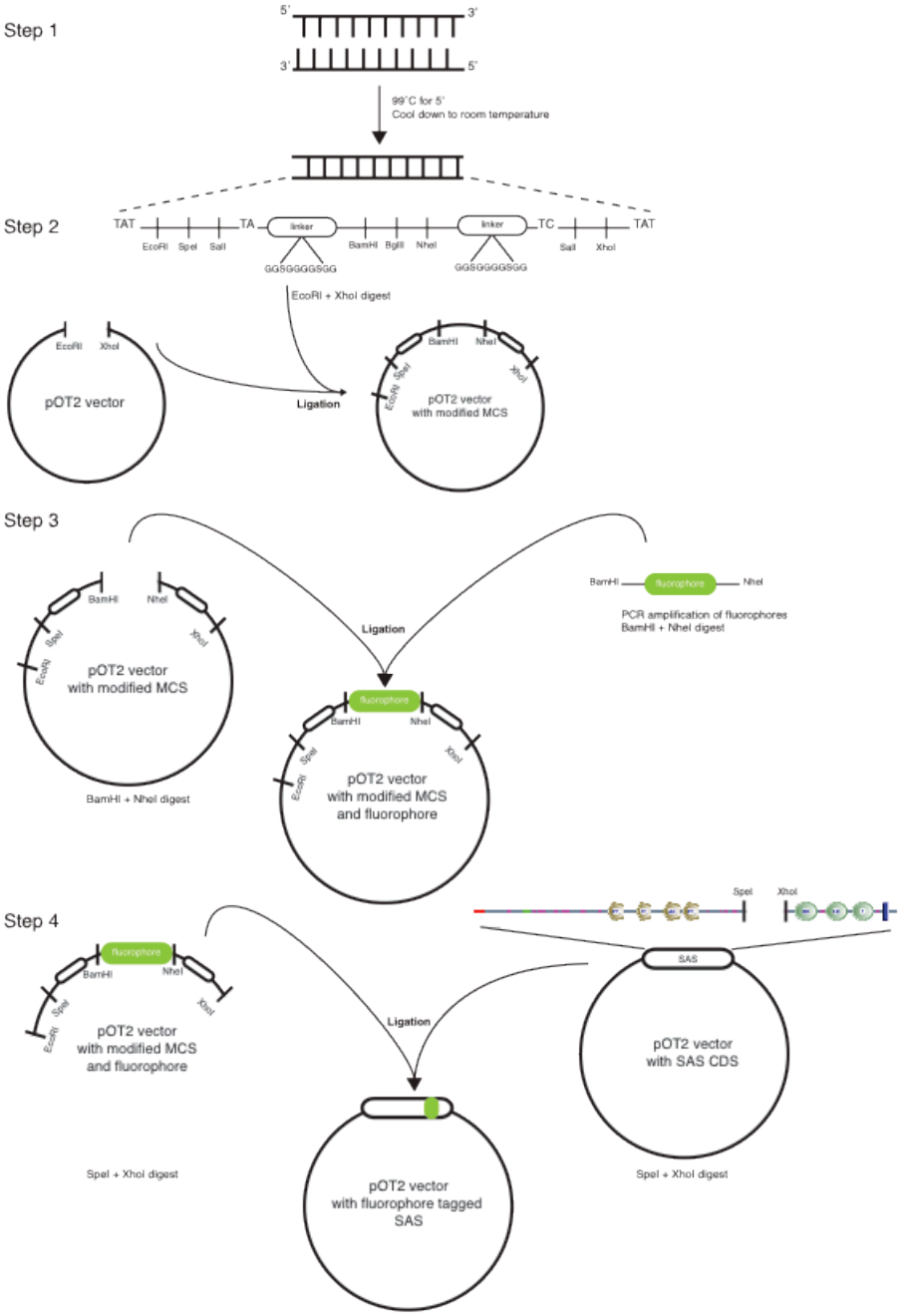

Figure F7 – The four initial cloning steps of fluorescently tagging SAS. Step 1 consisted in annealing the complementary artificial MCS primers. Once a double stranded DNA sequence of an artificial MCS was obtained, this sequence was cloned into a pOT2 vector by double digesting it with EcoRI and XhoI (Step 2). Step 3 consisted in inserting the different fluorophores between the 2 linker sequences (coding for GGSGGGGSGG) present in the artificial MCS. To achieve this, the fluorophore sequences were amplified by PCR using primers containing BamHI and NheI restriction sites. After digesting the PCR amplified sequences and the pOT2 vector containing the artificial MCS with these restriction enzymes, both products were ligated. Four different pOT2 vectors were obtained via this process – each one with a different fluorophore. Finally, step 4 consisted in inserting the fluorophore sequences surrounded by the linkers into the SAS CDS sequence. To do this, a double digest with SpeI and XhoI was performed, thus leading to the replacement of the low complexity region of SAS by a suitable fluorophore for live imaging. For primer and vector sequences see Supplementary Data.

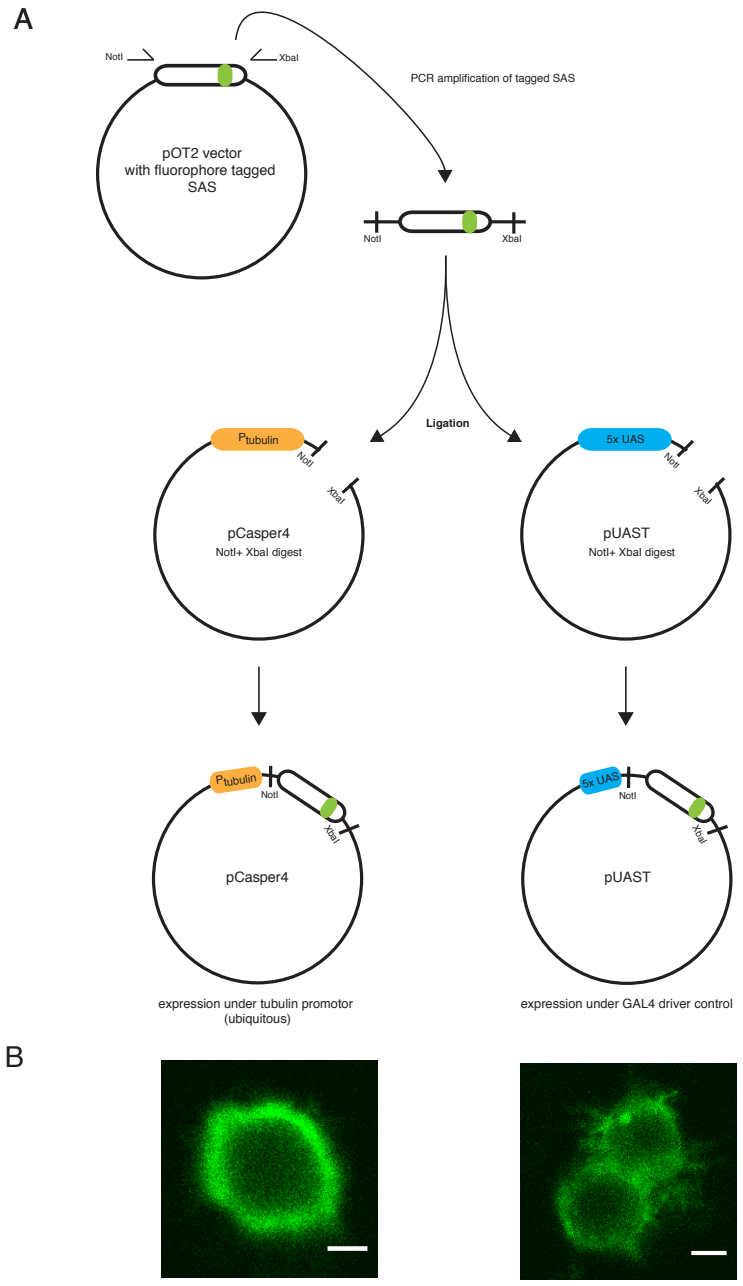

Figure F8 – Cloning fluorophore tagged SAS into an expression vector suitable for *Drosophila* transgenesis. (A) Once the four fluorescent flavours of SAS were obtained as explained in Figure F7, it was decided to clone them into two different expression vectors: pCasper4 with a tubulin promoter (low overexpression levels) and pUAST (for high levels of overexpression). To achieve this, specific primers with NotI and XbaI restriction sites were used to amplify the SAS sequence. Once digested, the PCR products could be inserted into the two different expression vectors. (B) To test the success and fluorescent signal of the tagged protein, transient expression in S2 cells was conducted. The protein not only localised to the membrane but also showed a strong fluorescent signal. Scalebar: 5μm.

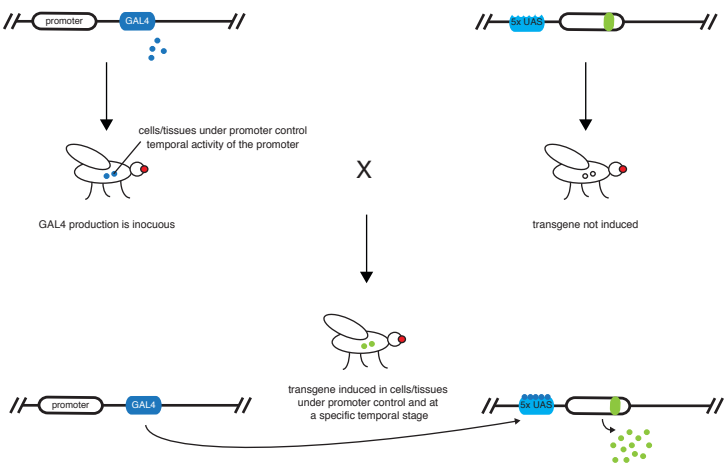

Figure F9 – The UAS/GAL4 system.

SAS Transgenic Lines	Chromosome insertion	SAS Transgenic Lines	Chromosome insertion
Casper SAS-Cherry 1	3	UAS SAS-Cherry 7	2
Casper SAS-Cherry 2	3	UAS SAS-Cherry 8	3
Casper SAS-Cherry 3	3	UAS SAS-Cherry 9	3
Casper SAS-Cherry 4	2	UAS SAS-Eos 1	2
Casper SAS-Cherry 5	2	**UAS SAS-Eos 2**	**3**
Casper SAS-Cherry 6	2	UAS SAS-Eos 3	3
Casper SAS-Cherry 7	2	UAS SAS-Eos 4	3
Casper SAS-Cherry 8	3	UAS SAS-Eos 5	3
Casper SAS-Cherry 9	3	UAS SAS-Eos 6	2
Casper SAS-Eos 1	2	UAS SAS-Eos 7	X
Casper SAS-Eos 2	2	UAS SAS-Eos 8	3
Casper SAS-Eos 3	3	UAS SAS-PAGFP 1	3
Casper SAS-Eos 4	3	UAS SAS-PAGFP 2	X
Casper SAS-PAGFP 1	2	UAS SAS-PAGFP 3	X
Casper SAS-Venus 1	**3**	UAS SAS-PAGFP 4	X
Casper SAS-Venus 2	3	UAS SAS-PAGFP 5	3
UAS SAS-Cherry 1	3	UAS SAS-Venus 1	3
UAS SAS-Cherry 2	3	**UAS SAS-Venus 2**	**3**
UAS SAS-Cherry 3	3	UAS SAS-Venus 3	3
UAS SAS-Cherry 4	2	UAS SAS-Venus 4	3
UAS SAS-Cherry 5	2	UAS SAS-Venus 5	3
UAS SAS-Cherry 6	2	UAS SAS-Venus 6	3

Table F1 – List of transgenic fly lines obtained. Fly lines in bold were used in this study.

Digest conditions

5µl NEB Buffer

1µl Enzyme A

1µl Enzyme B

0.5µl BSA

xµl template DNA (1000ng)

xµl H_2O (until 20µl)

Hybridisation of 116-nucleotide primer

Denaturation	99°C	7min
Hold	22°C	

PCR protocols

PCR reactions were done with the following conditions

4µl 5xPhusion HF Buffer

1µl dNTPs

1µl forward primer

1µl reverse primer

0.2µl Phusion DNA Polymerase

1µl template DNA (500-1000 ng)

11.8µl H_2O

Template PCR protocol for Phusion DNA Polymerase

Initial denaturation	98°C	3min	
Denaturation	98°C	10s	35x
Annealing	X°C	20-30s	
Extension	72°C	30s/kb	
Final extension	72°C	7min	
Hold	4°C		

PCR protocol for fluorophore amplification using Phusion DNA Polymerase

Initial denaturation	98°C	3min	
Denaturation	98°C	10s	35x
Annealing	62°C	30s	
Extension	72°C	20s	
Final extension	72°C	7min	
Hold	4°C		

PCR protocol for SAS amplification using Phusion DNA Polymerase

Initial denaturation	94°C	3min	
Denaturation	94°C	30s	3x
Annealing	45°C	30s	
Extension	72°C	4min	
Denaturation	94°C	30s	36x
Annealing	65°C	30s	
Extension	72°C	4min	
Final extension	72°C	10min	
Hold	4°C		

4. Recombination of *crb*^{11A22} with SpiderGFP and pCasper SAS-Venus 1

This section highlights the genetic crosses undertaken to obtain recombinant fly lines with *crb*^{11A22} and Spider GFP (Figure F10) and pCasper SAS-Venus1 (Figure F11). In order to distinguish homozygous *crb*^{11A22} embryos from heterozygous ones during the live imaging sessions, a fluorescent balancer – TTG - was used. When in the presence of a heterozygous embryo, a strong GFP signal will be present inside cells and in a stripy pattern in the embryo. This makes selecting for homozygous embryos much easier.

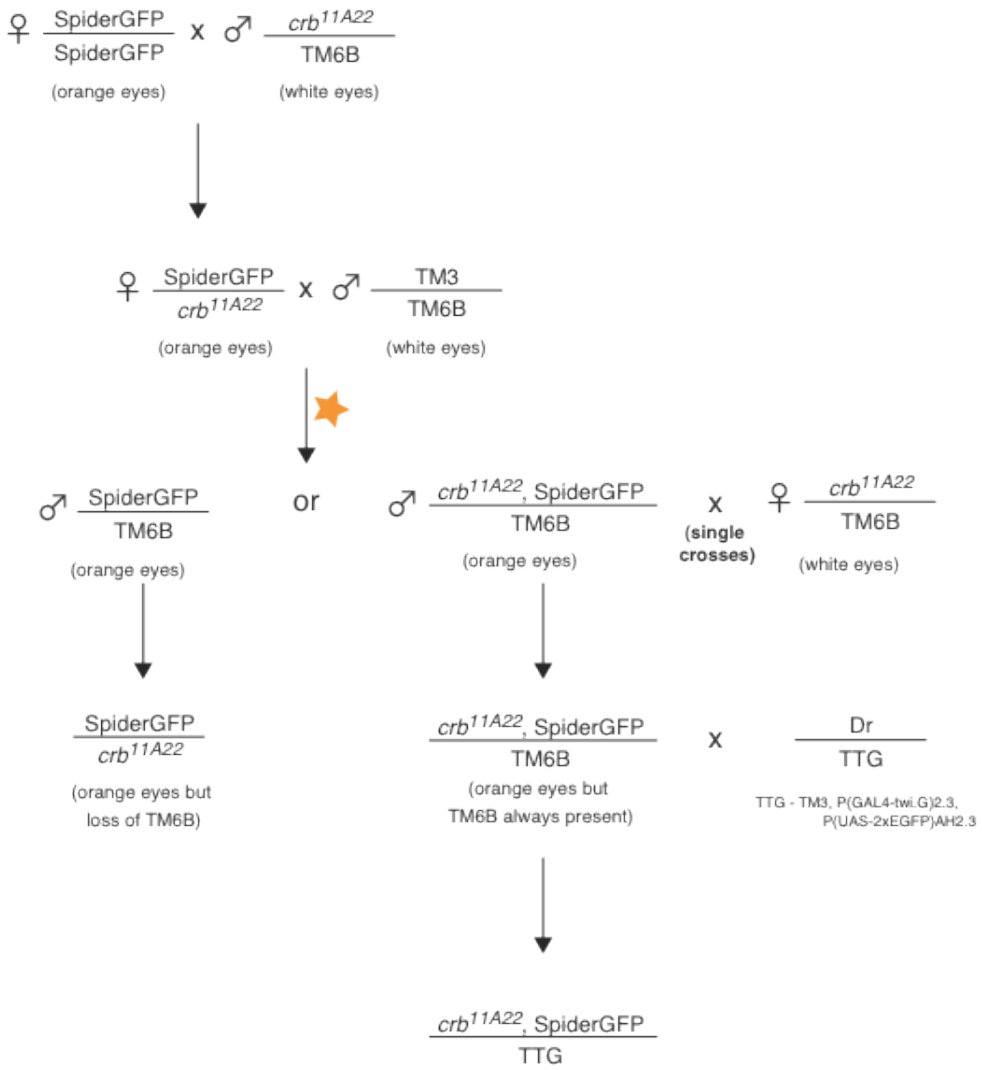

Figure F10 – Scheme highlighting the fly crosses undertaken to recombine SpiderGFP with *crb*^{11A22}. The star represents the recombination event.

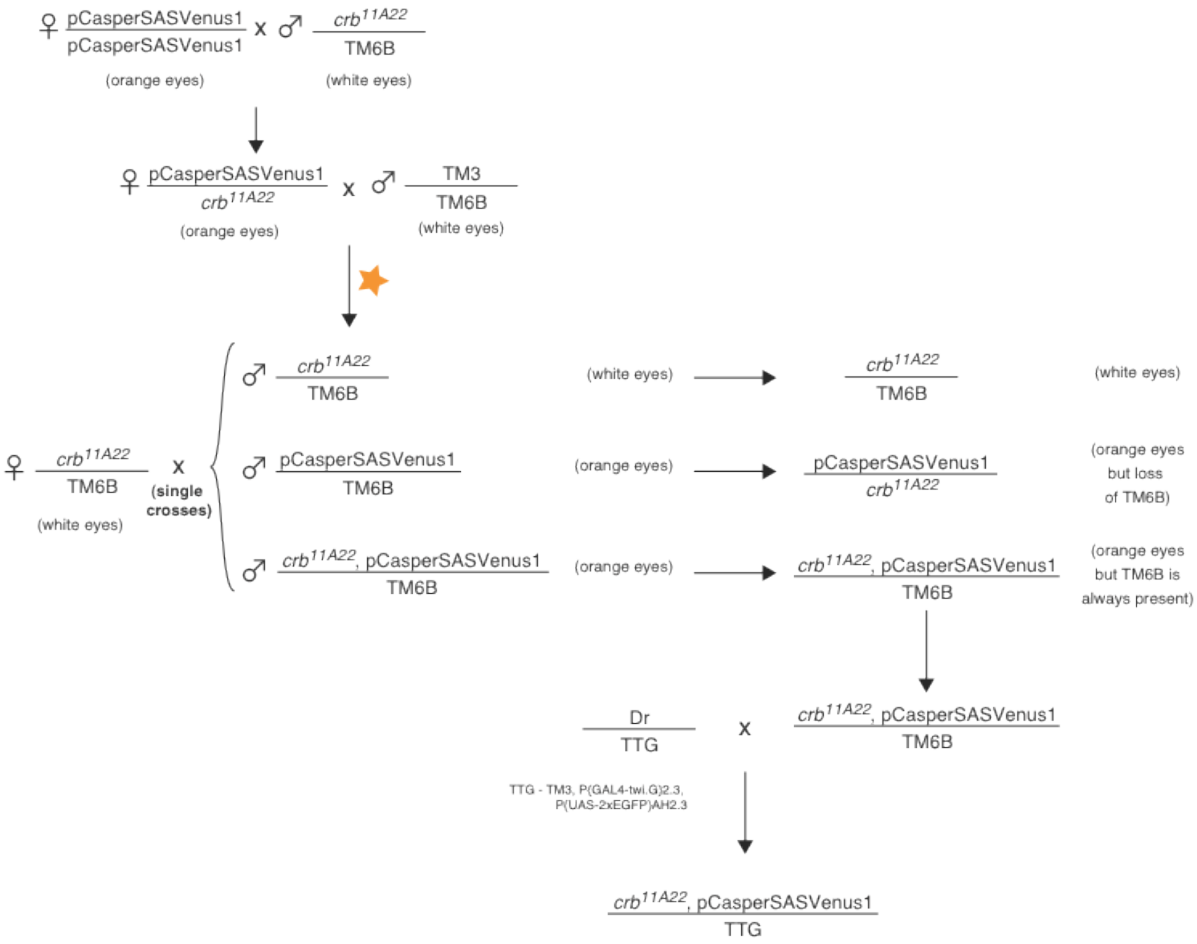

Figure F11 – Scheme highlighting the fly crosses undertaken to recombine pCasper SAS-Venus 1 with *crb*^{11A22}. The star represents the recombination event.

G. Supplementary Data

1. Information regarding SAS CDS ordered from DGRC

SAS clone (LD44801): made by Ling Hong: mRNA source--0-22hr embryos, from an isogenic *y; cn bw sp* strain, polyA+ selected twice. cDNA made using Stratagene ZAP-cDNA synthesis kit; oligo(dT) primed with XhoI site at end of primer for first strand synthesis; EcoRI adapter on 5' ends of clones; size fractionated on Sephacryl S-500--approximately 1-6kb., cDNA directionally cloned into EcoRI/XhoI-digested pOT2 plasmid.

2. SAS CDS (from FlyBase)

ATGCAAACGTGTAGAAGAAGAAAAGCCTCCGGCGGCCAATCCACGATCAAGTGGAGTAGAATGTGCCTGGCCAC
TCTCTGCGGATTACTTTTGCTTGGCATTCAAATTGAGCGTGCGGCGTCTGCGCCCGCAGGCGAAGACGCAGCGG
CCACAACGATGCCACCTTTGGATACCACAACAGATGCCCCAGACGCCGTTGCAGCCACCACCACTCCAGCCACA
ACTGCCGCAGAACAAAGCAGCAGCATCAGCAGCATAACCACCGAGGCGGCGGATGGTTCAACGACTTCCACGA
CGACAACAACTGAGGCGGCCAACAAATCCAATGCGACCGAAACTGATTTTACGACAAATGTGCCGGTGGCAAGC
AGCCTGCCAGAGGAGACCAGCGTGCGATCGACGAGCATTGAACCCATCACCTCCACGGAGCCCACGACAACGC
CCCGCCAGGAAACGGAGGGACCCGATCAGCACATGGTCTTCTCCAACACGGAACCAGATCAGAGCCACATTCA
GCACATTCCGCTGCGGGATGAGCACGCCGAGAGCAGTGGCGCCGACGATGCCACCACCGAGATGCAACGGCA
GCGTGAGCAGGATCAGCAGCAGAATGAGCTTAATCAGATCTCTAATGAGCAGGACGATGTGGTCAAGGATCTCA
ACAATTTCCGACATCCGGCCACGCTCATAACGGCCAGCAACAGCAACAGCGAGGAGAACGTCGAGATCGAAAGT
GACAAACAAGTTGAGACAACGACGACGGCGGTGCCGGCAGCAGCAACCTCCACATCCACAGAGGCAACAGGTA
CACCGCCAACAGGTACACCAGCAACATCCACATCCACAGTCCCGAACGAACGCGAAGAAGATCCCTATCATGTG
CATATACTGTCCGAGAATCATGATCGCCTGGCCGAACACGAAGATTATCAAATGCTCTCGACCAGCACCGAGGA
ATCGTCAACAACCTCTACCACTTCGACTACTAACAGCACCACAGAGTCGGGCATTGTGGCTGGTATTGTTGTCAG
TCAGGAGAACAAGGCAACCGCTGAGCCATCAACTGCAACCGAGTCTACATCCATATCCACATCCACAACAACTG
CAGCAACAGCCGCAACTTCAACCACATCGCGAGCACGCGCCATGCATATGAATGATCCAGAAGATGAAGCGGCC
ACCACAATAATGCCGGACAGCGAGTCGGTGCCAGTGATTAACATTGTTGAAGGACAACACATGCTGCAGCAGGA
GGATCAGAAGGATGAGGAGGAGGAGGGGGTGGTCAAGGAGTCGGAGAGCAGTTCCACCACCGAGGCGTCGAC
CACCACCACCGAGCCATCGCCATTTGTGGCCTTTGCTGGCGAGGGACGATCGGCGGGTGGCGGCAATGATATC
GAGCTGTTTCTGCACCACAATGGCTCTACACACGAGCAGCTCATGGATCTTAGTGATGTCAGCATGGACGGAGA
TCAGAACGAGGGCAGCAGCAAAACAGAGAGCAGCACTACTAGCACCACCACGACCACTGCTCAGCCGGAAACG
GAAATGCCGAAAATTGTGGAGATCACTGCCAGCGGGGATACCATGCAGCGGGAATGCCTGGCCAACAACAAGA
GCTATAAGCACGGCGAGTTGATGGAGCGGGATTGCGACGAGCGTTGCACCTGCAACCGCGGCGACTGGATGTG
CGAGCCAAGGTGCAGGGGACTAAGTTATCCGCGCGGCAGCCAGCGCAGCATGGCCAATCCCAACTGTCTGGAG
AAGATGGTGGAGGAGGACGAATGCTGTCGGGTGATGGAATGCAGTGAGCCGCAGCTGGAGCCCACGGTGGTAG
CCACAGAGGGTGCTGCACCTTCCACCAATGGAACGGGAGAATCGGCTGTGACCCTGCCCACGACCGATGATGA
AGCCACGCCCAAGCCCCGAACTGATTGCCACTACAACAGCGGTGTCTACAAATTCCGGGAGCGTCTGGAGATCG
GGTGCGAGCAGATCTGTCATTGTGCCGAAGGAGGCGTCATGGATTGCAGGCCACGCTGCCCGGAACGGAATCA
CACGCGTCTGGACAAGTGTGTGTATGTAAAGGACCCGAAGGACGTGTGCTGCCAACTGGAGCTCTGCGATGTCA

CGCTGGACGATCACGAACAGCAGCCAACGCCGCTGCAGAGCAACAACAACGAAGATCCAGAGGAGATCGACCC
CTTCCGCTTCCAGGAGCAGGCTCGCGACGCCGGAGGCGCCAAGCCCACTTGCACATTCAAGGGCGCAGAATAT
GATGTGGGTCAGCAGTTCCGCGATGGCTGCGACCAGTTGTGCATTTGCAATGAGCAGGGCATTCACTGTGCCAA
GCTGGAGTGCCCCTCGAACTTTGGCCTGGATGTCCAGGATCCGCACTGCATACGCTGGGAACCGGTTCCGGCG
GACTTCAAGCCCTCGCCGCCGAATTGCTGTCCGGAGAGCATGCGTTGCGTCGACAATGGCACATGCAGTTACCA
AGGCGTCCAGATCGAGAACTGGTCCCCTGTCCCAGCCAACCTGACAGGTTGCGATCAGCATTGTTATTGCGAGA
ATGGACGGGTAGAGTGCAGGGCAGCTTGTCCTCCGGTTCCAGCTCTTCCTCCGGCGGACTTGCCCTGCCATCCA
GCCTTGGCCCGCCTGCTGCCCATTCCCGATGACGAGTGCTGCAAGCACTGGATGTGTGCCCCCCAAATCCCGAA
AATCGGAGGTGCGGGTCAGGACGAAGAGACGGAAGCTACTTCAACCCATTCCTCGATTCCAGCAAATGAAACAA
CAACAACGACAGCGACAGCAAATAAATCGACCAGTATACCTAGCAAAGTACCCCAAATCAAGAAGGACGAGGAG
AAGAGACCACCAGCAAGTGGCGCCTTCTATCCAACCTTGGATGGCAAGCCACCCAAGTCGATTGGTGGTCTTGG
TATCTTCGAGAAGCCGGAAAAACCAGAGAAGGCCCACAAGAAAGTGCAACATCAACAGCAGCAGCATCAGCAGC
AGGAGCAGCAGGAGCAGCAGCAGCACCAGAATGATGTTATATTCGACGGTGATCGCACAGAGGAGCAGGAGGA
GCCTTTGCCACCGAACGGCGGTTTTGTGCCCTTCCAATTCGGCCAGCAGCATCCGCATCAGCCACATCTTGGTC
CGTATGGCTTCTACAATCCCGTGAAGCCCGTTTACGAGGACTATAATCCCTATGAGCCGTACGACATCAATCCCA
ATGGCACACCACAGGGCAAACCGCCTCCAGTGCCCACTAGTCAGTCCGATTTGTTCAATATATTAGGTGCGGAA
CAACCAGGACACCCGGTTCATCCTGGCCATGGTGGACCCCCCCGCATTCATCCTGGGCAAACGCAAAAAGACAA
TCACAACCTGGGACCACAAGTTAGAATCGAACAGATACTGCAGCACCTGCAGCAAACTGTTCCAGGTGGACCAC
CACCACCTCCGCCCCACCAGCAACACCAATCCCTGACACCGCAGCTGCATCCGCAGCAGCAACAAATTTCGCAG
CAACATCCTGGTCATTATGTGCCCATCGTGCACAGTGGAGTGCCGCCACCGCCACCAGGACATGGCATTGCCAT
TGTCGATGGGCAAACAGTGGCCTATGAGAGTTATCCTGTGATCCCGGGACTGGGAGTACCACAGCACCATCCCC
AGCAGCACCAGACGACCCCGCAGCAACACTTGCAGCAGACAATCCTGCCTAGCTCGAGCACCACCTCCGGACT
CTCGACGCAGGCTAGTGAGCACAGTCTGCACCAGAACCAGGGCAAGCTGGCCAAACAGCAGCAGTCAGGAGCC
AACAACCTGCAACCTGATATCGAAGTTCACACACTGGAGGCCATCGATCCTCGTTCCATTCGCATCGTCTTCACC
GTTCCCCAGGTCTATGTGAACCTCCATGGACGCGTGGAGCTGCGCTACTCGAATGGACCCAGTAACGATACATC
CACCTGGGAACAACAGATTTTTGCTCCGCCCGAGGACCTCATTGCCACATCCCAGATGGAGTTCGATCTGCCCA
GTCTGGAACCAAACTCACTGTACAAGGTGAAGATCACCTTAATCCTTCGTGATCTAAACTCGCAGCCCACGAGCA
GTATCTACACCGTGAAGACGCCACCTGAAAGGACCATCACTCCGCCACCTCCGTTCCCCGATTACAGGCCAGAC
TTCCAGGACATCTTTAAGAACGTTGAGGATCCAGAACTGACGGTCAGCGAAACGAATGCCAGCTGGTTGCAGTT
GACATGGAAGAAACTTGGAGACGACCAAATGGAATATGTGGACGGAGTTCAGCTGCGCTACAAGGAACTGACGG
GCATGATCTACTCCTCAACGCCTCTGATCCATCGCACGTTGACCAGCTACACCATCCAGAACCTTCAGCCGGATA
CGGGCTACGAGATTGGGCTGTACTACATCCCATTGGCTGGACATGGAGCTGAATTGCGTGCCGGACACATGATT
AAGGTGCGAACTGCCCAGAAGGTGGACGTGTATGGCTTCGATGTGACCGTTAACGTAACCAAGGTGAAGACCCA
GAGTGTCGAGATCTCATGGAACGGAGTGCCCTATCCGGAGGACAAGTTCGTGCACATTTATCGTGCCATCTACC
AGAGCGACGCTGGCAAGGAGGACTCCAGCGTCTTCAAGGTGGCCAAGCGGGACAGCACCACTGGTACCCTGAT
CATGGATCTCAAACCAGGCACCAAGTACCGCCTCTGGCTGGAAATGTACCTGACCAACGGCAACACCAAGAAGA
GCAACGTTGTCAACTTCATCACGAAGCCAGGTGGTCCAGCCACTCCCGGAAAGACTGGAAAACTCCTAACGGCG
GGAACGGACCAACCCGTAGGCGATTACTACGGCCCCCTTGTGGTGGTTTCTGTGATCGCCGCTCTGGCGATCAT
GTCTACTTTGGCCCTGCTACTTATTATCACCAGGAGACGAGTTCATCAAACGGCATCCATTACGCCACCACGAAA
AAGCGACGCTGCCTACGATAATCCCTCATACAAGGTGGAGATCCAACAGGAGACTATGAATCTGTAA

- **SpeI recognition site**
- **XhoI recognition site**

3. SAS protein sequence

MQTCRRRKASGGQSTIKWSRMCLATLCGLLLLGIQIERAASAPAGEDAAATTMPPLDTTTDAPDAVAATTTPATTAAE
QSSSISSITTEAADGSTTSTTTTTEAANKSNATETDFTTNVPVASSLPEETSVRSTSIEPITSTEPTTTPRQETEGPDQH
MVFSNTEPDQSHIQHIPLRDEHAESSGADDATTEMQRQREQDQQQNELNQISNEQDDVVKDLNNFRHPATLITASNS
NSEENVEIESDKQVETTTTAVPAAATSTSTEATGTPPTGTPATSTSTVPNEREEDPYHVHILSENHDRLAEHEDYQML
STSTEESSTTSTTSTTNSTTESGIVAGIVVSQENKATAEPSTATESTSISTSTTTAATAATSTTSRARAMHMNDPEDEAA
TTIMPDSESVPVINIVEGQHMLQQEDQKDEEEEGVVKESESSSTTEASTTTTEPSPFVAFAGEGRSAGGGNDIELFLH
HNGSTHEQLMDLSDVSMDGDQNEGSSKTESSTTSTTTTTAQPETEMPKIVEITASGDTMQRECLANNKSYKHGELME
RDCDERCTCNRGDWMCEPRCRGLSYPRGSQRSMANPNCLEKMVEEDECCRVMECSEPQLEPTVVATEGAAPSTN
GTGESAVTLPTTDDEATPKPRTDCHYNSGVYKFRERLEIGCEQICHCAEGGVMDCRPRCPERNHTRLDKCVYVKDPK
DVCCQLELCDVTLDDHEQQPTPLQSNNNEDPEEIDPFRFQEQARDAGGAKPTCTFKGAEYDVGQQFRDGCDQLCIC
NEQGIHCAKLECPSNFGLDVQDPHCIRWEPVPADFKPSPPNCCPESMRCVDNGTCSYQGVQIENWSPVPANLTGCD
QHCYCENGRVECRAACPPVPALPPADLPCHPALARLLPIPDDECCKHWMCAPQIPKIGGAGQDEETEATSTHSSIPA
NETTTTTATANKSTSIPSKVPQIKKDEEKRPPASGAFYPTLDGKPPKSIGGLGIFEKPEKPEKAHKKVQHQQQQHQQQ
EQQEQQQHQNDVIFDGDRTEEQEEPLPPNGGFVPFQFGQQHPHQPHLGPYGFYNPVKPVYEDYNPYEPYDINPNG
TPQGKPPPVPTSQSDLFNILGAEQPGHPVHPGHGGPPRIHPGQTQKDNHNLGPQVRIEQILQHLQQTVPGGPPPPPP
HQQHQSLTPQLHPQQQQISQQHPGHYVPIVHSGVPPPPPGHGIAIVDGQTVAYESYPVIPGLGVPQHHPQQHQTTPQ
QHLQQTILPSSSTTSGLSTQASEHSLHQNQGKLAKQQQSGANNLQPDIEVHTLEAIDPRSIRIVFTVPQVYVNLHGRVE
LRYSNGPSNDTSTWEQQIFAPPEDLIATSQMEFDLPSLEPNSLYKVKITLILRDLNSQPTSSIYTVKTPPERTITPPPPFP
DYRPDFQDIFKNVEDPELTVSETNASWLQLTWKKLGDDQMEYVDGVQLRYKELTGMIYSSTPLIHRTLTSYTIQNLQP
DTGYEIGLYYIPLAGHGAELRAGHMIKVRTAQKVDVYGFDVTVNVTKVKTQSVEISWNGVPYPEDKFVHIYRAIYQSDA
GKEDSSVFKVAKRDSTTGTLIMDLKPGTKYRLWLEMYLTNGNTKKSNVVNFITKPGGPATPGKTGKLLTAGTDQPVG
DYYGPLVVVSVIAALAIMSTLALLLIITRRRVHQTASITPPRKSDAAYDNPSYKVEIQQETMNL*

- **Region between SpeI and XhoI**

4. pOT2 vector sequence

Taken from (www.fruitfly.org/about/methods/pOT2vector.html).

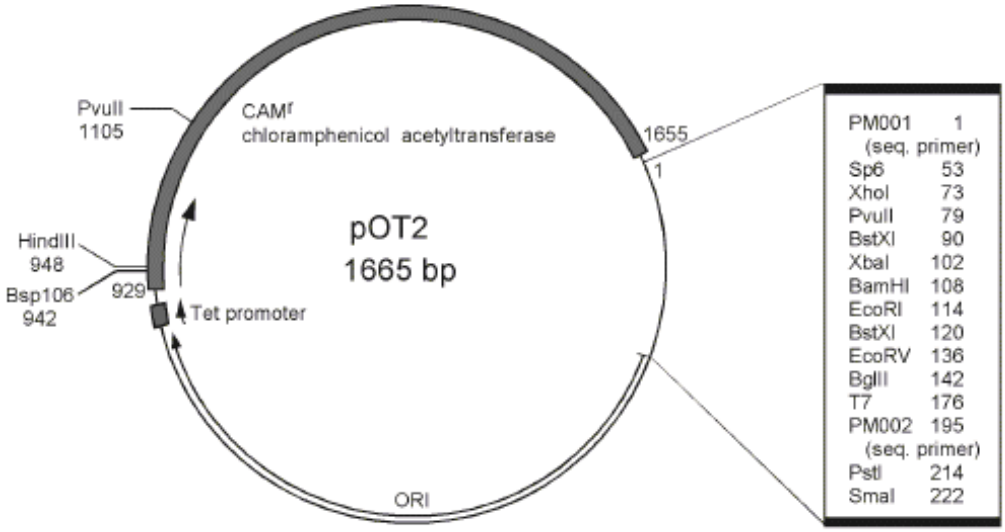

CGTTAGAACGCGGCTACAATTAATACATAACCTTATGTATCATACACATACGATTTAGGTGACACTATAGAACTCG
AGCAGCTGAAGCTCCAATGTGATGGTCTAGAGGATCCGAATTCCCAGCACAGTGGCGATGATATCAGATCTGCC
GGTCTCCCTATAGTGAGTCGTATTAATTTCGATAAGCCAGGTTAACCTGCATTAATGAATCGGCTGCAGTACCCG
GGAATTTAACCCGCCTAATGAGCGGGCTTTTTTTTGTGATCCAAAGGATCTTCTTGAGATCCTTTTTTTCTGCGCG
TAATCTGCTGCTTGCAAACAAAAAAACCACCGCTACCAGCGGTGGTTTGTTTGCCGGATCAAGAGCTACCAACTC
TTTTTCCGAAGGTAACTGGCTTCAGCAGAGCGCAGATACCAAATACTGTTCTTCTAGTGTAGCCGTAGTTAGGCC
ACCACTTCAAGAACTCTGTAGCACCGCCTACATACCTCGCTCTGCTAATCCTGTTACCAGTGGCTGCTGCCAGTG
GCGATAAGTCGTGTCTTACCGGGTTGGACTCAAGACGATAGTTACCGGATAAGGCGCAGCGGTCGGGCTGAAC
GGGGGGTTCGTGCACACAGCCCAGCTTGGAGCGAACGACCTACACCGAACTGAGATACCTACAGCGTGAGCTA
TGAGAAAGCGCCACGCTTCCCGAAGGGAGAAAGGCGGACAGGTATCCGGTAAGCGGCAGGGTCGGAACAGGA
GAGCGCACGAGGGAGCTTCCAGGGGGAAACGCCTGGTATCTTTATAGTCCTGTCGGGTTTCGCCACCTCTGACT
TGAGCGTCGATTTTTGTGATGCTCGTCAGGGGGGCGGAGCCTATGGAAAAACGCCAGCAACGCGGATCACAACA
AAAAGCCCGCTCATTAGGCGGGCTAAATTCTCATGTTTGACAGCTTATCATCGATAAGCTTTAATGAGTTATCGAG
ATTTTCAGGAGCTAAGGAAGCTAAAATGGAGAAAAAAATCACTGGATATACCACCGTTGATATATCCCAATGGCAT
CGTAAAGAACATTTTGAGGCATTTCAGTCAGTTGCTCAATGTACCTATAACCAGACCGTTCAGCTGGATATTACGG
CCTTTTTAAAGACCGTAAAGAAAAATAAGCACAAGTTTTATCCGGCCTTTATTCACATTCTTGCCCGCCTGATGAA
TGCTCATCCGGAGTTCCGTATGGCAATGAAAGACGGTGAGCTGGTGATATGGGATAGTGTTCACCCTTGTTACAC
CGTTTTCCATGAGCAAACTGAAACGTTTTCATCGCTCTGGAGTGAATACCACGACGATTTCCGGCAGTTTCTACA
CATATATTCGCAAGATGTGGCGTGTTACGGTGAAAACCTGGCCTATTTCCCTAAAGGGTTTATTGAGAATATGTTT
TTCGTCTCAGCCAATCCCTGGGTGAGTTTCACCAGTTTTGATTTAAACGTGGCCAATATGGACAACTTCTTCGCC
CCCGTTTTCACCATGGGCAAATATTATACGCAAGGCGACAAGGTGCTGATGCCGCTGGCGATTCAGGTTCATCAT
GCCGTTTGTGATGGCTTCCATGTCGGCAGAATGCTTAATGAATTACAACAGTACTGCGATGAGTGGCAGGGCGG
GGCGTAATTGGTACGTCGA

- **EcoRI site**
- **XhoI site**

5. Primer List

Primer name	Sequence 5'-3'
Step1	
Artificial MCS forward	TATGAATTCACTAGTCGACTAGGCGGGTCAGGTGGAGGCGGGTCTGGAGGGGGATCCAGATCTGCT AGCGGCGGGTCAGGTGGAGGCGGGTCTGGAGGGTCGTCGACCTCGAGTAT
Artificial MCS reverse	ATACTCGAGGTCGACGACCCTCCAGACCCGCCTCCACCTGACCCGCCGCTAGCAGATCTGGATCCCCC TCCAGACCCGCCTCCACCTGACCCGCCTAGTCGACTAGTGAATTCATA
Step3	
Cherry forward	TATGGATCCATGGTGAGCAAGGGCGAG
Cherry reverse	TATGCTAGCCTTGTACAGCTCGTCCATGC
Eos forward	TATGGATCCATGAGTGCGATTAAGCCAGACAT
Eos reverse	TATGCTAGCTCGTCTGGCATTGTCAGG
PAGFP forward	TATGGATCCATGGTGAGCAAGGGCGAG
PAGFP reverse	TATGCTAGCCTTGTACAGCTCGTCCATGC
Venus forward	TATGGATCCATGGTGAGCAAGGGCGAGGAG
Venus reverse	TATGCTAGCCTTGTACAGCTCGTCCATGC
Step5:	
SAS amplification forward	ATATGCGGCCGCATGCAAACGTGTAGAAGAAGAAAAGCC
SAS amplification reverse	GCGCTCTAGATTACAGATTCATAGTCTCCTGTTGGATCTC

6. Fluorophore sequences

mCherry

ATGGTGAGCAAGGGCGAGGAGGATAACATGGCCATCATCAAGGAGTTCATGCGCTTCAAGGTGCACATGGAGG
GCTCCGTGAACGGCCACGAGTTCGAGATCGAGGGCGAGGGCGAGGGCCGCCCCTACGAGGGCACCCAGACCG
CCAAGCTGAAGGTGACCAAGGGTGGCCCCCTGCCCTTCGCCTGGGACATCCTGTCCCCTCAGTTCATGTACGGC
TCCAAGGCCTACGTGAAGCACCCCGCCGACATCCCCGACTACTTGAAGCTGTCCTTCCCCGAGGGCTTCAAGTG
GGAGCGCGTGATGAACTTCGAGGACGGCGGCGTGGTGACCGTGACCCAGGACTCCTCCCTGCAGGACGGCGA
GTTCATCTACAAGGTGAAGCTGCGCGGCACCAACTTCCCCTCCGACGGCCCCGTAATGCAGAAGAAGACCATGG
GCTGGGAGGCCTCCTCCGAGCGGATGTACCCCGAGGACGGCGCCCTGAAGGGCGAGATCAAGCAGAGGCTGA
AGCTGAAGGACGGCGGCCACTACGACGCTGAGGTCAAGACCACCTACAAGGCCAAGAAGCCCGTGCAGCTGCC
CGGCGCCTACAACGTCAACATCAAGTTGGACATCACCTCCCACAACGAGGACTACACCATCGTGGAACAGTACG
AACGCGCCGAGGGCCGCCACTCCACCGGCGGCATGGACGAGCTGTACAAG

Eos

ATGAGTGCGATTAAGCCAGACATGAAGATCAACCTCCGTATGGAAGGCAACGTAAACGGGCACCACTTTGTGAT
CGACGGAGATGGTACAGGCAAGCCTTTTGAGGGAAAACAGAGTATGGATCTTGAAGTCAAAGAGGGCGGACCTC
TGCCTTTTGCCTTTGATATCCTGACCACTGCATTCCATTACGGCAACAGGGTATTCGCCGAATATCCAGACCACA
TACAAGACTATTTTAAGCAGTCGTTTCCTAAGGGGTATTCGTGGGAACGAAGCTTGACTTTCGAAGACGGGGGCA
TTTGCATTGCCAGAAACGACATAACAATGGAAGGGGACACTTTCTATAATAAAGTTCGATTTCACGGTGTAAACTT
TCCCGCCAATGGTCCAGTTATGCAGAAGAAGACGCTGAAATGGGAGCCCTCCACTGAGAAAATGTATGTGCGTG
ATGGAGTGCTGACGGGTGATATTACCATGGCTTTGTTGCTTGAAGGAAATGCCCATTACCGATGTGACTTCAGAA
CTACTTACAAAGCTAAGGAGAAGGGTGTCAAGTTACCAGGCTACCACTTTGTGGACCACTGCATTGAGATTTTAA
GCCATGACAAAGATTACAACAAGGTTAAGCTGTATGAGCATGCTGTTGCTCATTCTGGATTGCCTGACAATGCCA
GACGATAA

paGFP

ATGGTGAGCAAGGGCGAGGAGCTGTTCACCGGGGTGGTGCCCATCCTGGTCGAGCTGGACGGCGACGTAAAC
GGCCACAAGTTCAGCGTGTCCGGCGAGGGCGAGGGCGATGCCACCTACGGCAAGCTGACCCTGAAGTTCATCT
GCACCACCGGCAAGCTGCCCGTGCCCTGGCCCACCCTCGTGACCACCTTCAGCTACGGCGTGCAGTGCTTCAG
CCGCTACCCCGACCACATGAAGCAGCACGACTTCTTCAAGTCCGCCATGCCCGAAGGCTACGTCCAGGAGCGC
ACCATCTTCTTCAAGGACGACGGCAACTACAAGACCCGCGCCGAGGTGAAGTTCGAGGGCGACACCCTGGTGA
ACCGCATCGAGCTGAAGGGCATCGACTTCAAGGAGGACGGCAACATCCTGGGGCACAAGCTGGAGTACAACTA
CAACAGCCACAACGTCTATATCATGGCCGACAAGCAGAAGAACGGCATCAAGGCCAACTTCAAGATCCGCCACA
ACATCGAGGACGGCAGCGTGCAGCTCGCCGACCACTACCAGCAGAACACCCCCATCGGCGACGGCCCCGTGCT
GCTGCCCGACAACCACTACCTGAGCCACCAGTCCGCCCTGAGCAAAGACCCCAACGAGAAGCGCGATCACATG
GTCCTGCTGGAGTTCGTGACCGCCGCCGGGATCACTCTCGGCATGGACGAGCTGTACAAG

Venus

ATGGTGAGCAAGGGCGAGGAGCTGTTCACCGGGGTGGTGCCCATCCTGGTCGAGCTGGACGGCGACGTAAAC
GGCCACAAGTTCAGCGTGTCCGGCGAGGGCGAGGGCGATGCCACCTACGGCAAGCTGACCCTGAAGCTGATCT
GCACCACCGGCAAGCTGCCCGTGCCCTGGCCCACCCTCGTGACCACCCTGGGCTACGGCCTGCAGTGCTTCGC
CCGCTACCCCGACCACATGAAGCAGCACGACTTCTTCAAGTCCGCCATGCCCGAAGGCTACGTCCAGGAGCGC
ACCATCTTCTTCAAGGACGACGGCAACTACAAGACCCGCGCCGAGGTGAAGTTCGAGGGCGACACCCTGGTGA
ACCGCATCGAGCTGAAGGGCATCGACTTCAAGGAGGACGGCAACATCCTGGGGCACAAGCTGGAGTACAACTA
CAACAGCCACAACGTCTATATCACCGCCGACAAGCAGAAGAACGGCATCAAGGCCAACTTCAAGATCCGCCACA
ACATCGAGGACGGCGGCGTGCAGCTCGCCGACCACTACCAGCAGAACACCCCCATCGGCGACGGCCCCGTGC
TGCTGCCCGACAACCACTACCTGAGCTACCAGTCCGCCCTGAGCAAAGACCCCAACGAGAAGCGCGATCACATG
GTCCTGCTGGAGTTCGTGACCGCCGCCGGGATCACTCTCGGCATGGACGAGCTGTACAAG

H. Bibliography

Afonso, C., and Henrique, D. (2006). PAR3 acts as a molecular organizer to define the apical domain of chick neuroepithelial cells. J Cell Sci *119*, 4293-4304.

Axelrod, D., Koppel, D.E., Schlessinger, J., Elson, E., and Webb, W.W. (1976). Mobility Measurement by Analysis of Fluorescence Photobleaching Recovery Kinetics. Biophysical Journal *16*, 1055-1069.

Bachmann, A., Schneider, M., Theilenberg, E., Grawe, F., and Knust, E. (2001). Drosophila Stardust is a partner of Crumbs in the control of epithelial cell polarity. Nature *414*, 638-643.

Baum, B., and Georgiou, M. (2011). Dynamics of adherens junctions in epithelial establishment, maintenance, and remodeling. J Cell Biol *192*, 907-917.

Berger, S., Bulgakova, N.A., Grawe, F., Johnson, K., and Knust, E. (2007). Unraveling the genetic complexity of Drosophila stardust during photoreceptor morphogenesis and prevention of light-induced degeneration. Genetics *176*, 2189-2200.

Bertet, C., Sulak, L., and Lecuit, T. (2004). Myosin-dependent junction remodelling controls planar cell intercalation and axis elongation. Nature *429*, 667-671.

Bilder, D., Li, M., and Perrimon, N. (2000). Cooperative regulation of cell polarity and growth by Drosophila tumor suppressors. Science *289*, 113-116.

Bilder, D., and Perrimon, N. (2000). Localization of apical epithelial determinants by the basolateral PDZ protein Scribble. Nature *403*, 676-680.

Blankenship, J.T., Fuller, M.T., and Zallen, J.A. (2007). The Drosophila homolog of the Exo84 exocyst subunit promotes apical epithelial identity. J Cell Sci *120*, 3099-3110.

Bolognesi, R., Farzana, L., Fischer, T.D., and Brown, S.J. (2008). Multiple Wnt genes are required for segmentation in the short-germ embryo of Tribolium castaneum. Curr Biol *18*, 1624-1629.

Braga, J., McNally, J.G., and Carmo-Fonseca, M. (2007). A reaction-diffusion model to study RNA motion by quantitative fluorescence recovery after photobleaching. Biophys J *92*, 2694-2703.

Buszczak, M., Paterno, S., Lighthouse, D., Bachman, J., Planck, J., Owen, S., Skora, A.D., Nystul, T.G., Ohlstein, B., Allen, A.*, et al.* (2007). The carnegie protein trap library: a versatile tool for Drosophila developmental studies. Genetics *175*, 1505-1531.

Butler, L.C., Blanchard, G.B., Kabla, A.J., Lawrence, N.J., Welchman, D.P., Mahadevan, L., Adams, R.J., and Sanson, B. (2009). Cell shape changes indicate a role for extrinsic tensile forces in *Drosophila* germ-band extension. Nat Cell Biol *11*, 859-864.

Campbell, K., Knust, E., and Skaer, H. (2009). Crumbs stabilises epithelial polarity during tissue remodelling. J Cell Sci *122*, 2604-2612.

Cavey, M., Rauzi, M., Lenne, P.F., and Lecuit, T. (2008). A two-tiered mechanism for stabilization and immobilization of E-cadherin. Nature *453*, 751-756.

Chen, X., and Macara, I.G. (2005). Par-3 controls tight junction assembly through the Rac exchange factor Tiam1. Nat Cell Biol *7*, 262-269.

Cheong, J.K., and Virshup, D.M. (2011). Casein kinase 1: Complexity in the family. Int J Biochem Cell Biol *43*, 465-469.

Classen, A.K., Anderson, K.I., Marois, E., and Eaton, S. (2005). Hexagonal packing of Drosophila wing epithelial cells by the planar cell polarity pathway. Dev Cell *9*, 805-817.

Cliffe, A., Mieszczanek, J., and Bienz, M. (2004). Intracellular shuttling of a Drosophila APC tumour suppressor homolog. BMC Cell Biol *5*, 37.

Davies, J.A., and Garrod, D.R. (1997). Molecular aspects of the epithelial phenotype. Bioessays *19*, 699-704.

Drees, F., Pokutta, S., Yamada, S., Nelson, W.J., and Weis, W.I. (2005). Alpha-catenin is a molecular switch that binds E-cadherin-beta-catenin and regulates actin-filament assembly. Cell *123*, 903-915.

Ebnet, K., Suzuki, A., Horikoshi, Y., Hirose, T., Meyer Zu Brickwedde, M.K., Ohno, S., and Vestweber, D. (2001). The cell polarity protein ASIP/PAR-3 directly associates with junctional adhesion molecule (JAM). EMBO J *20*, 3738-3748.

Goldman, R.D., and Spector, D.L. (2005). Live cell imaging : a laboratory manual (Cold Spring Harbor, N.Y., Cold Spring Harbor Laboratory Press).

Grawe, F., Wodarz, A., Lee, B., Knust, E., and Skaer, H. (1996). The *Drosophila* genes *crumbs* and *stardust* are involved in the biogenesis of adherens junctions. Development *122*, 951-959.

Harris, K.P., and Tepass, U. (2008). Cdc42 and Par proteins stabilize dynamic adherens junctions in the Drosophila neuroectoderm through regulation of apical endocytosis. J Cell Biol *183*, 1129-1143.

Harris, T.J., and Peifer, M. (2005). The positioning and segregation of apical cues during epithelial polarity establishment in Drosophila. J Cell Biol *170*, 813-823.

Hartenstein, V. (1993). Atlas of Drosophila development (Plainview, N.Y., Cold Spring Harbor Laboratory Press).

Hartenstein, V., and Campos-Ortega, J.A. (1984). Early neurogenesis in wildtype *Drosophila melanogaster*. Roux's Archives of Developmental Biology *193*, 308-325.

Hong, Y., Ackerman, L., Jan, L.Y., and Jan, Y.N. (2003). Distinct roles of Bazooka and Stardust in the specification of Drosophila photoreceptor membrane architecture. Proc Natl Acad Sci U S A *100*, 12712-12717.

Hurd, T.W., Gao, L., Roh, M.H., Macara, I.G., and Margolis, B. (2003). Direct interaction of two polarity complexes implicated in epithelial tight junction assembly. Nat Cell Biol *5*, 137-142.

Itoh, M., Sasaki, H., Furuse, M., Ozaki, H., Kita, T., and Tsukita, S. (2001). Junctional adhesion molecule (JAM) binds to PAR-3: a possible mechanism for the recruitment of PAR-3 to tight junctions. J Cell Biol *154*, 491-497.

Izaddoost, S., Nam, S.C., Bhat, M.A., Bellen, H.J., and Choi, K.W. (2002). Drosophila Crumbs is a positional cue in photoreceptor adherens junctions and rhabdomeres. Nature *416*, 178-183.

Johnson, K., Grawe, F., Grzeschik, N., and Knust, E. (2002). Drosophila crumbs is required to inhibit light-induced photoreceptor degeneration. Curr Biol *12*, 1675-1680.

Johnson, K., and Wodarz, A. (2003). A genetic hierarchy controlling cell polarity. Nat Cell Biol *5*, 12-14.

Jurgens, G., Wieschaus, E., Nussleinvolhard, C., and Kluding, H. (1984). Mutations Affecting the Pattern of the Larval Cuticle in Drosophila-Melanogaster .2. Zygotic Loci on the 3rd Chromosome. Wilhelm Rouxs Archives of Developmental Biology *193*, 283-295.

Kempkens, O., Medina, E., Fernandez-Ballester, G., Ozuyaman, S., Le Bivic, A., Serrano, L., and Knust, E. (2006). Computer modelling in combination with in vitro studies reveals similar binding affinities of Drosophila Crumbs for the PDZ domains of Stardust and DmPar-6. Eur J Cell Biol *85*, 753-767.

Knust, E., and Bossinger, O. (2002). Composition and formation of intercellular junctions in epithelial cells. Science *298*, 1955-1959.

Knust, E., Dietrich, U., Tepass, U., Bremer, K.A., Weigel, D., Vassin, H., and Campos-Ortega, J.A. (1987). EGF homologous sequences encoded in the genome of Drosophila melanogaster, and their relation to neurogenic genes. EMBO J *6*, 761-766.

Kohjima, M., Noda, Y., Takeya, R., Saito, N., Takeuchi, K., and Sumimoto, H. (2002). PAR3beta, a novel homologue of the cell polarity protein PAR3, localizes to tight junctions. Biochem Biophys Res Commun *299*, 641-646.

Krahn, M.P., Buckers, J., Kastrup, L., and Wodarz, A. (2010). Formation of a Bazooka-Stardust complex is essential for plasma membrane polarity in epithelia. J Cell Biol *190*, 751-760.

Langevin, J., Morgan, M.J., Sibarita, J.B., Aresta, S., Murthy, M., Schwarz, T., Camonis, J., and Bellaiche, Y. (2005). Drosophila exocyst components Sec5, Sec6, and Sec15 regulate DE-Cadherin trafficking from recycling endosomes to the plasma membrane. Dev Cell *9*, 365-376.

Laprise, P., and Tepass, U. (2011). Novel insights into epithelial polarity proteins in Drosophila. Trends Cell Biol.

Lecuit, T. (2004). Junctions and vesicular trafficking during Drosophila cellularization. J Cell Sci *117*, 3427-3433.

Lemmers, C., Medina, E., Delgrossi, M.H., Michel, D., Arsanto, J.P., and Le Bivic, A. (2002). hINADl/PATJ, a homolog of discs lost, interacts with crumbs and localizes to tight junctions in human epithelial cells. J Biol Chem *277*, 25408-25415.

Lemmers, C., Michel, D., Lane-Guermonprez, L., Delgrossi, M.H., Medina, E., Arsanto, J.P., and Le Bivic, A. (2004). CRB3 binds directly to Par6 and regulates the morphogenesis of the tight junctions in mammalian epithelial cells. Mol Biol Cell *15*, 1324-1333.

Martin-Belmonte, F., Gassama, A., Datta, A., Yu, W., Rescher, U., Gerke, V., and Mostov, K. (2007). PTEN-mediated apical segregation of phosphoinositides controls epithelial morphogenesis through Cdc42. Cell *128*, 383-397.

McGill, M.A., McKinley, R.F., and Harris, T.J. (2009). Independent cadherin-catenin and Bazooka clusters interact to assemble adherens junctions. J Cell Biol *185*, 787-796.

Medina, E., Lemmers, C., Lane-Guermonprez, L., and Le Bivic, A. (2002). Role of the Crumbs complex in the regulation of junction formation in Drosophila and mammalian epithelial cells. Biol Cell *94*, 305-313.

Morais-de-Sa, E., Mirouse, V., and St Johnston, D. (2010). aPKC phosphorylation of Bazooka defines the apical/lateral border in Drosophila epithelial cells. Cell *141*, 509-523.

Muller, H.A., and Wieschaus, E. (1996). armadillo, bazooka, and stardust are critical for early stages in formation of the zonula adherens and maintenance of the polarized blastoderm epithelium in Drosophila. J Cell Biol *134*, 149-163.

Nam, S.C., and Choi, K.W. (2006). Domain-specific early and late function of Dpatj in Drosophila photoreceptor cells. Dev Dyn *235*, 1501-1507.

Oda, H., and Tsukita, S. (1999). Dynamic features of adherens junctions during Drosophila embryonic epithelial morphogenesis revealed by a Dalpha-catenin-GFP fusion protein. Dev Genes Evol *209*, 218-225.

Pellikka, M., Tanentzapf, G., Pinto, M., Smith, C., McGlade, C.J., Ready, D.F., and Tepass, U. (2002). Crumbs, the Drosophila homologue of human CRB1/RP12, is essential for photoreceptor morphogenesis. Nature *416*, 143-149.

Petrasek, Z., Ries, J., and Schwille, P. (2010). Scanning FCS for the characterization of protein dynamics in live cells. Methods Enzymol *472*, 317-343.

Pilot, F., and Lecuit, T. (2005). Compartmentalized morphogenesis in epithelia: from cell to tissue shape. Dev Dyn *232*, 685-694.

Pinal, N., Goberdhan, D.C., Collinson, L., Fujita, Y., Cox, I.M., Wilson, C., and Pichaud, F. (2006). Regulated and polarized PtdIns(3,4,5)P3 accumulation is essential for apical membrane morphogenesis in photoreceptor epithelial cells. Curr Biol *16*, 140-149.

Pocha, S.M., Wassmer, T., Niehage, C., and Knust, E. (2011). Retromer Controls Epithelial Cell Polarity by Trafficking the Apical Determinant Crumbs. Curr Biol *21*.

Richard, M., Grawe, F., and Knust, E. (2006). DPATJ plays a role in retinal morphogenesis and protects against light-dependent degeneration of photoreceptor cells in the Drosophila eye. Dev Dyn *235*, 895-907.

Roh, M.H., Liu, C.J., Laurinec, S., and Margolis, B. (2002a). The carboxyl terminus of zona occludens-3 binds and recruits a mammalian homologue of discs lost to tight junctions. J Biol Chem *277*, 27501-27509.

Roh, M.H., Makarova, O., Liu, C.J., Shin, K., Lee, S., Laurinec, S., Goyal, M., Wiggins, R., and Margolis, B. (2002b). The Maguk protein, Pals1, functions as an adapter, linking mammalian homologues of Crumbs and Discs Lost. J Cell Biol *157*, 161-172.

Schonbaum, C.P., Organ, E.L., Qu, S., and Cavener, D.R. (1992). The *Drosophila melanogaster stranded at second* (*sas*) gene encodes a putative epidermal cell surface receptor required for larval development. Dev Biol *151*, 431-445.

Sotillos, S., Diaz-Meco, M.T., Caminero, E., Moscat, J., and Campuzano, S. (2004). DaPKC-dependent phosphorylation of Crumbs is required for epithelial cell polarity in Drosophila. J Cell Biol *166*, 549-557.

Sprague, B.L., and McNally, J.G. (2005). FRAP analysis of binding: proper and fitting. Trends Cell Biol *15*, 84-91.

Takekuni, K., Ikeda, W., Fujito, T., Morimoto, K., Takeuchi, M., Monden, M., and Takai, Y. (2003). Direct binding of cell polarity protein PAR-3 to cell-cell adhesion molecule nectin at neuroepithelial cells of developing mouse. J Biol Chem *278*, 5497-5500.

Tan, Y., Yu, D., Pletting, J., and Davis, R.L. (2010). Gilgamesh is required for rutabaga-independent olfactory learning in Drosophila. Neuron *67*, 810-820.

Tepass, U. (1996). Crumbs, a component of the apical membrane, is required for zonula adherens formation in primary epithelia of *Drosophila*. Dev Biol *177*, 217-225.

Tepass, U., and Knust, E. (1990). Phenotypic and developmental analysis of mutations at the *crumbs* locus, a gene required for the development of epithelia in *Drosophila melanogaster*. Roux's Archives of Developmental Biology, 189-206.

Tepass, U., and Knust, E. (1993). Crumbs and stardust act in a genetic pathway that controls the organization of epithelia in Drosophila melanogaster. Dev Biol *159*, 311-326.

Tepass, U., Theres, C., and Knust, E. (1990). crumbs encodes an EGF-like protein expressed on apical membranes of Drosophila epithelial cells and required for organization of epithelia. Cell *61*, 787-799.

Totong, R., Achilleos, A., and Nance, J. (2007). PAR-6 is required for junction formation but not apicobasal polarization in C. elegans embryonic epithelial cells. Development *134*, 1259-1268.

Vincent, J.P., and Girdham, C. (1997). Promoters to express cloned genes uniformly in Drosophila. Methods Mol Biol *62*, 385-392.

von Stein, W., Ramrath, A., Grimm, A., Muller-Borg, M., and Wodarz, A. (2005). Direct association of Bazooka/PAR-3 with the lipid phosphatase PTEN reveals a link between the PAR/aPKC complex and phosphoinositide signaling. Development *132*, 1675-1686.

Wang, Q., Hurd, T.W., and Margolis, B. (2004). Tight junction protein Par6 interacts with an evolutionarily conserved region in the amino terminus of PALS1/stardust. J Biol Chem *279*, 30715-30721.

Wei, S.Y., Escudero, L.M., Yu, F., Chang, L.H., Chen, L.Y., Ho, Y.H., Lin, C.M., Chou, C.S., Chia, W., Modolell, J.*, et al.* (2005). Echinoid is a component of adherens junctions that cooperates with DE-Cadherin to mediate cell adhesion. Dev Cell *8*, 493-504.

Wodarz, A., Grawe, F., and Knust, E. (1993). CRUMBS is involved in the control of apical protein targeting during Drosophila epithelial development. Mech Dev *44*, 175-187.

Wodarz, A., Hinz, U., Engelbert, M., and Knust, E. (1995). Expression of Crumbs confers apical character on plasma membrane domains of ectodermal epithelia of *Drosophila*. Cell *82*, 67-76.

Wu, H., Feng, W., Chen, J., Chan, L.N., Huang, S., and Zhang, M. (2007). PDZ domains of Par-3 as potential phosphoinositide signaling integrators. Mol Cell *28*, 886-898.

Yu, S.R., Burkhardt, M., Nowak, M., Ries, J., Petrasek, Z., Scholpp, S., Schwille, P., and Brand, M. (2009). Fgf8 morphogen gradient forms by a source-sink mechanism with freely diffusing molecules. Nature *461*, 533-536.

Zallen, J.A., and Wieschaus, E. (2004). Patterned gene expression directs bipolar planar polarity in Drosophila. Dev Cell *6*, 343-355.

I. Acknowledgements

This work would not have been possible without the support and encouragement of many people to whom I would like to express my gratitude.

Firstly, I would like to thank Elisabeth Knust for allowing me to do my PhD work in her lab and for her support and scientific input.

I would also like to thank the members of my Thesis Advisory Committee, Teymuras Kurzchalia and Andrew Oates for their helpful comments and insightful and stimulating discussions.

I would also like to thank the Max-Planck Society for their financial support but also for allowing me to do a PhD in an institute with some of the best facilities I ever encountered.

A special thank you to Jean-Yves Tinevez for our extremely fruitful and engaging collaboration. When Physics meets Biology, beautiful things can happen. It was and still is a pleasure to work you. Thank you for making me wish to pursue a more biophysical approach to developmental problems.

A very special thank you to all my previous tutors: high school teachers, university professors who made me aware of the problems that Science tries to solve. My curiosity and resolve to try and get answers is in great part due to all of you.

I could not forget about Isabel Palacios, my former supervisor in Cambridge, who told me all there is to know about *Drosophila* and greatly supported (and still supports) me in my starting scientific career. Cambridge was a great experience and you were a major part of it. I will never forget our lab bench time together while listening to the craziest music and Philippe dancing to it! Thank you all!

During my PhD I met several people and made several friends who made life so much more pleasant and fun.
The Portuguese mafia was always there and made my adaptation time to Dresden and the MPI quite the experience. Pedro Campinho, Lara Carvalho, Maria Carvalho, Miguel Coelho, Antonio Domingues, Ana Violeta Fonseca, Tiago Ferreira, familia Junqueira (Magno, Livia, Huguinho e Artur), Marta Luz, João Matos, Julio Sampaio, you are all great and I am proud to

consider myself your friend. You were always there for me - the good times, the bad times and especially the fun times! Thank you!
A very big thanks also goes to the “you know what” gang – Alex Bussek, Fernando Carrillo, Claire Poulet, Stephan Preibisch, Daniele Soroldoni, Jakub Sedzinski – you guys rock! I have no words to describe the bond we established during these 4 years – it was great!
I could not forget about the Penkovismo Movement started here in Dresden. Sider Penkov (el ‘Comandante’) and Vili (la Presidenta) you are special. Thank you for allowing me to be your Subcomandante!

Life in the lab wasn’t always easy but certain people made it special and memorable. Rosana Blawid and Shirin Pocha were such people. Thank you from the bottom of my heart for all the moments and experiences we shared – good and bad, lest we forget. We endured a lot and persevered. I learned a lot from both of you and we had good fun while at it! I will never forget both of you and hope to keep calling you Gabi2 and Novsky for a long time. Thank you!

I also want to thank a group of people who already left Dresden but left their mark – Hristio Boytchev, Vanessa Barone, Julien Compagnon, Eugeni Entchev, Marzuk Kamal, Jesse Lipp and Elwy Okaz. But also people still in Dresden who make my life much nicer – Sebastian Boland, Marko Brankatschk, Andreas Ettinger, Volker Khroehne, Ali Mahmoud and Jens Roeper. Thank you!

Another special thanks goes to my club – SLBenfica (Glorioso SLB!) - for their majestic win in the championship in 2010. Wish I could have been in Lisbon to celebrate!

Thanks to my friends from Portugal for their support – Pepe, Rocha, Joaninha, Lontra, Carla, Hany, Veliça, Max, Carraça, Caiado, Marconi, Eurico and all the others I probably forgot – ‘Sois grandes!’.

I also have to thank a very special person – Ana Mateus – for all the moments, joys in life and fun we shared. Thank you for all the support, encouragement and motivation you gave me. You will always have a special place in my heart.

And finally, a very big, if not HUGE, thank you to my family – ‘as cotas’ – who were always there for me! Thank you for raising me properly, for giving me moral values, for teaching me to respect others and for loving me unconditionally. You will always be my compass in life!